Master's thesis

AgriGenomics

Microfluidic single-cell physiology analysis of *Corynebacterium glutamicum and Bacillus subtilis* under antibiotic stress

Thesis written at

Forschungszentrum Jülich, GmbH

by

Abhijeet Singh

First reviewer – JuniorProf. Dr. Dietrich Kohlheyer

Second reviewer – Prof. Dr. Ralf-Udo Ehlers

Faculty of Agricultural and Nutritional Sciences

Christian-Albrechts-Universität zu Kiel

Kiel, June 2015

Table of contents

I. Abstract

The antibiotic susceptibility of bacteria is an important criterion, as it has high relevance in the clinical treatment of infectious bacterial diseases and pharmacological research for new antimicrobial drug development. Antibiotic susceptibility testing is widely used for the analysis of bacterial sensitivity for an antibiotic. There is an increasing demand for an ideal analysis method, which can provide susceptibility information on the basis of physiology of bacteria at single-cell level. In this thesis, a novel microfluidic single-cell analysis (MSCA) method was developed for fast and accurate antibiotic susceptibility testing (AST). The method is based on the fluorescence time lapse imaging of bacterial growth and physiology under antibiotic stress. In MSCA, bacteria were cultivated in monolayer growth chambers (MGC) of a PDMS-glass based microfluidic device. The device contains four cultivation channels, each with hundreds of MGC, which allowed testing three different concentrations of an antibiotic along with a reference in parallel. Dynamic staining was used for bacterial cells growing in the MGCs with the perfusion media mixed with fluorescent dyes and desired antibiotic. For the experiments, two model bacteria *C. glutamicum* and *B. subtilis* were chosen that are close relatives of the human pathogenic strains, *e.g. M. tuberculosis* and *B. anthracis*, respectively. For the dynamic staining of *C. glutamicum,* fluorescent dyes calcein-AM and PI were used for sensing of metabolic activity of viable cells and dead cell differentiation, respectively. In case of *B. subtilis*, fluorescent dyes PO-PRO1 and PI were used for detection of cells without membrane potential and dead cells, respectively. Using MSCA, *C. glutamicum* and *B. subtilis* were tested with five different antibiotics *i.e.* ampicillin, chloramphenicol, kanamycin, streptomycin and mitomycin C. As MSCA is based on the accurate measurement of physiological changes of cells, it bypasses the need of time consuming conventional methods of AST. We have successfully demonstrated our method for two model organism with five antibiotics in four different concentrations, for accurate analysis of AST based on the physiological changes of bacterial cells under antibiotic stress. In addition to AST, MSCA method has a great potential to be used as a powerful tool in several microbiological studies focusing on the heterogeneity, phenotypic and physiological changes of bacteria under different conditions at a single-cell level.

II. Abbreviations and Symbols

Abbreviations	
3D	3 dimensional
AMP	Ampicillin
AST	Antibiotic susceptibility testing
ATCC	American type cell collection
B. subtilis	*Bacillus subtilis*
BHI	Brain Heart Infusion
C. glutamicum	*Corynebacterium glutamicum*
Calcein-AM	Calcein acetoxymethyl ester
CFU	Colony forming units
CHL	Chloramphenicol
CLSI	Clinical and Laboratory Standards Institute
DNA	Deoxyribose Nucleic Acid
FACS	Fluorescence assisted cell sorting
GFP	Green fluorescent protein
KAN	Kanamycin
MAC	Microfluidic agarose channel
MIC	Minimum inhibitory concentration
MMC	Mitomycin C
mRNA	Messenger Ribose Nucleic Acid
MSCA	Microfluidic single-cell analysis
PDMS	Poly(dimethyl)siloxane
PI	Propidium Iodide
PLBR	Picoliter bioreactor
RFP	Red fluorescent protein
RNA	Ribose Nucleic Acid
SCMA	Single-cell morphological analysis
STR	Streptomycin

Symbols	
µ	Growth rate
µg	Microgram
µm	Micrometer
g	Gram
L	Liter
mL	Milliliter
nL	Nanoliters
nm	Nanometer
nM	Nanomolar
^{o}C	Degree Celsius
OD_{600}	Optical density at 600 nanometer
pg	Pictogram
rpm	Revolutions per minute
W	Watt
μ_{max}	Maximum growth rate per hour

III. List of figures

IV. List of tables

1. Introduction

1.1. Motivation

Bacteria are ubiquitous and found in various environments like soil, water, air, on and within animals and plants, hot springs and glaciers (Logan and De Vos 2011). The ability to survive unfavorable conditions and to produce multiple progenies in a very short period of time makes them very successful organism on earth. Bacteria have evolved many mechanisms to acquire energy and nutrients for growth and reproduction. They influence human life in many ways, being either useful in the form of mutualistic or communalistic associations or harmful by being pathogenic to living organisms. Among all bacterial species that occur on earth, a very small fraction is pathogenic and causes different diseases in humans, animals and plants. Therefore, the study of bacteria with the new and advancing technologies is continuously carried out by scientists on the basis of different parameters like morphology (*i.e.* rod, coccoid and spiral shape), staining properties (gram positive and gram negative) and physiology.

Physiology of bacteria is a very important parameter in microbiology. The question that whether a cell is alive or dead has always been a matter of debate for microbiologists and biotechnologists. Hence, different terminologies like viable, nonviable, viable-but-nonculturable have been used to resolve this discussion (Kell *et al.* 1998). Physiology analysis to differentiate the live and dead cells is a very important aspect related to bacteria (Breeuwer and Abee 2000). Pathogenic bacteria infect humans and cause various diseases. These bacterial infections are treated by antibiotic therapies under a supervision of a physician. Antibiotics are the low molecular weight compounds produced by microorganisms which in minute quantities inhibit or kill bacteria. In case of clinical management of infectious diseases, the knowledge of antibiotics and bacterial physiology in terms of viability or in other words alive or dead, is very important to administer the antibiotic therapy. The prescription of antibiotics for the treatment of bacterial infection is carried out on the basis of antibiotic susceptibility assays.

1.2. Antibiotic susceptibility assay

Antibiotic susceptibility testing (AST) is an important method commonly used in clinical and microbiological laboratories to detect the sensitive or resistant status of a bacterial isolate and validate the susceptibility of bacteria against a particular drug (Jorgensen and Ferraro 2009). Rapid and accurate phenotype based clinical diagnosis of bacterial infection is needed to prevent the spread of infection and absolute treatment by antibiotics (Choi *et al.* 2013; Kalashnikov *et al.* 2012). The principle of AST is to evaluate the physiological response of a pathogen and to monitor its ability to grow in different concentrations of antibiotics as specified by the Clinical and Laboratory Standards Institute (CLSI). The performance of AST is also crucial in confirming the susceptibility of individual bacterial strain against the choice of antibacterial agent. Growth based AST and phenotyping are the current gold standard in clinical microbiological laboratories (Chen *et al.* 2010).

Conventional methods like agar plate, broth dilution, disk diffusion and antibiotic gradient (Etest strips) methods are commonly used in diagnostic laboratories. They are time consuming (24 - 48 hours) as they are based on the observation of bacterial growth on agar plates or in broth to determine the minimum inhibitory concentrations (MIC) of relevant antibiotics (Choi *et al.* 2012). MIC is defined as the lowest concentration of an antimicrobial that can inhibit the visible growth of a microorganism after an overnight incubation (Andrews 2001). Conventional methods of AST are broad and sensitive, nevertheless, they are time consuming, labor intensive and provide only limited information (Kahlmeter *et al.* 2003; Hou *et al.* 2014). Due to the increasing need of rapid and accurate AST, several automated methods are developed for the rapid and high throughput analysis for antibiotic susceptibility. For instance, WalkAway systems from Siemens, the Phoenix automated microbiology system from BD diagnostics, flow cytometry method and microfluidic method are few examples (Pulido *et al.* 2013). In the last decade, the development of important techniques like microfluidics and automated time-lapse fluorescence microscopy have revolutionized AST for the basic research of clinical infectious diseases (Chen *et al.* 2010).

1.3. Microfluidic antibiotic susceptibility testing

An ideal AST assay would be one which interprets susceptibility of bacteria against an antibiotic, based on the analysis of phenotypic variations and physiology of particular single-cells over a long period of time. Additionally, it would be fast enough to deliver the antibiotic susceptibility information to treat a patient in minimum possible time (Kalashnikov *et al.* 2012). The rapid and accurate analysis method will be also helpful in many other fields. For instance, agriculture and veterinary, waste water treatment plants, environmental studies, veterinary care and antibiotics development. The development of bioengineering and nanotechnology have promoted the miniaturization of AST assay into a rapid and portable forms which are easily customizable according to the experimental requirements (Pulido *et al.* 2013). These portable forms are generally termed as lab-on-a-chip device and have an advantage of effective sample usage which is in the range of picoliters to microliters. Bacteria are isolated from patient, animals and natural environments like fields, waste water treatment sites and are cultured to prepare a usable sample for the analysis. The use of small sample volumes is also a crucial factor in the rapid susceptibility testing (less than 12 hours). Microfluidic devices can be used to perform multiple tests with different concentrations of a particular antibiotic or with different antibiotics at the same time (Kalashnikov *et al.* 2012). Moreover, microbial growth, phenotypes and physiology can also be monitored with the use of phase-contrast and fluorescence microscopic techniques for the evaluation of growth rates and phenotypic variations at single-cell level.

In this thesis, a novel, rapid and accurate method for AST has been developed. This method is based on the fast and precise detection of antibiotic susceptibility by the use of advanced technologies like microfluidics and high resolution automated time-lapse fluorescence microscopy. The new method is called as microfluidic single-cell analysis based antibiotics susceptibility assay. The new method is presented and discussed in the following.

1.4. Microfluidic single-cell analysis based antibiotic susceptibility assay

Microfluidic single-cell analysis (MSCA) based antibiotic susceptibility assay is a rapid method in which bacteria are cultured with different concentrations of antibiotics in a microfluidic device and simultaneously analyzed for the sensitivity against antibiotics. In 2014, Gruenberger has developed a single use poly(dimethyl)siloxane (PDMS) based microfluidic device incorporating monolayer growth chamber (MGC). Single bacteria were cultivated in MGC to form isogenic microcolonies in which all bacterial cells are present in same plane (Figure 1). The microfluidic device contained four parallel cultivation channels with hundreds of MGCs each. These cultivation channels were continuously perfused with fresh culture medium to maintain constant environmental conditions. These MGCs were applied by Binder et al. 2014 for the light responsive control of gene expression in bacteria. Furthermore, Krämer (unpublished) has developed a dynamic method of bacterial staining using the aforesaid microfluidic device. This dynamic staining method is based on the instantaneous sensing of bacterial physiology by using fluorescent dyes. Krämer has demonstrated an online staining method for live and dead bacterial cells with the use of two fluorescent dyes, calcein acetoxymethyl ester (calcein-AM) and Propidium Iodide (PI). PI stained the disintegrated cells (red) and the non-fluorescent calcein-AM is metabolized to fluorescent calcein (blue) by the living bacteria (unpublished) (Figure 2). Another combination of fluorescent dyes *i.e.* PO-PRO1 and PI was also used for the sensing of physiology of bacteria. PI can enter the cells which had damaged cell walls and stained them while the counter stain PO-PRO1 entered the cells which lack membrane potential and give fluorescence (Krämer, unpublished). Details of the online staining method are presented in the following chapters.

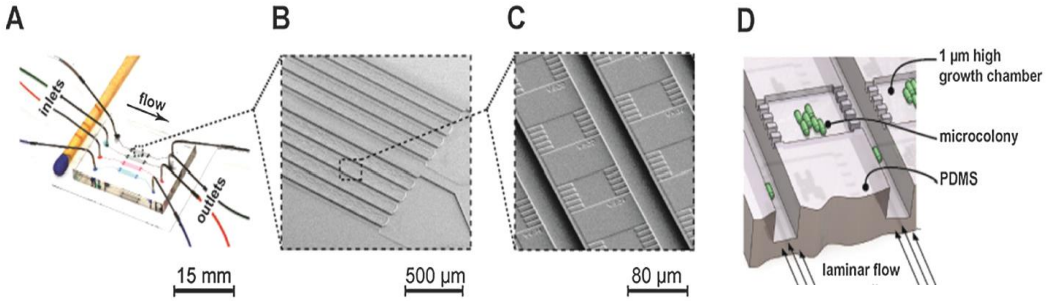

Figure 1. Microfluidic single-cell analysis device. (A) Assembled PDMS-glass based microfluidic device. Colored ink indicates parallel cultivation channels in the device. The direction of the flow is indicated by the arrow from inlets towards outlets. (B) Each cultivation channel has several lanes of sub-channels which incorporate hundreds of monolayer growth chambers indicated in image of plane (C). (D) Schematic representation of monolayer growth of a bacterial microcolony, arrow indicates the flow of culture medium in microfluidic device. (Binder *et al.* 2014).

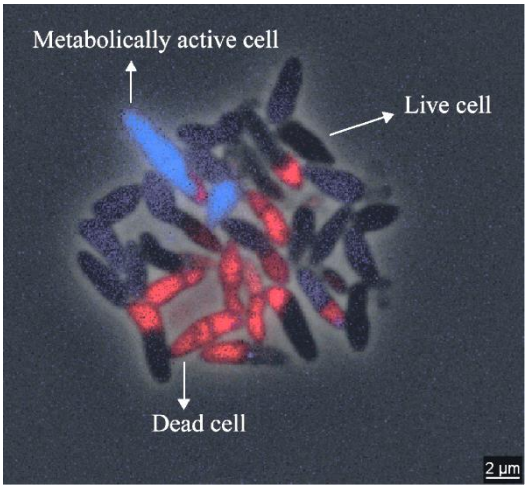

Figure 2. Demonstration of an online live and dead staining method in a microfluidic monolayer growth chamber. *C. glutamicum* ATCC 13032 were grown in the presence of ampicillin in a microfluidic device. calcein-AM and PI were perfused in the optimized concentration with the medium. Metabolically active cells converted non-fluorescent calcein-AM to fluorescent calcein (blue). Disintegrated cells were stained by PI and indicated with red fluorescence (Krämer, unpublished)

The basic principle of MSCA is to evaluate the response of bacteria to antibiotics on the basis of high-throughput single-cell fluorescence analysis. The possibilities to use different concentrations of antibiotics at the same time in a microfluidic device generate high-throughput data which is very beneficial in accurate AST. Since high resolution time-lapse microscopy provides real time information of bacterial response to antibiotics on a single-cell level,

bacterial physiological changes can be interpreted on the basis of fluorescence signals and projected area of bacteria. Most of the assays interpret antibiotic sensitivity of bacteria on the basis of their macroscopic growth in the presence of antibiotics (Figure 3A). On the contrary, MSCA based antibiotic susceptibility assay not only provide information about growth of bacteria in the presence of antibiotics, it also give an information about phenotypic variations, physiological state (live or dead) and size of individual cells. Moreover, the dynamic information of microbial heterogeneity caused due to different responses of individual bacterial cell to antibiotics in a micro population is an added advantage (Figure 3B). Heterogeneity can be explained on the basis of different response of individual bacterial cells to an antibiotic. Bacteria under antibiotic treatment can be susceptible, persistent, tolerant or resistant. Susceptible bacteria cannot survive in the presence of an antibiotic and die. A physiological state of bacteria, in which it does not die upon antibiotic treatment, but shut down its metabolic activities, is called persistent. Tolerant bacteria are able to grow at a reduced rate in the antibiotic environment. The physiological states namely persistence and tolerance are not considered as genetic phenomenon and are the responses of individual bacteria due to its physiology. Resistant bacteria grow, divide and do not show any response to the antibiotics. Antibiotic resistance is a genetic phenomenon, which occurs due to antibiotic resistance genes in the genome (Gefen and Balaban 2009).

To evaluate MSCA method on the basis of its performance against conventional test methods, agar plate based antibiotic susceptibility tests were conducted for comparison of the MSCA based antibiotic susceptibility assay. A schematic representation of the new MSCA is presented and compared with the agar plate method of antibiotic susceptibility testing in the following.

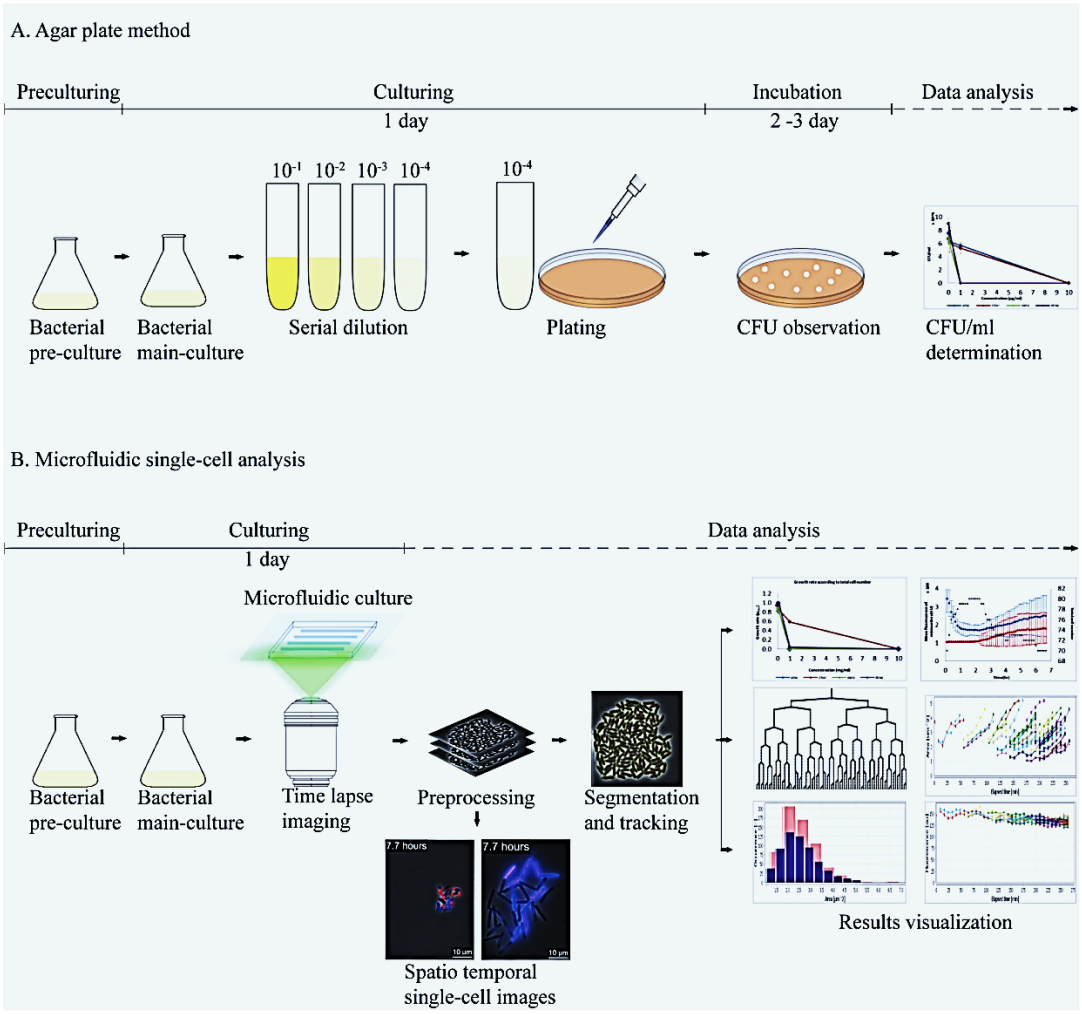

Figure 3. A schematic representation of agar plate method and microfluidic single-cell analysis for antibiotic susceptibility testing. (A) The agar plate method has several steps of serial dilution and plating before culturing of bacteria on the agar medium containing antibiotics. It is time consuming and provides information of bacterial susceptibility on the basis of viable cell number by colony forming unit (CFU) in unit volume of bacterial suspension. (B) Microfluidic single-cell analysis method is rapid and provides information of bacterial susceptibility on the basis of cell number, growth rate, cell division rate, size distribution. High resolution time-lapse fluorescence images provide information of the phenotypic changes and viability of bacterial cells. Interpretation of the fluorescence signals gives information about the physiological state of bacterial cells in terms of viable or dead.

1.5. Microbial single-cell analysis and population heterogeneity

The development of new and sophisticated methods for the study of individual microbial cells has opened the door to characterize microorganisms in detail and to precisely monitor their dynamic activity in a changing environment. Bulk and average based measurements indicates an average value of bacterial samples and can hide the contribution of individual bacterial cells to the average value (Probst *et al.* 2013). Single-cell techniques are constantly

being developed to decode the unexplored phenomenon of the bacterial physiology (Brehm-stecher *et al.* 2004). Recent developments in technologies and the growing interests for single-cell analysis is an impetus to study individual bacterial cells. The studies of bacteria at single-cell level have revealed many characteristics of bacteria which were not identified before. For instance, single individuals of a clonal population may differ widely in terms of gene regulation, physiology, biochemistry and behavior. Microorganisms are naturally heterogeneous and display wide range of genetic and non-genetic difference. The heterogeneity of bacterial population is very important and has practical influence on antibiotic therapy to the patient, veterinary animals and livestock (Brehm-stecher *et al.* 2004). Additionally, bacterial heterogeneity also has a huge influence on the food processing industry to monitor and maintain food safety including regulatory standards (Gram *et al.* 2002; Chmielewski, R. A. N. 2003). In case of clinical microbiology, if the antibiotic therapy is not supervised properly, bacteria may survive antibiotic treatment in the persistent or tolerant form and can cause recurrence of diseases like tuberculosis and *Clostridium difficile* infection (Keller and Kuijper 2015). In this thesis, two model bacteria namely *Corynebacterium glutamicum* and *Bacillus subtilis* were used. They are non-pathogenic, closely related to human pathogenic strains and are commonly used as a model organisms for different fields of research.

1.6. *Corynebacterium glutamicum* and *Bacillus subtilis*

C. glutamicum is a small, rod shaped, gram positive, non-motile, non-spore forming, heterotrophic, aerobic, non-pathogenic bacterium that is found in soil and can grow on a variety of sugars and organic acids (Ikeda and Nakagawa 2003; Kalinowski *et al.* 2003). It is extensively used in industries for the production of amino acids (L-glutamate, L-lysine, L-aspartate), food additives (Monosodium Glutamate – MSG) and also used for the bioremediation of phenol and arsenic from environment (Lee *et al.* 2010; Mateos *et al.* 2006). The complete genome of *C. glutamicum* has been sequenced in year 2003 and it consists of single circular chromosome comprising of 3,282,708 base pairs (3.2 Mbp). The genome contains high GC

content, 3002 protein coding genes out of which 2489 genes show homologies to the known protein coding genes (Kalinowski *et al.* 2003). Hence, it is widely used as a model organism. *C. glutamicum* belongs to a suborder *Corynebacterianeae* and is a close relative of human pathogens like *Mycobacterium tuberculosis, Mycobacterium laprae and Corynebacterium diphtheriae* (Donovan and Bramkamp 2014). The microcolony of *C. glutamicum* ATCC 13032, a model bacteria used in this thesis, is presented in Figure 4.

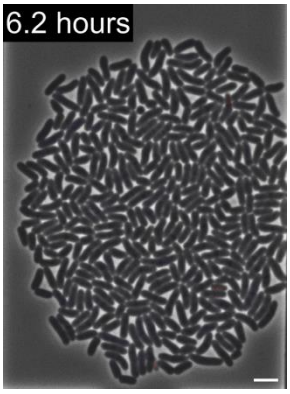

Figure 4. *C. glutamicum* ATCC 13032 microcolony grown in a MGC. BHI broth was used as a perfusion medium for culturing. Scale bar - 5 µm.

B. subtilis is a long, rod shaped, gram positive, heterotrophic, aerobic, non-pathogenic bacteria commonly found in soil. *B. subtilis* has an industrial importance, as it can produce enzymes like amylases and proteases in very high concentrations (g/L) (Kunst *et al.* 1997). It can produce more than two dozen antibiotics and antibiotic like compounds with wide variety of structures, which contribute to its morphology and physiology to survive in natural environment (Stein, Mikrobiologie, and Goethe- 2005). It also produces some fungicidal compounds, which are investigated as a control agent of fungal pathogens. It is used as a biocontrol agent for the control of diseases in plants and seeds (Ferreira, Matthee, and Thomas 1991). Complete genome of *B. subtilis* has been sequenced and it contains 4,214,810 base pairs (4.2 Mbp) and 4,100 protein coding genes. *B. subtilis* is a one of the best characterized gram positive bacteria (Kunst *et al.* 1997). In unfavorable conditions, *B. subtilis* vegetatively differentiates into cells with different morphologies. It can

produce long cell filaments, which are enclosed in a matrix secreted by the cells itself. Such structure is called biofilm. If the unfavorable conditions prevail, *B. subtilis* produces endospores. Endospores are resistant structures produced in response to the environmental changes for the survival in harsh conditions. Due to the unique characteristics of producing biofilm and endospores, *B. subtilis* is extensively used as a research subject (Piggot and Hilbert 2004). *B. subtilis* is related with *Bacillus anthracis*, which is a pathogenic bacterium for human. Spores of *B. anthracis* cause respiratory infections in human called anthrax. Microcolony of model bacteria *B. subtilis* 168 is presented in Figure 5.

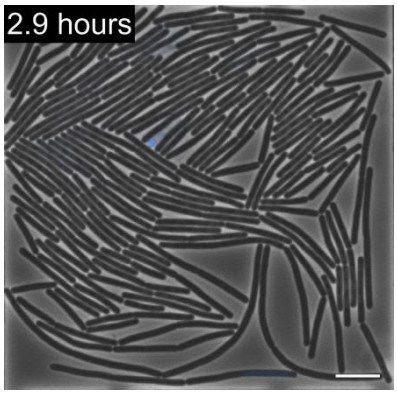

Figure 5. *B. subtilis* 168 microcolony grown in a MGC. BHI broth was used as a perfusion medium for culturing. Scale bar - 10 μm.

2. Technical state-of-the-art

As microfluidic methods can provide a wide range of information on bacterial antibiotic susceptibility, physiological and morphological changes, efforts are being made to develop an ideal assay with a microfluidics based susceptibility analysis. These methods are gaining huge attention of the scientific community as a rapid and accurate tool for AST. In recent years, several state-of-the-art microfluidic assays have been developed, which will be discussed in the following.

Choi *et al.* in 2013 have developed a rapid antimicrobial susceptibility test based on single-cell morphological analysis (SCMA). It is an automatic system for the analysis of morphological changes in bacterial cells under different antibiotic conditions. In this method, bacterial cells were mixed and immobilized in the microfluidic agarose channel (MAC). The chip has 96 wells. Medium containing antibiotic was loaded into well surrounded by microfluidic channels. An antibiotic diffuses through an opening present between the well and the channel. Immobilized cells were analyzed for morphological changes during antibiotic treatment with the help of time-lapse bright field microscopy. This method is rapid, easy and AST can be performed accurately. The method is described in Figure 6.

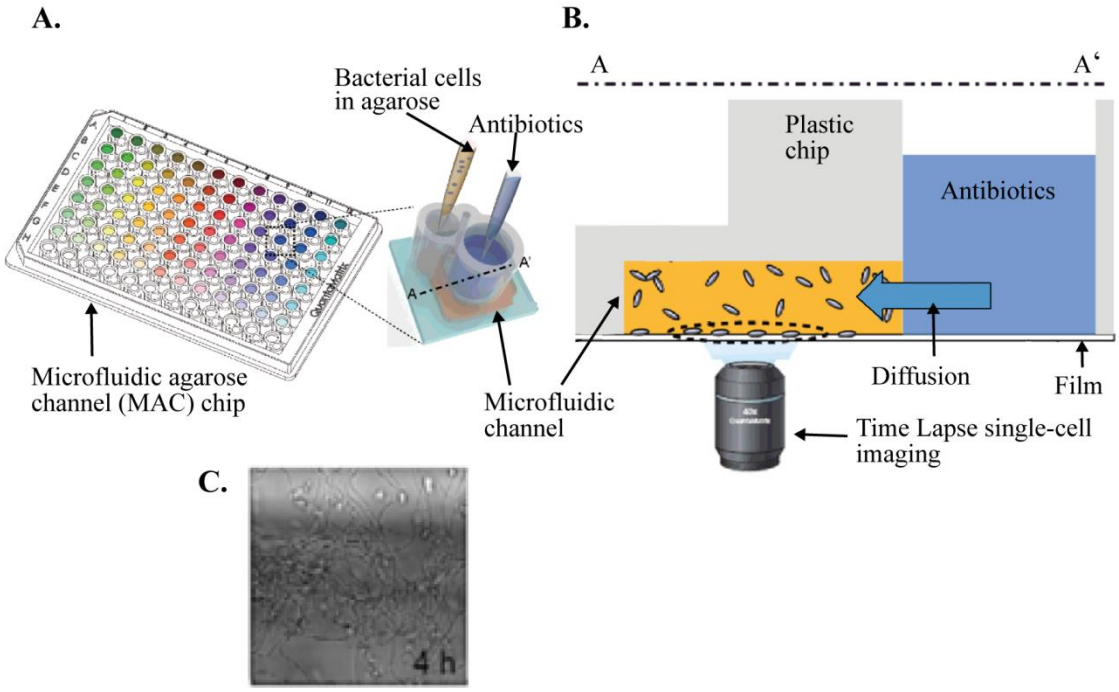

Figure 6. Single-cell morphological analysis (SCMA) for antimicrobial susceptibility testing. (A) 96 well chip with integrated microfluidic agarose channels. Individual microfluidic well with bacterial cells immobilized in agarose and antibiotics. (B) Imaging of immobilized cells under antibiotic treatment. Antibiotics diffuse into microfluidic channel in which cells are immobilized in agarose. Time lapse images were acquired for the cells present at the bottom of the channel agarose. Bacterial cell were counted automatically and change in cell number was used to generate the information about antibiotic susceptibility. (C) Time lapse single-cell image after 4 hour of antibiotic treatment (Choi *et al.* 2013).

In another study Hou *et al.*, developed a time lapse investigation method for antibiotic susceptibility testing using a microfluidic gradient 3D culture device in year 2014. This method was based on the microfluidic culture of bacteria in a linear concentration gradient of antibiotic and the investigation by time-lapse micrography. Bacterial cells were immobilized in the 3D microfluidic culture device with the help of low temperature melting agarose. Culture media with and without antibiotics were continuously introduced in the channels present on both side of an agarose channel, which creates a constant antibiotic concentration gradient. Time lapse images were used for the detection of antibiotic susceptibility on the basis of MIC. The method is presented in the following Figure *7*.

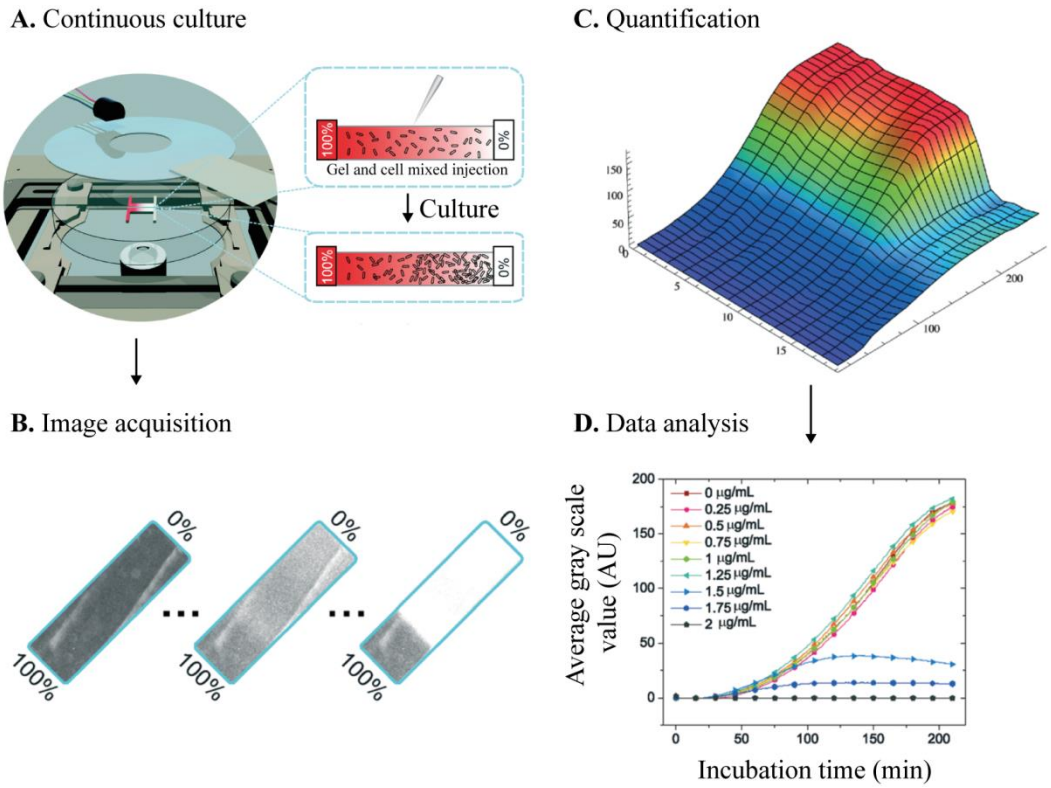

Figure 7. Schematic representation of the Microfluidic gradient 3D culture method. (A) continuous culture in a microfluidic gradient generator chip, placed on an inverted bright field microscope and time lapse images were captured. (B) Micrographs of 3D agarose channel. First micrograph represent background at the start of experiment, second is a lighter micrograph after some time of incubation and in third micrograph white part represent high cell concentreation. The gray part represent no bacterial growth. The intersection of white and grey part represent the MIC. (C) After processing the images, the images were quantified as a 2D optical intensity graphs against time and antibiotic concentration which indicates about the growth of bacteria in chip. (D) The quantified data will give temporal and concentration information of bacterial growth. The generated data can be used to determine MIC and to build a pharmacodynamics model (Hou *et al.* 2014).

Mohan *et al.* in 2015, develop a method to study the effect of bacterial interactions on antimicrobial susceptibility in polymicrobial cultures. It is an extension of the method developed by the same research group in 2013. This method is based on the fluorescence microscopy assisted determination of antibiotic suseptibility in a multiplex manner by using a two layered PDMS microfluidic device. The device can detect the polymicrobial interactions with different antibiotics in 12 combinations. The bacteria used in this study were genetically modified to express green and red fluorescent proteins (GFP and RFP). The method is illustrated in Figure 8.

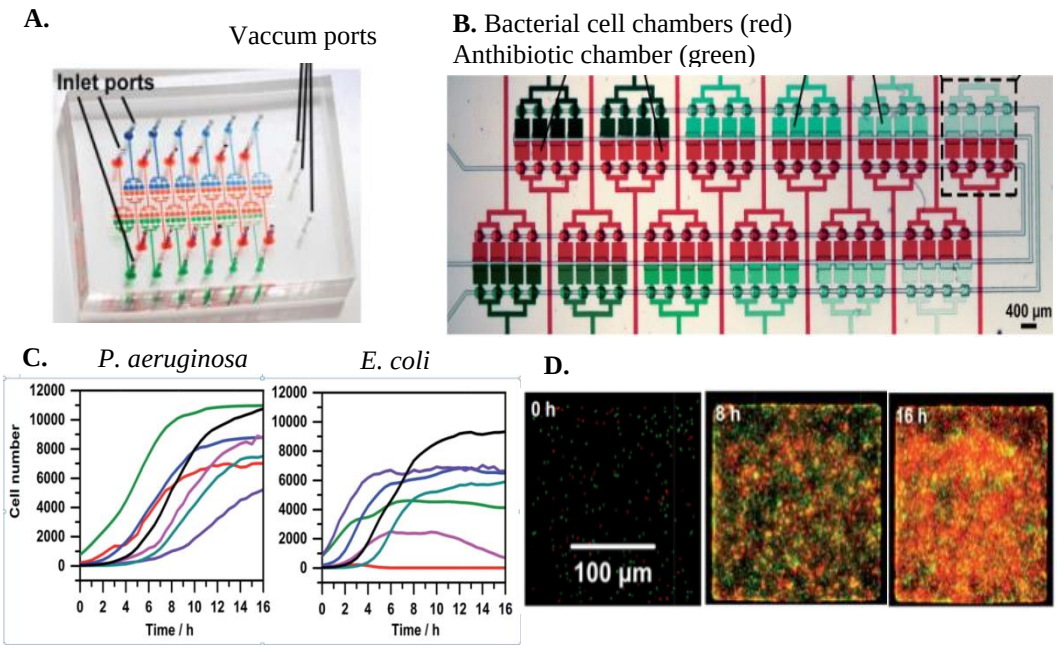

Figure 8. Microfluidic platform for polymicrobial interactions and antimicrobial susceptibility analysis. (A) Two layered PDMS microfluidic device, chambers are indicated with colored dyes. (B) Close-up of the 48 well array that is capable of testing 12 combinations of bacteria and antibiotics. (C) Cell numbers of two different bacteria growing in the microfluidic chambers are counted with ImageJ algorithm. Mean cell number of three experiment were used for analysis and to prepare the graphs which indicated about the interaction of one bacteria with other and also with antibiotic. (F) Time-lapse fluorescence images of two bacteria expressing GFP and RFP (Mohan *et al.* 2015).

The microfluidic method from Kalashnikov *et al.* is a rapid method for stress induced antibiotic susceptibility testing on the basis of time-lapse fluorescence microscopy. This method uses epoxy coated glass slide to immobilize bacterial cells. Thereafter, the glass slide with immobilized bacteria was clamped together with a PDMS device with 4 channels in a system indicated in figure 9. The assembly was placed on an inverted microscope and continuously flushed with the culture media containing antibiotics, fluorescent dye and stress inducing enzyme. Cell death was monitored by the fluorescent dye Sytox Green. Time-lapse images were used to quantify the percentage of bacterial death count to estimate the antibiotic susceptibility. The schematic description of the method is presented in Figure 9.

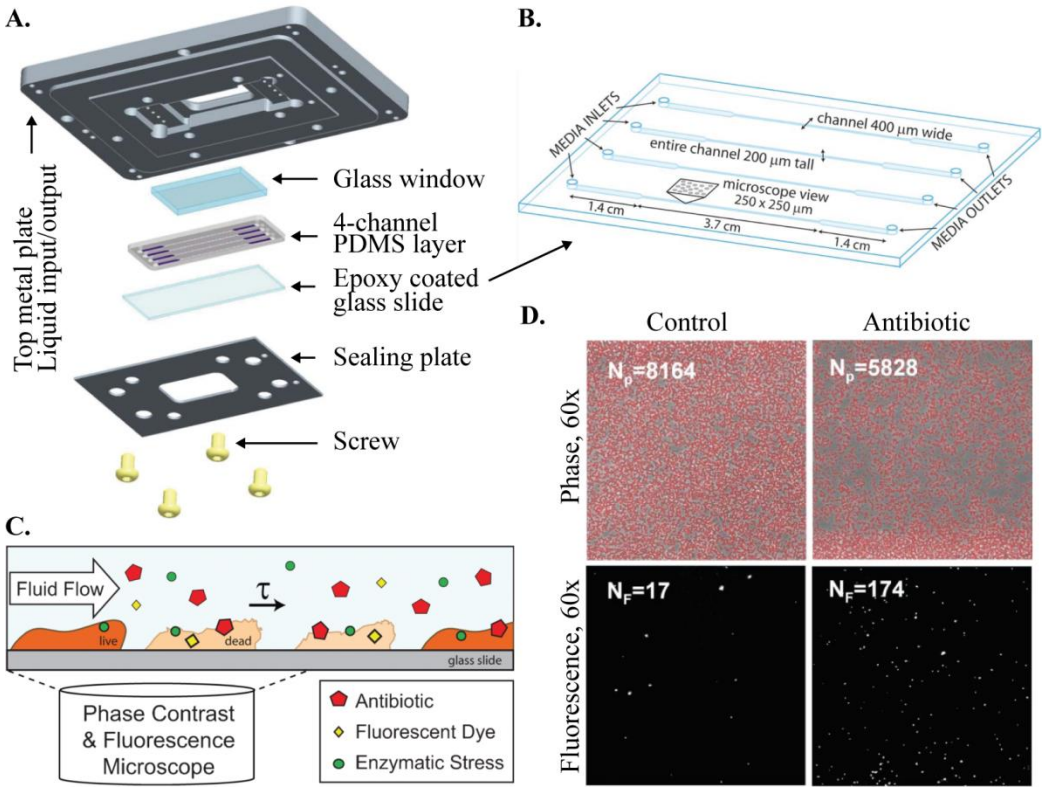

Figure 9. Microfluidic platform for rapid, stress induced antibiotic susceptibility testing. (A) Microfluidic chip assembly to clamp the bacterial cells, which were immobilized on the epoxy-coated glass slide. (B) Drawing of the microfluidic device indicating the dimensions. (C) Cross-sectional view of an individual channel illustrating the interaction of immobilized bacteria with antibiotics, fluorescent dye and stress inducing enzyme. (D) Time-lapse phase contrast and fluorescence images for the quantification of bacterial cell death (Kalashnikov *et al.* 2012).

In this thesis, a MSCA method was developed for an accurate determination of antibiotic susceptibility based on the high resolution time-lapse fluorescence microscopy. In addition to the antibiotic susceptibility, several important parameters like growth rate, phenotypic variations, viability, and metabolic activity can also be analyzed. As described earlier, this method relies on time-lapse fluorescence image based detection of bacterial responses to the antibiotic treatment. The bacterial cells are cultivated in a high-throughput PDMS-glass device. The culture medium mixed with fluorescent dyes and desired amount of antibiotics was continuously perfused into the cultivation channels. Single bacterial cells were introduced into hundreds of MGCs present in the cultivation channels. *C. glutamicum* and *B. subtilis* were used as model bacteria in this thesis. Different fluorescence staining strategies were carried out for each bacterium (Figure 11A-B). Calcein-AM and PI were used for *C.*

glutamicum which can differentiate the metabolically active cells from dead cells (Figure 11A). PI was used as a dead cell stain, which can enter the cell that have lost its cell wall integrity and intercalate with the DNA. PI incorporated in the DNA is highly fluorescent with bright red color. Calcein-AM is a non-fluorescence compound and can be hydrolyzed by the cellular esterase enzyme to fluorescent calcein and ethanol. Calcein fluorescence is the indication of the cellular metabolic activity.

The mechanism of the dynamic staining of metabolic activity in bacterial cells with calcein-AM includes different aspects of calcein-AM. When the calcein-AM mixed with the perfusion medium comes in contact with the viable cell, non-fluorescent calcein-AM diffuses into the cell. As soon as calcein-AM enters the cell, it is converted into fluorescent calcein and ethanol by the action of intracellular esterase. Fluorescent calcein is supposed to be actively transported out of the cell that was the focus in other studies. These studies suggested that cells which can grow normally, give calcein fluorescence that will reduce as the population of microcolony increases.

By the observations with conditions where bacteria grew and multiply, the division of bacterial cells caused the distribution of fluorescent calcein into two daughter cells. The division of cells and active efflux reduced the calcein signal from generation to generation (Figure 10). In such a situation, there was an equilibrium established between the process of diffusion of calcein-AM into the cell, conversion of calcein-AM to fluorescent calcein, efflux of calcein from the cell and the multiplication of cells. During this equilibrium condition the calcein signal did not increase and fluorescence signal reduced. If the equilibrium condition was disturbed, for example, due to the antibiotics, the alterations in the bacterial growth, enzymatic conversion, active efflux of fluorescent calcein occurred, which caused changes in the calcein fluorescence. By the interpretation of variations in calcein fluorescence, the changes in the metabolic activity due to antibiotic treatment could be analyzed. The schematic representation of the calcein fluorescence in the bacterial cell is presented in the Figure 10.

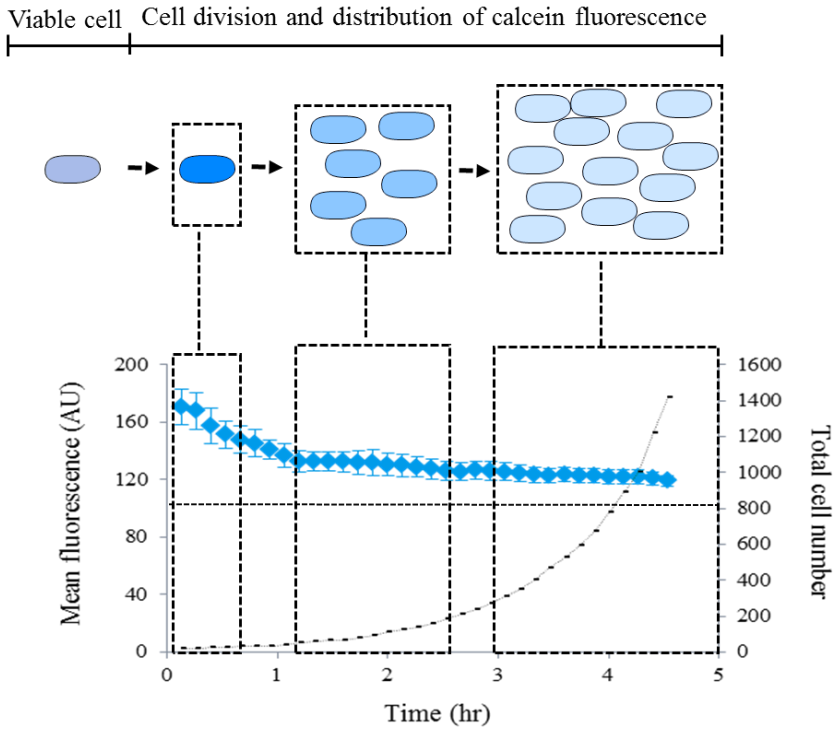

Figure 10. The mechanism of calcein-AM staining of *C. glutamicum*. The viable cell upon contact with calcein-AM, metabolize non-fluorescent dye into fluorescent calcein. The continuous multiplication of cells and active efflux of fluorescent calcein reduce fluorescence signals. Horizontal black line indicates the level of background calcein signal.

In case of *B. subtilis*, fluorescent dyes PO-PRO1 and PI were used. Viable cells maintain membrane potential between intra and extra cellular environment. PO-PRO1 is a dye that can enter the cells without membrane potential and intercalate with DNA to give fluorescence. The diagrammatic representation of the mechanism of online staining of *B. subtilis* cells is presented in Figure 11B. During the dynamic staining process, as metabolically active and dead cells of *C. glutamicum* can occur simultaneously, similarly, the physiological state of cells without membrane potential and dead cells can occur both together and solely. The time-lapse fluorescence images were generated for qualitative and quantitative analysis of bacterial physiology under antibiotic treatment.

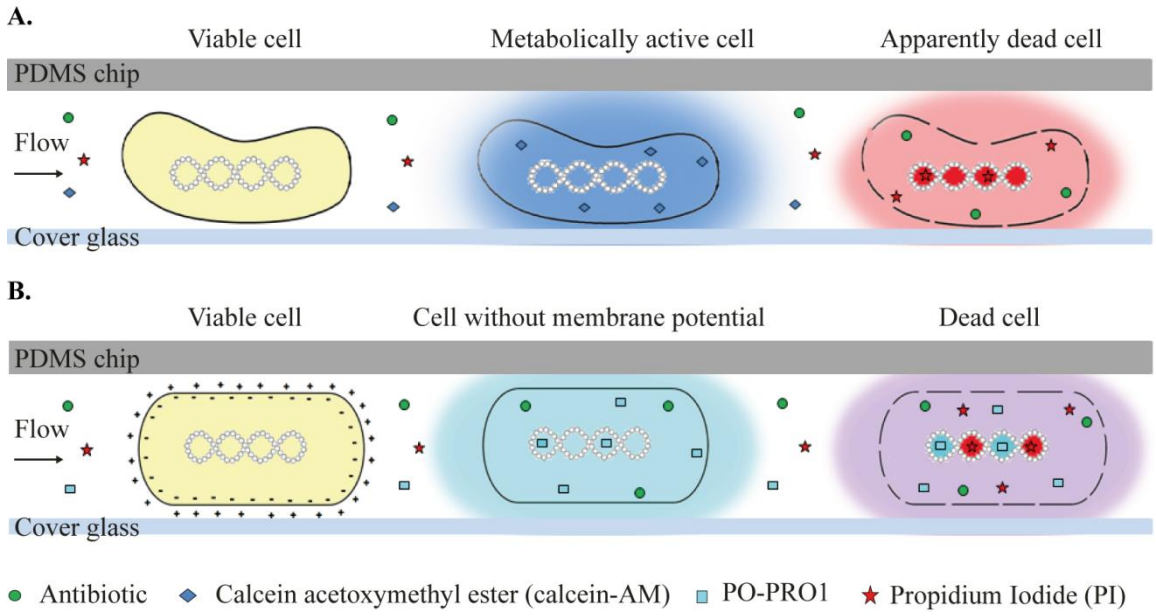

Figure 11. The microfluidic single-cell analysis (MSCA) method for antibiotic susceptibility testing presented in this thesis. (A) Online fluorescence staining of *C. glutamicum* with calcein-AM and PI. Viable cell is shown just before the start of an experiment. The metabolically active cells convert calcein-AM to fluorescent calcein and the cells which have lost their cell wall integrity due to the effect of antibiotics were stained by PI. (B) Online fluorescence staining of *B. subtilis* with PO-PRO1 and PI. Viable cell is shown just before the start and during an experiment. Due to the effect of antibiotics, the cells without membrane potential were stained by PO-PRO1 and disintegrated cells were stained by PO-PRO1 and PI.

3. Materials and methods

3.1. Bacterial strains

For this study, the wild type strain of *Corynebacterium glutamicum* ATCC 13032 and wild type strain of *Bacillus subtilis* 168 were used. The bacterial strains were stored at −80 °C in cryo culture. For *C. glutamicum*, Roti®-store Cryo-vials were used to produce the pre-culture and main-culture. For *B. subtilis*, bacterial culture stored in glycerin was used to produce pre-culture and main-culture. For culturing bacteria, brain heart infusion (BHI) medium from Becton-Dickinson and company was used in all the experiments.

3.2. Fluorescent dyes

Fluorescent dyes were used as the marker for physiological changes occurring under different antibiotic treatments. Propidium Iodide (PI – excitation/emission maximum ~535/617 nm) from Carl Roth was used to stain dead cells. Calcein acetoxymethyl ester (calcein-AM – excitation/emission maximum ~400/452 nm) from Life technologies for the live cells staining was used for *C. glutamicum*. PO-PRO1 (excitation/emission maximum ~435/455 nm) from Life technologies was used as counter stain for *B. subtilis*.

3.3. Antibiotics

Antibiotics with different modes of action were chosen for the experiments. The antibiotics used for the experiments are as follows:

S. no.	Name	Subclass	Nature	Action
1.	Ampicillin (AMP)	Beta-Lactams	Bactericidal	Cell wall synthesis inhibitor
2.	Chloramphenicol (CHL)	Phenethylamines	Bacteriostatic	Protein synthesis (50S) inhibitor
3.	Kanamycin (KAN)	Amino sugars	Bactericidal	Protein synthesis (30S) inhibitor
4.	Streptomycin (STR)	Amino sugars	Bactericidal	Protein synthesis (30S) inhibitor
5.	Mitomycin C (MMC)	Indolequinones	Antineoplastic	DNA synthesis inhibitor

Table 1. Antibiotics used in the experiments with *C. glutamicum* and *B. subtilis*

3.4. Bacterial culture and growth conditions

Pre-culture for *C. glutamicum* was prepared by inoculating one pearl from Roti®-store Cryo-vials in 20 mL of BHI broth and incubated overnight at 30 °C and 120 rpm. For *B. subtilis*, a loop full (10 µL) of the frozen culture was inoculated in BHI broth and incubated overnight at 37°C and 150 rpm. The main-culture was prepared by pipetting bacterial suspension from the pre-culture, so that the optical density (OD_{600}) of the start culture was 0.1 and incubated at particular temperature for about 2 – 3 hrs, till the bacteria were in early exponential phase.

S.no.	Bacteria	Temperature (^{o}C)	RPM
1.	*C. glutamicum*	30	120
2.	*B. subtilis*	37	150

Table 2. Culturing conditions for *C. glutamicum* and *B. subtilis*

3.5. Analytical methods

In this thesis, two analytical methods were performed and compared *i.e.* agar plate method and MSCA method. MMC is a temperature sensitive antibiotic and half-life at 37 ^{o}C is around 8-48 min (www.drugbank.ca/drugs/DB00305). Due to the temperature sensitivity of MMC,

shake flask method was used instead of agar plate method. Both analytical methods are described in the following.

3.5.1. Agar plate method

3.5.1.1. Pre-experimental preparations

Agar plates with antibiotics were prepared using BHI media and agar-agar. 1 liter medium was prepared by adding 37 g of BHI powdered ingredient and 1.5 % agar-agar as a solidifying agent in 1 liter of Millipore water. The medium was mixed and autoclaved. The media was allowed cooled to ~ 40 °C and specific antibiotic was added according to the desired concentration, mixed thoroughly and poured in Petri-plates under the clean bench.

McFarland standards were used as a reference to adjust the turbidity of bacterial suspensions, so that the number of bacteria per mL will be in a given range. McFarland standard of value 0.5 was prepared by mixing 0.05 mL of 1.175 % Barium chloride dihydrate ($BaCl_2.2H_2O$) and 9.95 mL of 1 % Sulfuric acid (H_2SO_4). This 0.5 McFarland standard was used as a reference to adjust the turbidity of bacterial suspension in NaCl which was equivalent to 1 x 10^8 CFU/mL. A schematic diagram for the experimental set-up for all antibiotics except MMC is presented in Figure 12. The set-up for the experiment with MMC is presented in experimental procedure section.

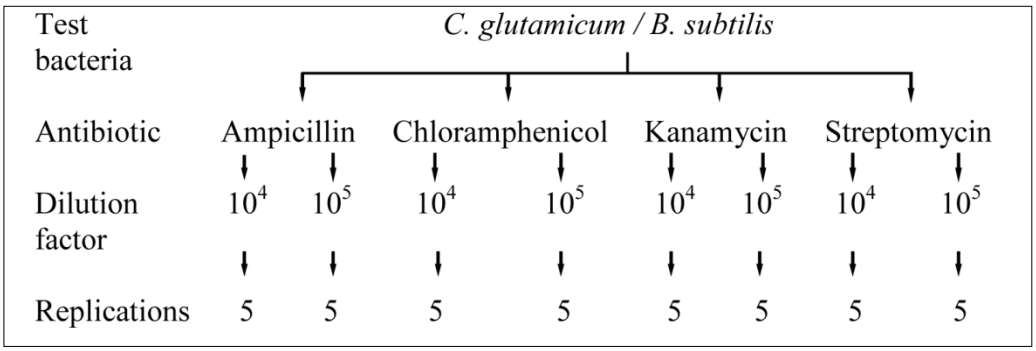

Figure 12. A schematic representation for the experiment carried out using agar plate method for *C. glutamicum* and *B. subtilis*.

3.5.1.2. Experimental procedure

Bacterial suspension was prepared in 0.9 % NaCl from main-culture (OD_{600} 0.1 – 0.2). Bacterial suspension was standardized with 0.5 McFarland standards using a spectrophotometer. A serial dilution row was prepared by adding 1 mL standardized bacterial suspension into 9 mL of 0.9 % NaCl (Figure 13A). Bacterial suspensions (100 µL) of dilution factor 10^4 and 10^5 were taken to plate on the antibiotic agar plates. The suspension was carefully spread on the agar surface with the help of a Drigalski spatula. Reference plates without antibiotics were prepared in parallel for comparison. An experiment was performed with five replicates (Figure 13B). Agar plates were labeled and incubated in upside down position for 24 hours in an incubator at specific temperature according to bacteria. Observations were taken after 24 hours and number of colonies appeared on the agar plates were counted.

In case of MMC, a shaking flask method was used (Figure 13C). A bacterial suspension was prepared in BHI and standardized with 0.5 McFarland standards to contain approximately 1 x 10^8 CFU/mL. The standardized suspension was then dispensed into separate flask to have same starting $OD_{600.}$ The addition of MMC was carried out according to the scheme as shown in Figure 13. Spectrophotometric observations were taken every 30 min to see the change in OD_{600} during the shaking flask experiment. The procedure is described in the following scheme.

A.

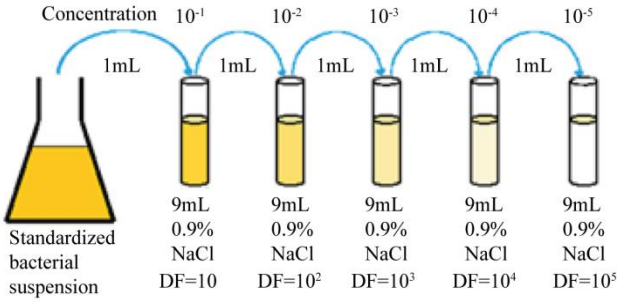

B.

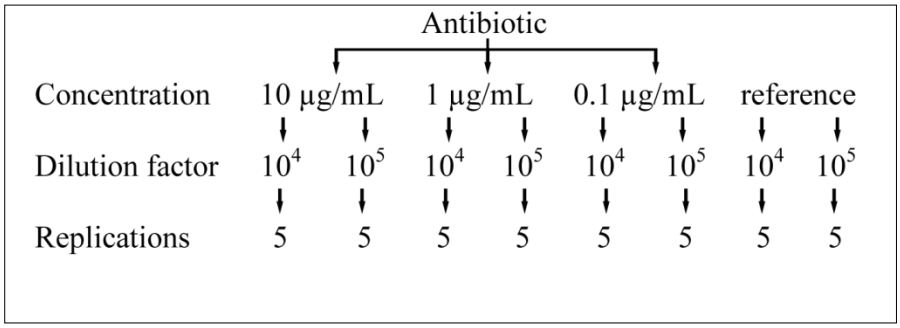

C.

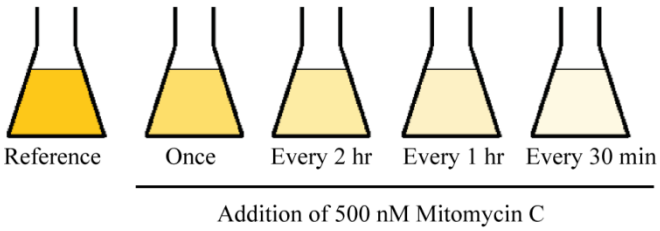

Figure 13. A schematic representation of the experimental procedure. (A) Dilution series was prepared by diluting 1 mL of standardized bacterial suspension with 9 mL of 0.9 % NaCl. Dilution series was prepared up to the dilution factor (DF) of 10^5. Suspension of dilution factor of 10^5 contained a concentration of approximately10^{-5} bacteria per mL. (B) Experimental setup for the agar plate test. Agar plates with a concentration of 10 µg/mL, 1 µg/mL and 0.1 µg/mL were prepared with specific antibiotics. (C) Schematic representation of shaking flask method with MMC.

3.5.1.3. Data analysis

Number of CFUs was used to calculate the CFU/mL in bacterial suspension with the help of following equation,

$$x = \frac{\text{number of colonies on agar plates} \times \text{dilution factor of bacterial suspension}}{\text{volume of suspension used}}$$

Where, x is the viable cell count = CFU/mL. Plotting CFU/mL against concentration of antibiotic gave the information about antibiotic susceptibility of bacteria. Normalized CFU/mL values were used to calculate percentage of the dose response of bacteria against particular antibiotics. Dose response is the inverse of normalized CFU/mL values at a particular antibiotic concentration.

3.5.2. Microfluidic single-cell analysis

3.5.2.1. Pre-experimental preparations

Photolithographic SU8 based silicon wafer with desired microchamber design was used for the preparation of the Poly(dimethyl)siloxane (PDMS) based microfluidic device (Gruenberger *et al*. 2013). For molding PDMS chips, the silicon wafer was kept in a large Petri plate and a degassed mixture of PDMS base and curing agent (10:1) was poured on the wafer under a laminar air flow. The PDMS mixture was polymerized at 80 ^{o}C for 3 hours in a convection oven. The baked PDMS slab was carefully cutted out from Petri plate using a sharp scalpel and individual chips were separated. Chemical treatment was carried out to remove un-polymerized monomers and dimers from PDMS chips. One washing step with n-pentane and two washing steps with acetone were carried out for 90 min each, and these chemically treated chips were dried overnight. Dried chips were stored and used as needed. Before the start of an experiment, chips were selected according to the desired microstructure design (High through-put device - HT3 for *C. glutamicum* and HT2 for *B. subtilis*) for the experiment. Inlet and outlet holes were punched with the help of a punching device under a microscope. The chip was then given multiply washes of Isopropanol and deionized water, to remove dust and PDMS particles. Nitrogen gun was used to dry the chip and adhesive tape to remove any traces of

dust and PDMS particles. Similarly, 170 µm thick glass slide (29.5 x 24.5 mm) was also cleaned. Surface oxygen plasma activation of PDMS device and glass slide was carried out in a pre-warmed (2000-3000 sec.) plasma chamber (Power = 50 W, time = 25 sec. and oxygen flow rate = 20 sccm) to bond them together. To ensure the strength of bonding, the assembly was kept at 80 °C in a convection oven for 10 sec. At the vicinity of the microscope, bonded chip was connected with the needles (inner diameter 0.2 mm – from Nordsen EFD) to connect the tubes (inner diameter 0.25 mm - from Tygon) for delivering perfusion medium (Figure 14).

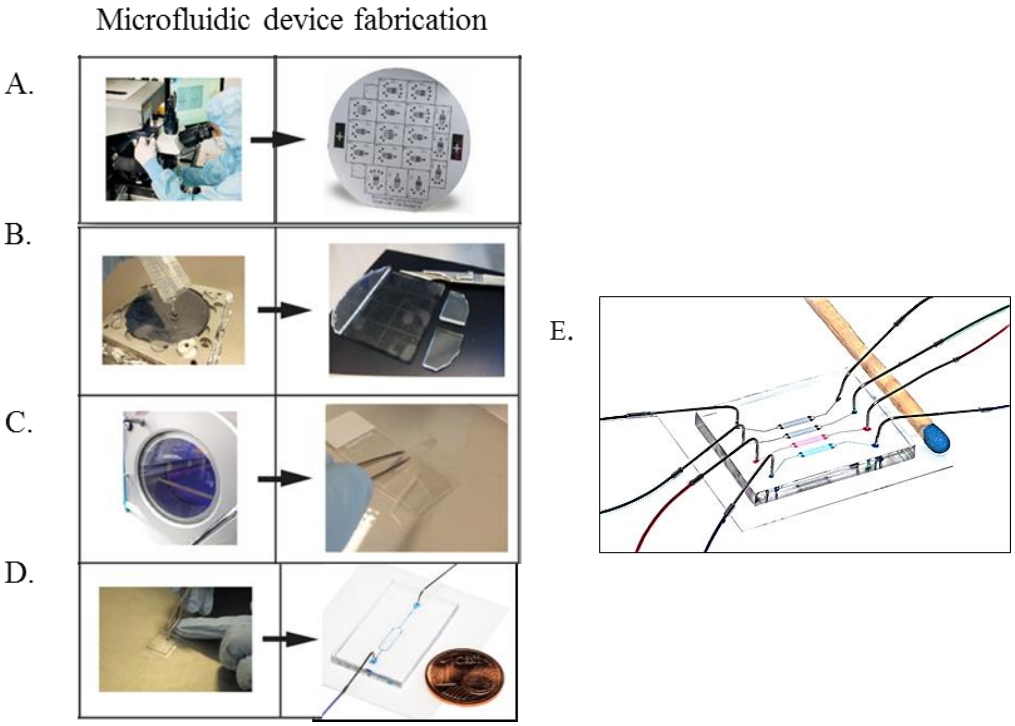

Figure 14. An overview for the steps involved in the fabrication of microfluidic device. (A) Production of the photolithographic SU8 based silicon wafer with engraved microfluidic structures. (B) Molding of PDMS device over silicon wafer and PDMS slap after baking in oven to cut individual device. (C) Surface activation in plasma chamber and bonding of PDMS device with glass slide. (D) Connecting needles and tubes with the device. (E) An illustration of ready to use microfluidic device, cultivation channels are indicated in colored ink.

3.5.2.2. Experimental procedure

Experiments were designed according to the test bacteria and the concentration of candidate antibiotic. Separate experiments were performed for *C. glutamicum* and *B. subtilis* with antibiotic concentrations at 10 µg/mL, 1 µg/mL and 0.1 µg/mL along with reference (without antibiotics). Perfusion

media contains BHI broth added with fluorescent dyes and antibiotics. Fluorescent dyes were selected according to test bacteria as described earlier. A scheme is presented in Figure 15, to describe the experimental procedure.

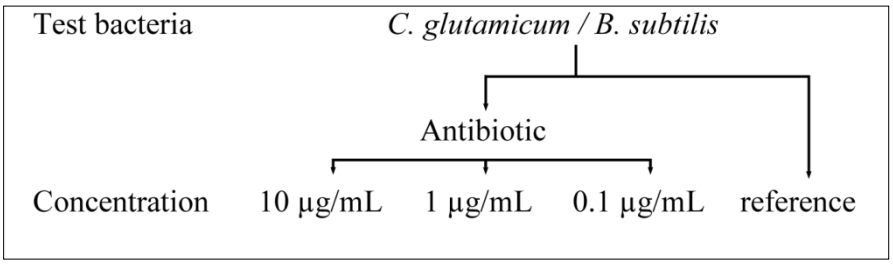

Figure 15. A schematic representation of the experimental procedure of MSCA for *C. glutamicum* and *B. subtilis* with AMP, CHL, KAN and STR in four different concentrations *i.e.* 10 µg/mL, 1 µg/mL, 0.1 µg/mL and reference. In Case of MMC, the concentrations at 50 nM, 500 nM and 1000 nM were used.

Before installing the microfluidic device on an inverted microscope (Nikon Eclipse Ti), the incubator was pre-warmed for 2 hours to prevent fluctuations in temperature. A fiber-glass incubator around the microscope stage maintained the temperature constant to the required optimum temperature for bacterial growth. The ready-to-use microfluidic device without tubes was fixed on the microscope objective with the help of inhouse designed chip holders. The microfluidic device was flushed with perfusion media to clean the cultivation channels. Bacterial suspension from the main-culture was prepared at optical OD_{600} ~0.2. Bacteria were hydro-dynamically trapped in MGCs with the help of 1 mL syringe. Approximately, 15 - 20 chambers/channel (60 – 80 chambers/chip) were selected and marked in the Nikon software component for time lapse imaging. The syringes with perfusion media were fixed on a software controlled syringe pump (neMESYS – Centoni GmbH), which perfused culture media continuously at a flow rate of 300 nL/min. The time lapse images were captured at an interval of 8 min for *C. glutamicum* and 5 min for *B. subtilis*. An experiment run time was up to 8-12 hrs, depending on the growth rate of the bacteria (for *C. glutamicum* 12 hrs and for *B. subtilis* 7.5 hrs). A photographic representation of the experimental setup is presented in Figure 16.

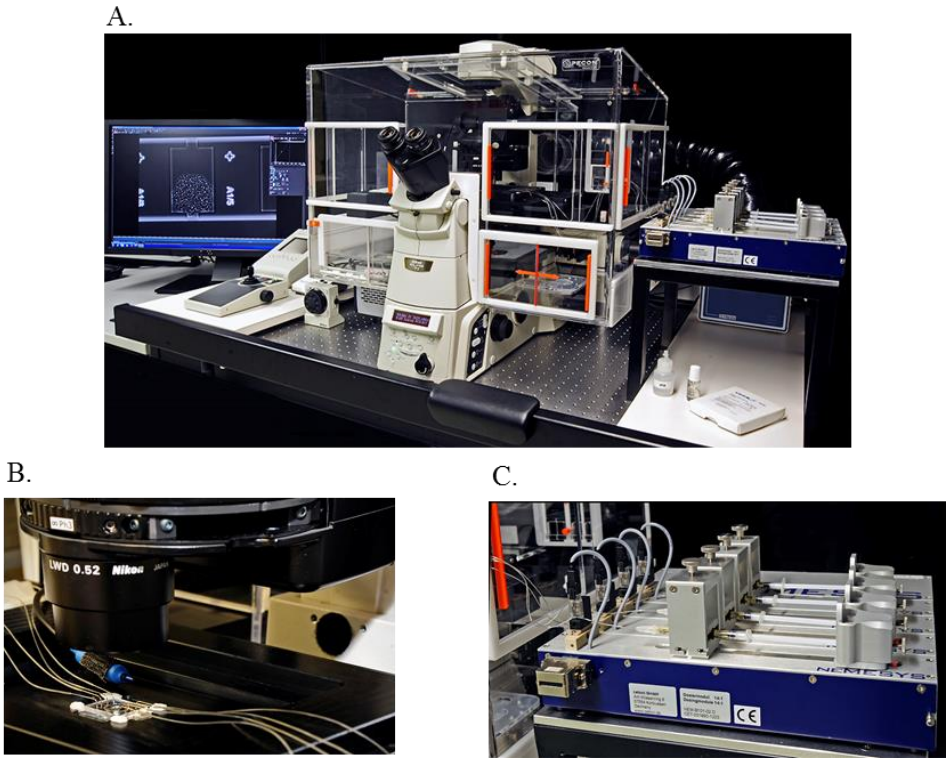

Figure 16. Experimental setup for MSCA. (A) Fully automated inverted Nikon Eclipse Ti microscope, surrounded by incubator. Computer system with NIS element software and microscopic stage controls (left) and neMESYS syringe pump (B) Microfluidic device installed on inverted microscope, connected with inlet and outlet tubes. Outlets were connected with Eppendorf tubes to collect flushed media. (C) Syringe pump with installed 1 mL syringes containing perfusion medium.

3.5.2.3. Data analysis

Out of 20 imaged chambers for each concentration of antibiotics, five chambers were analyzed in detail. Time lapse fluorescence images from individual MGC were processed by ImageJ/Fiji software (http://fiji.sc/Fiji). Preprocessing and segmentation was automatically done by ImageJ/Fiji with inhouse developed plugins to extract the data concerning cell number, projected length, projected area and fluorescence (Helfrich 2012). Cell number was used to calculate the maximum growth rate per hour (μ_{max}) using the equation,

$$\mu = \frac{ln(n2) - ln(n1)}{t2 - t1}$$

Where, $n_1 > 50$. In Microsoft Excel, mean fluorescence data was plotted against time to see the change in fluorescence of cells during the antibiotic treatment. Linage trees were prepared with ImageJ/Fiji and in-house developed software

Vizardous (Helfrich *et al.* 2015) was used to extract the single-cell fluorescence information. Single-cell fluorescence data was plotted against time to see the change in fluorescence of individual cell of a microcolony during the treatment.

4. Results and discussion

In this chapter, the results from all the experiments are presented and discussed. In section 4.1 antibiotic susceptibility assays carried out using agar plate method and MSCA method is presented and compared. The phenotypical changes of *C. glutamicum* and *B. subtilis* due to the effect of antibiotics are presented in section 4.2. In section 4.3 analysis based on the mean fluorescence of five microcolonies are presented for the respective experiments followed by section 4.4 which illustrates the single-cell fluorescence analysis of individual bacterial cells present in a single microcolony. In section 4.5 results from the regrowth experiments of *C. glutamicum* are presented and discussed thereafter.

4.1. Antibiotic susceptibility assay

Increase in cell number is the indicator for growth of bacteria under a specific condition. Commonly used viable count agar plate method is based on observing bacterial growth according to bacterial colonies also knows as colony forming units (CFU), formed on agar plate surface. However, CFU is only an estimate of bacterial cells present in a unit volume (per mL) of bacterial suspension. The limitation of this method is the relatively narrow countable range (25-250) of CFU on agar plate, which can cause large degree of variation in the data (Sutton 2011). Due to variations involved in the results of agar plate method, in recent years, it is less preferred as an antibiotic susceptibility assay. In such case, microfluidic single-cell analysis is very advantageous, as it provides information about bacterial growth and morphology on single-cell level with spatio-temporal resolution. In this chapter, the growth of *C. glutamicum* and *B. subtilis* was observed and growth rates in different antibiotic concentrations were calculated using agar plate and MSCA method. The results from different experiments are presented and compared in the discussion.

4.1.1. Antibiotic susceptibility assay for *C. glutamicum*

4.1.1.1. Agar plate method

C. glutamicum was grown on agar plates with different concentrations of antibiotics and number of CFUs on agar plates was used to calculate viable cell count (CFU/mL) (Figure 17A). Out of five replicates prepared, three were taken for the CFU/mL analysis. Normalized viable cell count was used to calculated percentage dose response of *C. glutamicum* for specific dose of antibiotics (Figure 17B). The reference agar plates were also prepared in parallel to the antibiotic plates, and the results from all the individual references were comparable.

AMP is a bactericidal antibiotic which kills bacteria. If AMP at a concentration of 0.1 µg/mL and 1 µg/mL was used, viable cell counts on agar plates were 6.3 x 10^6 CFU/mL and 5.7 x 10^6 CFU/mL and dose responses were 17 % and 25 %, respectively. No growth was observed if AMP was used at a concentration of 10 µg/mL. As described in the introduction, MIC is a concentration at which no visible growth of bacteria was observed (Figure 17A-B). Hence, it can be estimated that the MIC of AMP for *C. glutamicum* wild type ranges between a concentration of 1 µg/mL AMP and 10 µg/mL AMP.

CHL is a bacteriostatic antibiotic which suppresses the bacterial growth. CHL at a concentration of 10 µg/mL was lethal. The viable cell counts with CHL at a concentration of 0.1 µg/mL and 1 µg/mL were 6.0 x 10^6 CFU/mL and 5.3 x 10^6 CFU/mL and the corresponding dose responses were 10 % and 21 % (Figure 17A-B). The interpretation of results showed that MIC was between 1 µg/mL CHL and 10 µg/mL CHL.

If *C. glutamicum* was grown with KAN at a concentration of 1 µg/mL and 10 µg/mL, respectively, no visible growth was observed on agar plates. Viable cell count and dose response were 5.9 x 10^6 CFU/mL and 14 %, respectively, if KAN was used at a concentration of 0.1 µg/mL. KAN is a bactericidal antibiotic and was lethal at a concentration of 1 µg/mL and higher.

Similarly, STR is also a bactericidal antibiotic and was lethal for *C. glutamicum* at a concentration of 1 µg/mL and higher in this experiment. If STR was used at a concentration of 0.1 µg/mL, the viable cell count and dose response were 7.9 x 10^6 CFU/mL and 12 %, respectively (Figure 17A-B). A concentration of 1µg/mL and higher for both KAN and STR was lethal. Thus, it can be estimated that the MIC of both KAN and STR for *C. glutamicum* lies between a concentration of 0.1 µg/mL and 1 µg/mL.

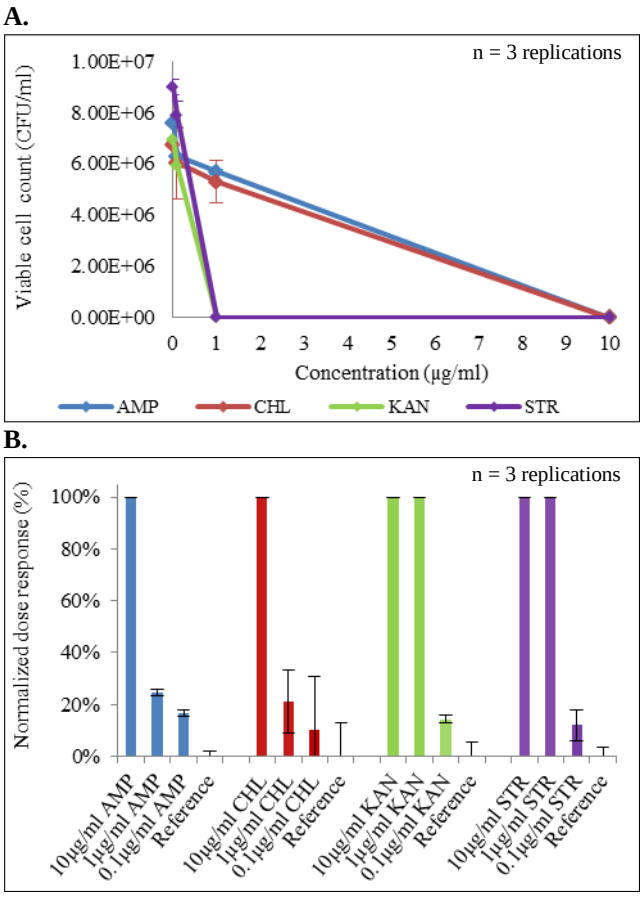

Figure 17. Results for the antibiotic susceptibility assay for *C. glutamicum* using agar plate method (A) Viable cell count (CFU/mL) for different concentrations of antibiotics, (B) Corresponding dose response normalized to reference for *C. glutamicum* at different concentrations of antibiotics. Error bars represent standard deviation of three replications.

MMC is sensitive to decay by temperature which doesn't allow the preparation of agar plates with desired concentrations. Due to the temperature sensitivity of MMC, shaking flask method was used. MMC at a concentration of 500 nM (167.17 pg/mL) was added at different time points (Figure 18A-B) and optical density at 600 nm (OD_{600}) was measured to calculate growth rate per hour. Growth rate per hour normalized to reference was then used to calculate

percentage of dose response. The growth rate for reference was 0.9 hr^{-1}. Dose response for all the combinations were found comparable for initial three time points and little differences were observed in the further time points, which might be due to the nutrient depletion. Furthermore, a slight decline in the growth rate was observed for the shaking flasks in which MMC was added. Hence, *C. glutamicum* was found less sensitive at different concentrations of MMC in shaking flask experiment.

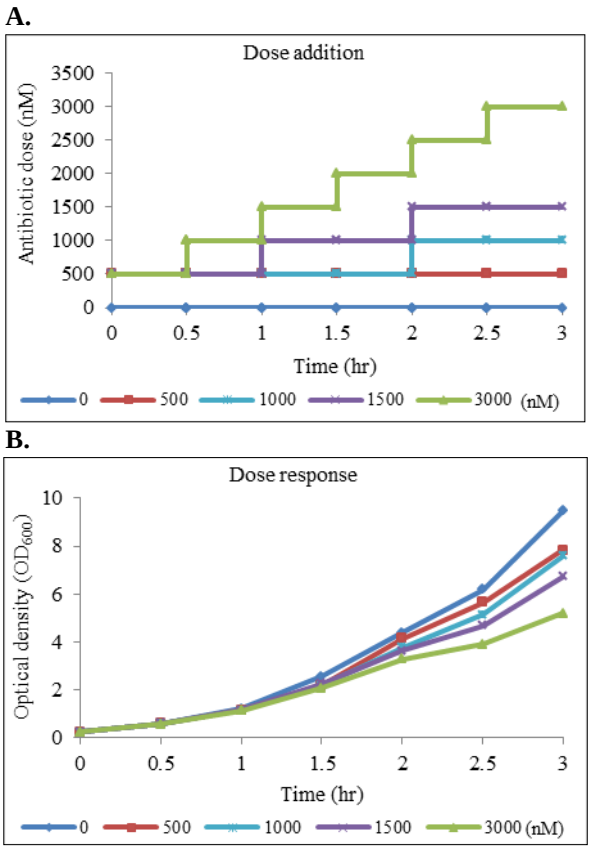

Figure 18. Results for the antibiotic susceptibility assay for *C. glutamicum* with MMC. (A) Addition of MMC at a concentration of 500 nM at different time points. (B) Changes in OD_{600} for different amount of MMC added. The change in OD_{600} represents the response of *C. glutamicum* against an added dose.

4.1.1.2. Microfluidic single-cell analysis method

C. glutamicum was cultivated in PDMS-glass microfluidic device under four different conditions. Time lapse images were used to count the number of cells. Total cell number from five micro-chambers was used to calculate maximum growth rate per hour (μ_{max}). Growth rate normalized to reference was

used to calculate the percentage dose response at different antibiotic concentrations (Figure 19A-C). The average growth rates for all the reference channels were found to be $\bar{\mu} = 0.93 \pm 0.66\ hr^{-1}$, where n = 5. A slight difference in the growth rates might be due to the microbial heterogeneity. Growth rate based on cell number depends on the growth rate of individual single-cells and might differ from the averaged population based growth rates (Dusny *et al.* 2015).

In single-cell analysis, if AMP was used with *C. glutamicum* at a concentration of 0.1 µg/mL, growth rate and dose response were 0.81 hr^{-1} and 13.6 %, respectively. As striking difference to the agar plate method, AMP was lethal at a concentration of 1 µg/mL and higher. Thus, MIC can be expected between a concentration of 0.1 µg/mL AMP and 1 µg/mL AMP. In an experiment with bacteriostatic antibiotic, CHL at a concentration of 10 µg/mL was lethal. CHL at a concentration of 1 µg/mL resulted in a growth rate of 0.59 hr^{-1} and a dose response of 36.4 %. If *C. glutamicum* was grown at a concentration of 0.1 µg/mL CHL, the growth showed minor impact by the antibiotic. The growth rate was found to be 0.85 hr^{-1} and the dose response was 7.7 %. Hence, the estimated MIC may lie between a concentration of 1 µg/mL CHL and 10 µg/mL CHL. KAN and STR are bactericidal and have a similar mode of action. If *C. glutamicum* was grown with KAN and STR at a concentration of 10 µg/mL and 1 µg/mL, no growth was observed. If KAN was used at a concentration of 0.1 µg/mL, the growth rate was 0.8 hr^{-1} and dose response was 7.6 %. In contrast to KAN, if STR was used at a concentration of 0.1 µg/mL, the growth rate was found comparable to the reference with undisturbed growth. Although, KAN and STR have the same mode of action, *C. glutamicum* react differently to the treatments. The MIC for both the antibiotics KAN and STR was estimated between a concentration of 1 µg/mL and 10 µg/mL (Figure 19 A).

In single-cell analysis, temperature sensitivity and decay due to light exposure of MMC can be neglected, due to the possibility of mixing it in the perfusion media that is kept at room temperature until it entered the incubator on its way through the microstructures. MMC was tested against *C. glutamicum* in the microfluidic cultivation device at three different concentrations

(Figure 19B). These were 1000 nM (334.33 pg/mL), 500 nM (167.16 pg/mL) and 50 nM (16.716 pg/mL) along with the reference. The growth rates at a concentration of 1000 nM and 500 nM were 0.7 $hr^{-1}$and 0.6 hr^{-1} and corresponding dose responses were 20.5 % and 27.6 %, respectively. MMC at a concentration of 50nM had no significant effect on *C. glutamicum* and its growth rate was comparable to reference. *C. glutamicum* was observed to have less effect on the growth rate due to MMC treatment. Therefore, the MIC for MMC against *C. glutamicum* is expected to be higher than 1000 nM in BHI media.

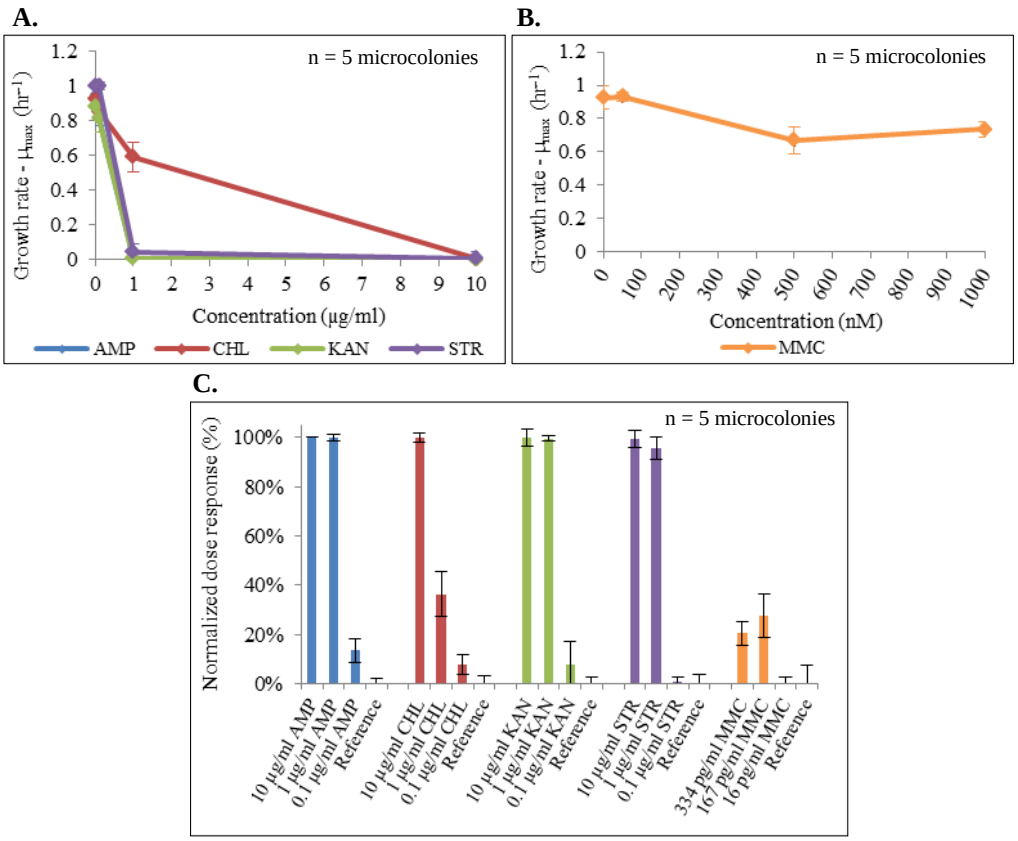

Figure 19. Results for the antibiotic susceptibility assay for *C. glutamicum* using single-cell analysis. (A) Growth rate per hour (μ_{max}) for different concentrations of AMP, CHL KAN and STR, (B) Growth rate per hour (μ_{max}) for different concentrations of MMC. (C) Corresponding dose response normalized to reference for *C. glutamicum* at different concentrations of antibiotics. Error bars represent standard deviation of five microcolonies.

B. subtilis is a fast growing bacteria and commonly used as a model organism for many microbiological studies. *B. subtilis* exhibits a characteristic behavior which includes rapid cell division, natural heterogeneity, autolysis and many more. To study its physiology in detail, high resolution spatio-temporal data is required. Unfortunately, limitations of the agar plate method do not

provide an opportunity to study its physiology in detail. Hence, single-cell analysis method is a very strong tool to analyze different aspects of *B. subtilis* physiology. Similar to *C. glutamicum* antibiotic susceptibility assay was performed for *B. subtilis* which is presented and discussed in the following.

4.1.2. Antibiotic susceptibility assay for *B. subtilis*

Agar plates with different concentrations of antibiotics were used to cultivate *B. subtilis* and viable cell count (CFU/mL) was calculated. The percentage dose response was calculated using the viable cell count normalized to the reference. The viable cell count of all the reference experiments with *B. subtilis* was comparable (Figure 20A-B).

4.1.2.1. Agar plate method

If AMP was used for *B. subtilis* in agar plate method, no growth was observed when AMP at a concentration of 10µg/mL and 1µg/mL was used. Furthermore, if AMP at a concentration of 0.1µg/mL was used, the viable cell count was 1.7 x 10^7 CFU/mL and dose response was 24.9 %. Hence, expected MIC may lie in the range of AMP at a concentration of 1µg/mL and 10µg/mL. CHL at a concentration of 10 µg/mL was lethal for *B. subtilis*. If *B. subtilis* was grown on agar plates with CHL at a concentration of 1µg/mL and 0.1µg/mL, viable cell counts were 2.0 x 10^7 CFU/mL and 2.2 x 10^7 CFU/mL and dose responses were 3.9 % and 12.6 %, respectively. Thus, MIC can be estimated between the range of 1 µg/mL and 10 µg/mL (Figure 20).

By using agar plate method, KAN at a concentration of 0.1µg/mL resulted in a viable cell count of 2.0 x 10^7 CFU/mL and a dose response of 12.8 %. Dose response was 100 % (no growth), if KAN at a concentration of 1µg/mL and higher was used. If *B. subtilis* was grown with STR at a concentration of 0.1µg/mL and 1µg/mL, respectively, viable cell counts were 2.0 x 10^7 CFU/mL and 1.8 x 10^7 CFU/mL and dose responses were 4.0 % and 14.4 %, respectively. STR at a concentration of 10µg/mL was lethal. Although, KAN and STR have same mode of action and both are bactericidal, *B. subtilis* responded differently to the respective treatments. It was found that *B. subtilis* is less susceptible for STR as compared to KAN. The MIC for both the antibiotic was supposed in different concentration range. On one hand, the expected MIC for KAN against

B. subtilis in BHI media was in the range of KAN 0.1 µg/mL and 1 µg/mL. On the other hand the expected MIC for STR in BHI media was between a concentration of 1 µg/mL and 10 µg/mL (Figure 20).

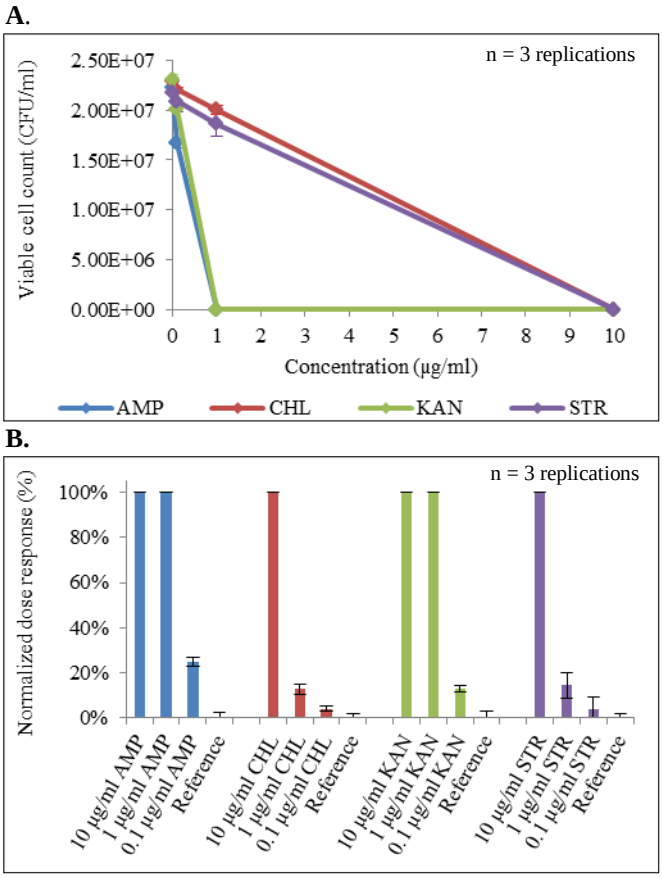

Figure 20. Results for the antibiotic susceptibility assay for *B. subtilis* using viable count agar plate method. (A) Viable cell count (CFU/mL) for different concentrations of antibiotics, (B) Corresponding dose response normalized to reference for *B. subtilis* at different concentration of antibiotics. Error bars represent standard deviation of three replications.

Similar to *C. glutamicum*, MMC was tested for *B. subtilis* using a shaking flask method. MMC at a concentration of 500 nM (167.17 pg/mL) was added at different time points (Figure 21A) and optical density at 600 nm ($OD6_{00}$) was measured every 30 min. The measurements were used to calculate growth rate per hour and percentage dose response was calculated by using growth rate normalized to reference (Figure 21B). The optical density for the reference was found to increase for 2 hours and decline in the OD_{600} was observed afterwards due to nutrition limitation, while an increase in OD_{600} was measured after 1.5 hours with MMC at an added concentration of 500 nM in the flask. If MMC was added at a concentration 1000 nM or higher to the shaking

flasks, OD_{600} values were below 0.1 (not significant). Thus *B. subtilis* was found to be sensitive to MMC. The expected MIC for MMC for *B. subtilis* in BHI media can be expected at an added concentration less than 1000 nM.

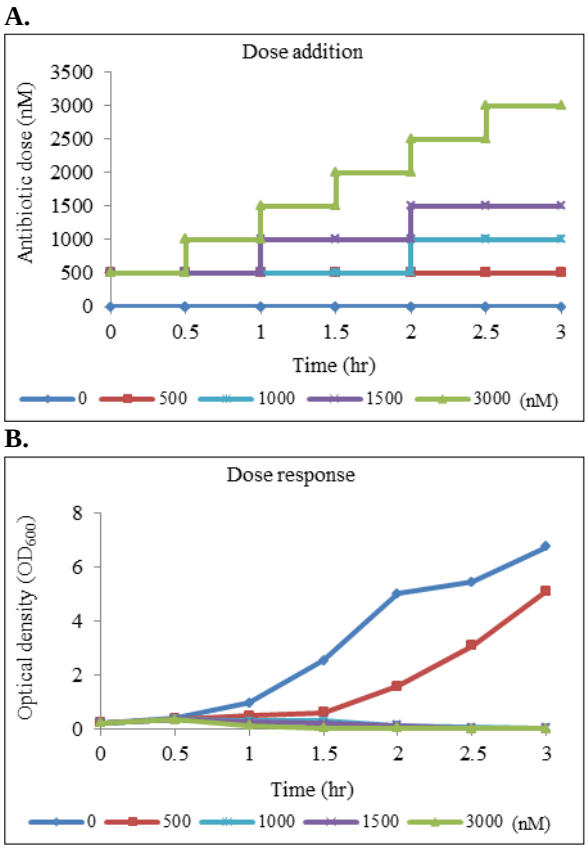

Figure 21. Results for the antibiotic susceptibility assay for *B. subtilis* with MMC. (A) Addition of MMC at a concentration of 500 nM at different time points. (B) Changes in OD_{600} for different amount of MMC added, as a measure of dose response. The change in OD_{600} represents the response of *B. subtilis* against an added dose.

4.1.2.2. Microfluidic single-cell analysis method

Microfluidic device was used to cultivate *B. subtilis* in microchambers, from which five microchambers were used to calculate the maximum growth rate per hour (μ_{max}). The normalized growth rate was used to calculate percentage dose response (Figure 22). The growth rate of the reference channels in different experiments was comparable to each other.

If AMP was used in the single-cell analysis at a concentration of 0.1 µg/mL the growth rate and dose response were 1.2 hr^{-1} and 3.9 %, respectively. If AMP at a concentration of 1 µg/mL and 10 µg/mL were used, complete

growth inhibition was observed (Figure 22A and C). The expected MIC ranges between a concentration of 0.1 µg/mL and 10 µg/mL AMP. In single-cell analysis, if CHL was used at a concentration of 10 µg/mL, the dose response was 97.1 % that means nearly no growth was observed. If CHL was used at a concentration of 1 µg/mL the growth was highly suppressed as compared to the agar plate method. The resulted growth rate was 0.4 hr^{-1} and dose response was 64.3 %. CHL at a concentration of 0.1 µg/mL had no effect on the growth and found comparable to the reference (Figure 22A and C). In the case of CHL the expected MIC may lie between a concentration of 1 µg/mL and 10 µg/mL.

If KAN was used at a concentration of 0.1 µg/mL there was no effect of KAN on growth of *B. subtilis* and it was comparable to the reference. If a KAN concentration at 1 µg/mL or higher was used, it resulted in total growth inhibition. Therefore, the MIC can be estimated in the range of KAN at a concentration lower than 1 µg/mL. Although KAN and STR have same mode of action, the response of *B. subtilis* against them was different. If STR was used at a concentration of 1 µg/mL or lower, the growth rate was found comparable to reference. STR at a concentration of 10 µg/mL resulted in the suppression of growth. The growth rate and dose response were 0.2 hr^{-1} and 82.9 %. Hence, it can be estimated that *B. subtilis* was less susceptible for STR and expected MIC should be higher than 10 µg/mL (Figure 22A and C).

The possibility to test MMC in single-cell analysis was very helpful in analyzing its effect on *B. subtilis*, because the effect of MMC cannot be seen in shake flask method. If MMC was used against *B. subtilis* at a concentration of 1000 nM (334.33 pg/mL) and 500 nM (167.16 pg/mL) total growth inhibition was observed. In addition to that, the cells were lysed due to the effect of MMC. The dose response was 12.4 %, if a MMC concentration at 50 nM was used and growth rate was highly suppressed to 0.5 hr^{-1} (Figure 22B and C). Thus, MIC was estimated to be between a MMC concentration at 50 nM and 500 nM.

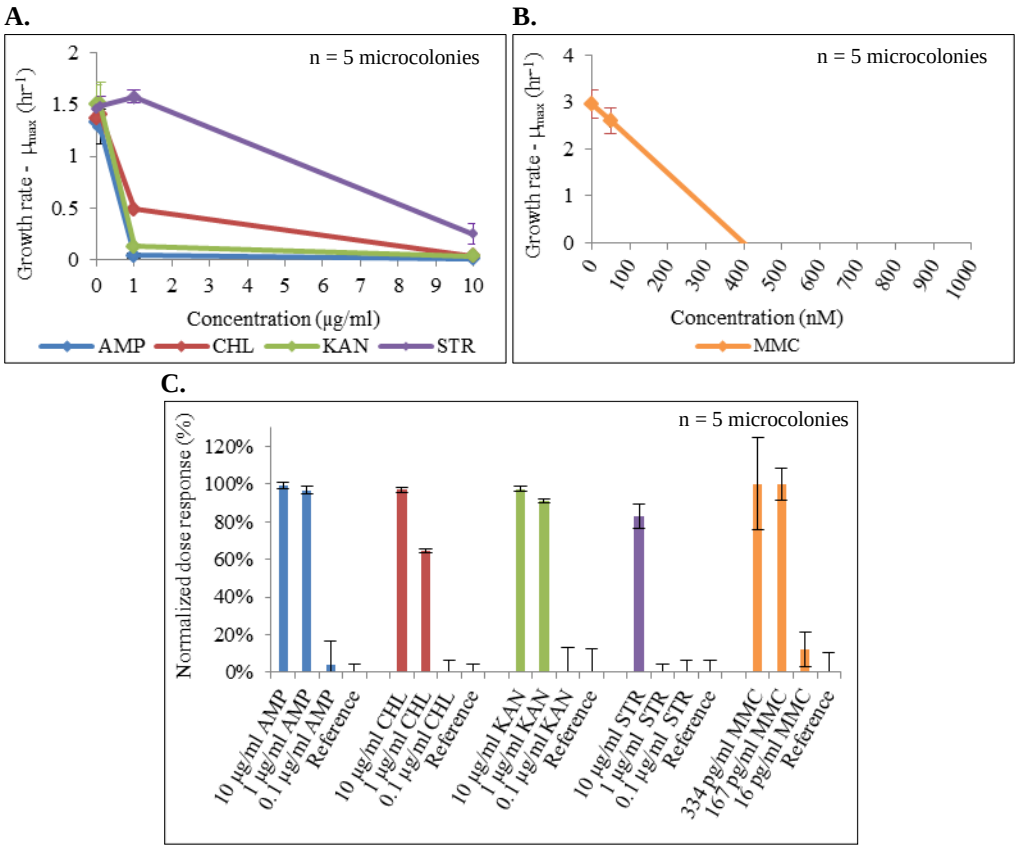

Figure 22. Results for the antibiotic susceptibility assay for *B. subtilis* using single-cell analysis. (A) Growth rate (μ_{max}) for different concentrations of AMP, CHL, KAN and STR (B) Growth rate (μ_{max}) for different concentrations of MMC (C) Corresponding dose response normalized to reference for *B. subtilis* at different concentrations of antibiotics. Error bars represent standard deviation of five microcolonies.

The results from the agar plate method and single-cell analysis method showed that both methods were comparable with some exceptions. Antibiotic susceptibility testing rely primarily on the MIC, which can be easily identified using both the methods. Different antibiotics act differently, for instance, bacteriostatic and bactericidal. Although, high concentrations of bacteriostatic antibiotics can be bactericidal. The effect of antibiotics might also be different for different bacteria. The limitation of precise visualization for bacteristatic or bactericidal effect of antibiotics in agar plate method may cause false interpretation of the results. MSCA can precisely illustrate the effect of antibiotic on a perticular bacterial sprecies.

Furthermore, *C. glutamicum* responded differently to AMP at a concentration of 1 µg/mL provided on solid medium (agar plates) and liquid perfusion medium (MSCA), respectively. The viable cell count calculated by

agar plate method had large difference in the results, if compared to the results calculated by using single-cell analysis method. The poosible reason might be, the fact that *C. glutamicum* can pump AMP out of the cell by efflux pumps (Sim *et al.* 2014). It might be possible that *C. glutamicum* cell can pump out AMP better if present on agar plates because the diffusion of the antibiotic might be slower due to the solid phase of agar medium. In case of MSCA, AMP is continuously perfused with the culture media in constant concentration and the diffusion of AMP in cells might be faster in the liquid phase. It is estimated that, the rate of diffusion of AMP was higher that the rate of active transport from the cells. Thus *C. glutamicum* was appeared more susceptible to AMP in MSCA. Therefore, in MSCA method, AMP at a concentration of 1 µg/mL inhibited the growth completely and did not produce viable colony. However, it can be seen from the microscopic images that cells changed their shape due to swelling.

Sim *et al.* in 2014, have described the MIC of different antibiotics for *C. glutamicum* by using agar diffusion assay. They used paper discs with specific amount of antibiotic on *C. glutamicum* wild type lawn and incubated for 24 hr at 30 ^{o}C. They have found that MIC of AMP is 15 µg/mL which is higher than expected MIC in our experiments (agar plate method and MSCA). Hence, there was an underestimation in MIC with agar plate method or disc diffusion method. Therefore, it can be concluded that there might be differences in the MIC when different antibiotic suseptibility assays are used. These differences might occur due difference dynamics involved in the analysing method. For instance, the concentration of antibiotics in the agar plate method might not remain constant through out the experiment and may decline with time, but in MSCA, a constant concentration of antibiotic is provided throughout an experiment. Hence, the effect of the antibiotic decay is eliminated from MSCA. Sim *et al.* had also calculated the MIC for CHL (6 µg/mL) and KAN (0.4 µg/mL) for *C. glutamicum* and MIC value found out by them lies in the range of concentrations estimated by our MSCA method.

There were also a minor difference observed between the results from agar plate method and MSCA method in case of *B. subtilis* with CHL and STR. It was observed that *B. subtilis* was more sensitive to CHL in the MSCA method, and the difference can be explained on the basis of the precision of the

methods, as discussed earlier. The MSCA method is more precise to observe the effect of CHL on *B. subtilis* growth and physiology. The difference in the growth rates of *B. subtilis* with STR in MSCA method might be due to the cell physiology. Additionally, *B. subtilis* also contain multidrug resistance efflux pump, which have funtional similarity to mammilian cells (Kunst *et al.* 1997). These efflux pumps which are related to different families of mambrane transporters can mediate the transport of structurally unrelated molecules across the cells. The abitlity of *B. subtilis* to produce antibiotics and transport of antibiotics like compound (Stein, Mikrobiologie, and Goethe- 2005) might be the reason for a slight variation observed with STR in MSCA. However, exact reason for the minor increase in growth rate was unclear and further experiments are needed to confirm the results. Nevertheless, it was confirmed from the results that *B. subtilis* was not sensitive towards STR at a concentration less than and equal to 1 µg/mL.

The composition of bacterial colony growing on agar plate is unknown attribute. The colony might be comprised of fast growing cells, slow growing cells, some cells which are active but not dividing, persistant, tolerant or resistant cells. Conventional assays are unable to differentiate subpopulations of nongrowing but metabolicllly active cells and also lack spatio-temporal tracking of phenotypic fluctuations at single-cell level (Maglica, Özdemir, and McKinney 2015). Same applies to fluorescence assisted cell sorting (FACS), as it also lacks a narrow spatio-temporal resoluted information at individual single-cell level. The use of different concentrations of antibiotics at same time also provide an option to compare the growth and physiology of bacterial cells at different concentrations, with high precision. The superiority of single-cell analysis lies in the generation of huge amount of useful information in relatively less time with high reliability of results. The MSCA method not only provides information about the antibiotic sensitivity of specific bacteria, but also provides a huge amount of information about the phenotypic changes and physiology of single-cell on real time scale, which are presented and disscussed for the MSCA results of this thesis in the section 4.2.

4.2. Phenotypic variations under antibiotic stress

As described before, *C. glutamicum* and *B. subtilis* were grown under different concentrations of antibiotics in BHI media, hence variations in the phenotype and morphology were detected, which are presented and discussed in this chapter.

4.2.1. Phenotypic variations of *C. glutamicum*

C. glutamicum is a straight or slightly curved rod shaped bacteria (Yassin, Kroppenstedt, and Ludwig 2003). Dusny *et al.* in year 2015, revealed the average size of *C. glutamicum* cells cultivated in monolayer growth chamber with BHI as a culture medium was 4.4 ± 0.4 µm and 2.7 ± 0.4 µm immediately before and after cell division, respectively. Similar results were obtained in this thesis. Cell length and morphology were found comparable under reference condition in all experiments (Figure 23 1A-5A). Similar to Neumeyer *et al.* 2013, a rare appearance of apparently dead cells was also observed in the reference population. Nevertheless, if *C. glutamicum* was grown in BHI media with different concentrations of antibiotic, a wide range of phenotypic variations were observed, which depended on the mode of action of antibiotic and its concentration. The appearance of specific phenotypes with antibiotics are presented and discussed henceforth.

4.2.1.1. Phenotypic variations of *C. glutamicum* due to AMP

The instance when *C. glutamicum* cells were grown in the presence of AMP at a concentration of 0.1 µg/mL, 1 µg/mL and 10 µg/mL, respectively, extensive alterations were observed in cell morphology. AMP is a bactericidal antibiotic, which inhibits cell wall synthesis (www.drugbank.ca/drugs/DB00415), thus it can cause phenotypic variations due to errors in cell wall formation. *C. glutamicum* cells appeared elongated and deformed when treated with AMP at a concentration of 0.1 µg/mL. The suppression in growth as well as formation of

some ‘Y’ shaped cells with bifurcated ends were noticed (Figure 23 1B). Moreover, AMP concentration at 1 µg/mL inhibited cell division. Additionally, changes in cell diameter were noticed. Thus cells appeared elongated and unsymmetrically segmented, with bulging at both ends, which might also have small metabolic activity indicated by blue fluorescence of calcein (Figure 23 1C). Bulging in the cell shape might occur due to loosening of cell wall during the process of cell division (Neumeyer *et al.* 2013). Internal pressure of cell might have caused the bacterial cell membrane to swell and change the diameter of cells. Complete inhibition of cell growth and division was observed when cells came in contact with perfusion media with an AMP concentration at 10 µg/mL (Figure 23 1D). As cells did not grow and divide, no distinct phenotypic changes were noticed at a concentration of 10 µg/mL AMP.

4.2.1.2. Phenotypic variations of *C. glutamicum* due to CHL

CHL is a bacteriostatic antibiotic, which stops bacterial growth by inhibiting protein synthesis, but may be bactericidal in high concentrations (www.drugbank.ca/drugs/DB00446). No clear difference was seen between cells when they were grown with CHL at a concentration of 0.1 µg/mL as compared to the reference condition without antibiotic addition. Although, a rare appearance of elongated cells was noticed (Figure 23 2B). Bacteriostatic activity of CHL was noticed at a concentration of 1 µg/mL for *C. glutamicum*, as the cell showed suppressed growth including few cells, which were abnormally elongated with tapering ends and divided to form deformed daughter cells which further grew and divided into deformed progenies (Figure 23 2C). CHL showed bactericidal activity at a concentration of 10 µg/mL which can be seen by the complete inhibition of division together with cells that were lysed and considered as dead due to the presence of PI fluorescence indicated in red (Figure 23 2D). Ghost cell could be observed, that are empty capsules of cell wall, which appeared translucent due to absence of cytoplasm and DNA within (Joux and Lebaron 2000). Ghost cell arises due to cell bursting under an influence of antibiotic in here and following experiments. The prominent presence of ghost cells also emphasized that CHL concentration at 10 µg/mL was bactericidal. Additionally, it is noteworthy to discuss the presence of cells

which were metabolically active as marked by the calcein fluorescence but were swelled and having spindle shaped. These cells were not PI positive; hence the cell wall was intact and may be considered as tolerant.

4.2.1.3. Phenotypic variations of *C. glutamicum* due to KAN

KAN is a bactericidal antibiotic that kills bacteria by causing misreading of mRNA during protein synthesis (www.drugbank.ca/drugs/DB01172). When treated with KAN at a concentration of 0.1 µg/mL cell shapes were comparable to those grown under reference conditions. However, few cells with a high calcein signal and unchanged morphology were observed (Figure 23 3B). KAN at a concentration of 1 µg/mL and higher inhibited cell division, nevertheless cells were highly heterogeneous (Figure 23 3C-D). These cells can be differentiated as metabolically active cells, apparently dead cells, ghost cells and segmented cells. Segmented cells are cells started to divide into two daughter cells, but have not separated and present in same envelop of cell wall. These cells were not connected and can have different physiological activity as seen in Figure 23. Segmented cells can be identified as metabolically active bigger cell attached to a smaller cell which was apparently dead. While discussing the results, a hypothesis can be drawn that cell division which occurred in the presence on KAN might remain incomplete and daughter cells cannot separate from each other. As an effect of KAN, incorrect amino acids are inserted in the polypeptides chain leading to production of nonfunctional or toxic peptides (www.drugbank.ca/drugs/DB01172), which might hinder cell division and causes death of cells.

4.2.1.4. Phenotypic variations of *C. glutamicum* due to STR

The mode of action of STR is same as that of KAN as described earlier. Moreover, the observations for different concentrations of streptomycin in combination with *C. glutamicum* were also similar. Changes in cell size and morphology of cells were found comparable to the cell under reference condition. STR at a concentration of 1 µg/mL and 10 µg/mL resulted in a

heterogeneous population comprising of metabolically active cells, apparently dead cells, ghost cells and segmented cells, while in contrary to KAN, less number of apparently dead cells were noticed for STR at a concentration of 1 µg/mL (Figure 23 4B-D).

4.2.1.5. Phenotypic variations of *C. glutamicum* due to MMC

C. glutamicum cells were found less sensitive if grown in different concentrations of MMC compared to *B. subtilis*. A slight growth suppression was observed along with swelled and elongated cells, which divided to give rise to deformed daughter cells, was observed if MMC at a concentration equal to or higher than 500 nM was used. Furthermore, many cells were lysed while other cells were growing (Figure 23 5B-D). No changes in cell phenotype were observed when cells were grown with MMC at a concentration of 50 nM (16.716pg/mL).

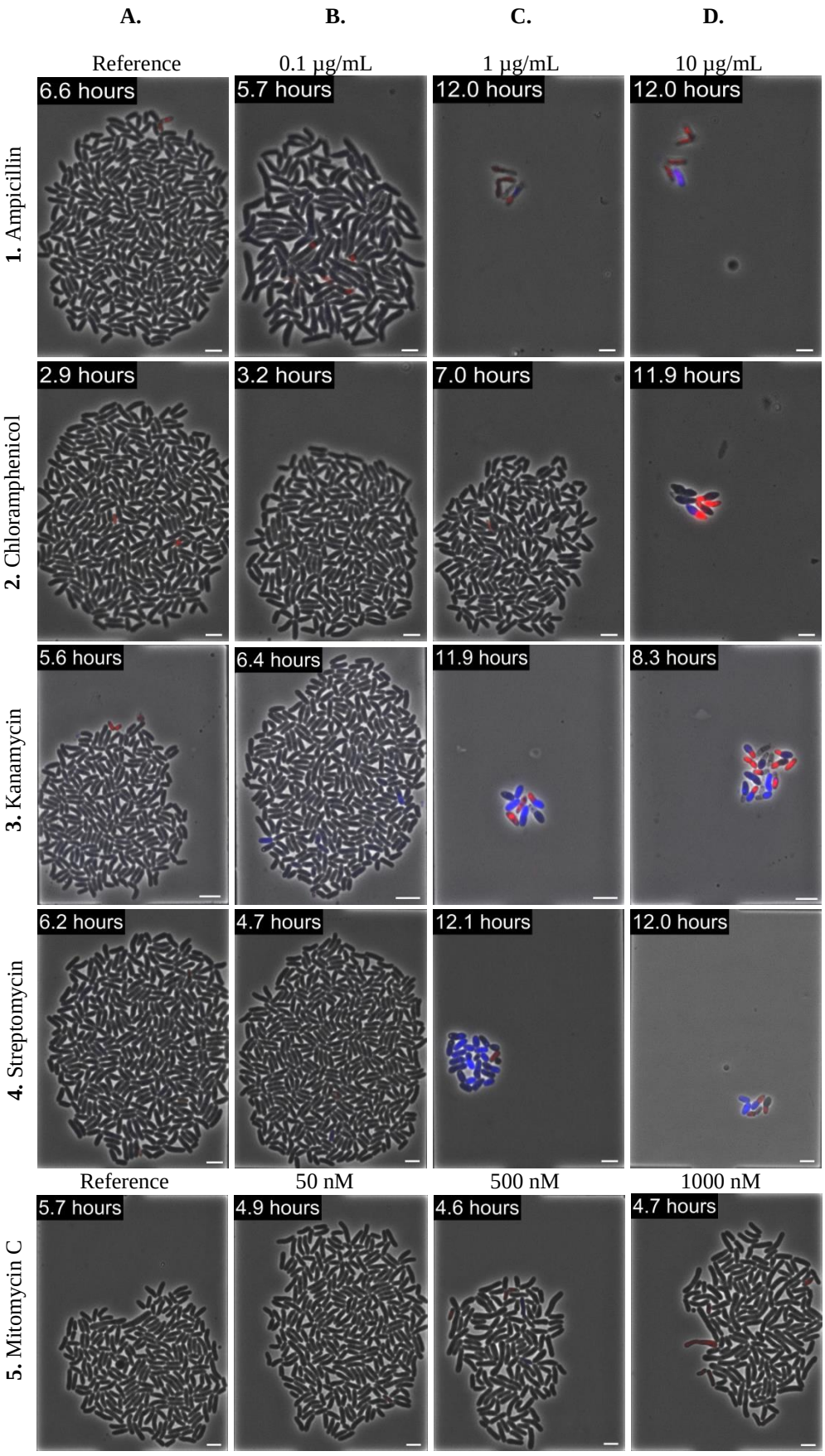

Figure 23. Phenotypic variations of *C. glutamicum* ATCC 13032 in response to different concentrations of antibiotics *C. glutamicum* was exposed to a concentration 0.1 µg/mL, 1 µg/mL and 10 µg/mL of AMP, CHL, KAN and STR, respectively. In case of MMC, concentrations 50 nM, 500 nM and 1000 nM were used. Changes in phenotype were observed and compared with reference. Viability and death of cells was interpreted on the basis of calcein (blue) and PI (red) fluorescence. Scale bar - 5 µm.

The occurrence of wide range of phenotypes of *C. glutamicum* under antibiotic treatment is of high relevance to the related bacteria which are pathogenic to human. The incidence of bacterial persistence and resistance to antibiotic treatment is also an alarming signal for more detailed physiological studies. Moving further, similar antibiotic stress experiments were conducted with *B. subtilis* in BHI media. The results obtained are presented and discussed in the following.

4.2.2. Phenotypic variations of *B. subtilis*

B. subtilis is very heterogeneous in nature and genetically identical cells may give rise to numerous distinct phenotypes. Heterogeneity may occur in terms of motility, extracellular matrix, filament formation, degradative enzymes or toxins secretion and cannibalism (Lopez, Vlamakis, and Kolter 2009). The average cell length of *B. subtilis* 168/S cell ranges from 2.46 µm – 6.52 µm in different culture media (Sargent 1975), while in this thesis an average individual cell length of *B. subtilis* 168 in MGC with BHI media was 10 ± 2 µm. *B. subtilis* 168 was observed to form long bacterial filaments also called macrofibers, which might measure up to 50 µm – 80 µm or even longer. Mendelson in year 1982, has described that *B. subtilis* macrofibers may be several millimeters in length when cells are cultured in the conditions which lead to reduction in autolytic enzymatic activity. In this thesis, average cell length of individual cells and morphology under reference growth conditions was found comparable for all the experiments (Figure 24 1A-5A). A rare occurrence of apparently dead cells was also noticed in reference, which might be due to specific autolytic phenotypes in the *B. subtilis* population. A narrow range of phenotypic variation in *B. subtilis* cells was observed when cells were grown under an influence of antibiotics.

4.2.2.1. Phenotypic variations of *B. subtilis* due to AMP

If an AMP concentration at 0.1 µg/mL was used in the perfusion media, no obvious phenotypic changes were observed as compared to the reference, while AMP at a concentration of 1 µg/mL was lethal. Similar observations were taken for AMP at a concentration of 10 µg/mL (Figure 24 1B-D). Since AMP at a concentration of 1 µg/mL was lethal, cells did not show any phenotypic variation in higher concentrations. At the time when cells lost their membrane potential, PO-PRO1 could enter the cell and bind to the DNA giving PO-PRO1 fluorescence indicated in light blue. Death of cells can be seen with both PO-PRO1 and PI fluorescence. No obvious changes were noticed in cell shape and size.

4.2.2.2. Phenotypic variations *B. subtilis* due to CHL

B. subtilis cells if treated with different concentrations of CHL, 0.1 µg/mL CHL had no effect on cell growth and division (Figure 24 2B). Severe effect on cell shape and size was observed if cells came in contact with CHL at a concentration of 1 µg/mL. Affected cells were long, undivided filaments having curly appearance. It should be noted that, however the cells were different in shape and sizes, membrane potential and cell wall was not damaged by CHL (Figure 24 2C). Heterogeneity in population was seen for CHL at a concentration of 10 µg/mL, where few cells were both PO-PRO1 and PI positive which indicated damaged cell wall while other cells were only PO-PRO1 positive *i.e.* cells lost their membrane potential. Nonetheless, CHL at a concentration of 10 µg/mL of was lethal for *B. subtilis* (Figure 24 2D).

4.2.2.3. Phenotypic variations of *B. subtilis* due to KAN

Despite the fact that KAN is a bacteriostatic antibiotic, KAN at a concentration of 0.1 µg/mL had no effect on *B. subtilis* and phenotype was comparable to the reference (Figure 24 3B). Furthermore, KAN at a concentration of 1 µg/mL and 10 µg/mL was lethal (Figure 24 3C-D). The dead cells were only PO-PRO1 positive, which showed that the cell wall was not damaged by 1 µg/mL and higher concentrations of KAN.

4.2.2.4. Phenotypic variations of *B. subtilis* due to STR

B. subtilis was observed to be less sensitive to STR, because the result showed that STR concentrations at 0.1 µg/mL and 1 µg/mL were comparable with the reference in growth behavior and morphology (Figure 24 4B-C). Cells growing in the presence of antibiotic were more filamented as compared to the reference. STR at a concentration of 10 µg/mL clearly suppressed growth and altered the morphology of the cells. Few cells appeared long and filamented while a minority of them was PO-PRO1 positive, all other cells were dividing at a reduced rate (Figure 24 4D).

4.2.2.5. Phenotypic variations of *B. subtilis* due to MMC

If *B. subtilis* was grown in the presence of MMC at a concentration of 50 nM (16.716 pg/mL) small suppression in growth was observed with no phenotypic changes in comparison to reference (Figure 24 5B). However, MMC is an antibiotic that had extreme impact on *B. subtilis* at a concentration of 500 nM (167.16 pg/mL) and higher. If *B. subtilis* cells were grown with MMC concentration at 500 nM and higher, cell were disintegrated and disappeared. Hence, no phenotypic variations in terms of cell morphology could be imaged (Figure 24 5C-D).

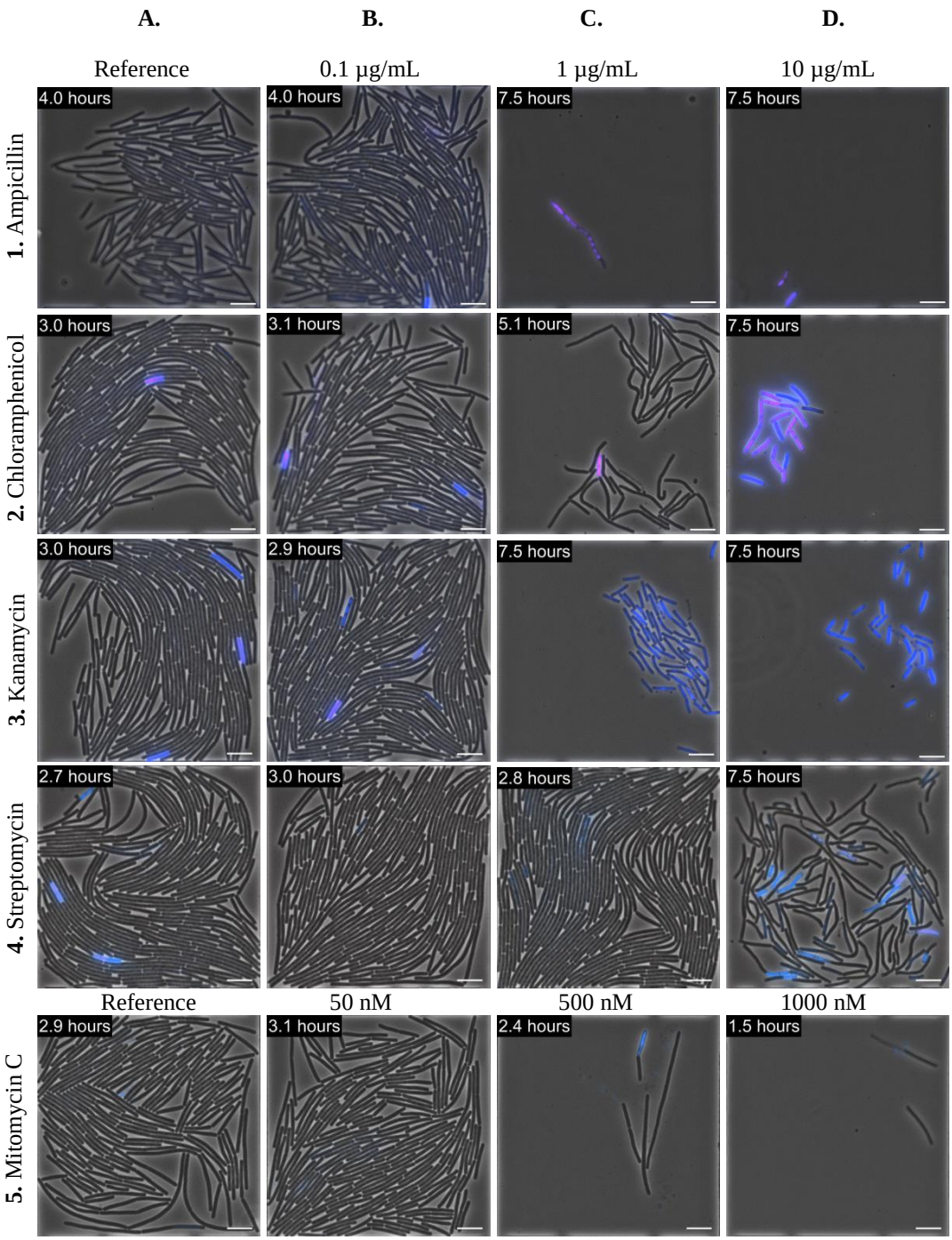

Figure 24. Phenotypic variations of *B. subtilis* 168 in response to different concentrations of antibiotics. *B. subtilis* was exposed to a concentration 0.1 µg/mL, 1 µg/mL and 10 µg/mL of AMP, CHL, KAN and STR, respectively. In case of MMC, concentrations 50 nM, 500 nM and 1000 nM were used. Changes in phenotype were observed and compared with reference. Viability and death of cells was interpreted on the basis of PO-PRO1 (blue) and PI (red) fluorescence. Scale bar - 10 µm.

The results of phenotype analysis can be further discussed on the basis of effective range of antibiotic against specific organism. The effective range of the antibiotic can be defined as the concentration of antibiotic at which degradative impact on growth, physiology and morphology can be observed. Comparing the effect of different antibiotics on the phenotype of *C. glutamicum* and *B. subtilis,* it can be seen that AMP inhibited cell growth and divisions at a concentration higher than 0.1 µg/mL, so the effective range of the AMP concentrations lies between 0.1 µg/mL and 1 µg/mL. The occurrence of distorted cell shapes of *C. glutamicum* at a concentration of 0.1 µg/mL can be explained by the fact that, AMP cannot penetrate the cell membrane. Therefore, it must bind to an external peptidoglycan precursor or newly inserted lipid linked subunits at the growing end of glycan strand of cell wall (Daniel and Errington 2003). *C. glutamicum* is a slow growing bacterium. During the growth of cells, the glycan fibers might be formed and incorporated in the cell wall, slowly. This might allow better penetration of AMP in the growing matrix of glycan network in cell wall. As AMP can penetrate cell wall in the slow growing glycan network, interruption in the cell wall synthesis might occur. The changes in *C. glutamicum* cell shape could be due to the wide penetration of AMP in the cell wall. This might have caused cells to have elongated and bifurcated morphology.

Likewise, both bacteria were equally sensitive towards KAN, and similar effective range was applicable. In case of CHL, the effective range was between a concentration at 1 µg/mL and 10 µg/mL. *B. subtilis* was found less sensitive for STR as compared to *C. glutamicum*, because *B. subtilis* cells were observed to grow and divide with a STR at a concentration less than and equal to 10 µg/mL. On the contrary, total growth inhibition was observed for *C. glutamicum* at a concentration equal to and higher than 1µg/mL, so the effective range for STR against *C. glutamicum* was between 0.1 µg/mL and 1 µg/mL, while effective range of STR against *B. subtilis* was higher than a concentration of 10 µg/mL. The phenomenon of ghost cells and segmented cells was not seen in *B. subtilis* as compared to *C. glutamicum*. It might have been because *B. subtilis* cell wall is more rigid and structurally different from *C. glutamicum*, therefore none of the cells were bursted and no ghost cells were observed. Segmented cells were not observed for *B. subtilis* because of the fact that

mechanism of cell division is different and staining methods used for *B. subtilis* and *C. glutamicum* were also different. PO-PRO1 bound to the DNA of metabolically dead cells which were devoid of membrane potential while calcein-AM was hydrolyzed by metabolically active cells to give fluorescence signal.

Furthermore, MMC was found to be less competent in suppressing the growth of *C. glutamicum* even at highest concentration of 1000 nM in respective experiment. On the contrary, *B. subtilis* was extremely sensitive towards MMC. The difference in the activity of MMC for both bacteria might be due to its mode of action. MMC is a strong DNA cross-linker have specificity for CpG sequence (Tomasz 1995). MMC inhibits DNA synthesis, induce mutagenesis and DNA repair (SOS) response in bacteria (Iyer and Szybalski 1964). Enzymatically reduced MMC is an active form which is only potent in hypoxic environment of cell, and activation of MMC is inhibited in the oxidizing environment (Teicher *et al.* 1981; Kennedy, Rockwell, and Sartorelli 1980). Different action of MMC against *B. subtilis* and *C. glutamicum* might be due to the difference of CpG sequences in the genome of both bacteria. The hypoxic intracellular environment is also a key parameter for MMC action. For instance, oxygen rich environment in *M. tuberculosis*, a close relative of *C. glutamicum*, induces up-regulation of central metabolism and less susceptibility to antibiotic targeting cell wall synthesis (Hett, Chao, and Rubin 2010; Koul *et al.* 2014). Hence, redox potential of cytoplasm also influences antibiotic activity. In addition to this, as a matter of fact, *B. subtilis* spontaneously produces degradative enzymes resulting in the autolysis of cell. this process is under the control of stress induced two component system DegS-DegU (López *et al.* 2009; Nicolas *et al.* 2012; Ogura *et al.* 2003). Upon phosphorylation, these regulators lead to the secretion of degradative enzymes. As MMC is a DNA cross-linker, it might also cause activation of degradative pathway which resulted in the self-degradation and bursting of cells in *B. subtilis*. One hypothesis can also be drawn on the basis of growth rates of bacteria. *B. subtilis* was faster growing as compared to *C. glutamicum*. The fast replication of DNA might provide better penetration of MMC to form cross-linkages in DNA strands and inhibit DNA synthesis. This might cause *B. subtilis* to be more

sensitive towards the degradative action of MMC. The difference in sensitivity of *B. subtilis* and *C. glutamicum* to MMC requires further explorations.

Simultaneously, while discussing the phenotype of *B. subtilis* and *C. glutamicum* in detail, one of the major differences between both organisms is the spore forming ability in *B. subtilis*. However, no spores were observed in *B. subtilis* micro population during the treatments with different antibiotics. To form spores, *B. subtilis* cells need to divide asymmetrically into two compartments of mother cell and forespore, under differential gene expression (Lopez, Vlamakis, and Kolter 2009). Nevertheless, in our experiments no morphological changes were observed in the compartmentalization of *B. subtilis* cells, hence it can be concluded that *B. subtilis* did not form spores in the antibiotic treatment in respective experiments. A yet another remarkable phenomenon of *B. subtilis* is the ability to produce extracellular matrix, which is known as biofilm. Biofilm production and sporulation are triggered by phosphorylation of a master regulator, Spo0A (Lopez, Vlamakis, and Kolter 2009). Under unfavorable conditions, cell can initiate biofilm formation before sporulation and encased in self-produced extracellular matrix (Branda *et al.* 2006; Morikawa *et al.* 2006). Moreover, not all of the cells in bacterial population produce a biofilm or endospores (Dubnau 1991; Lopez, Vlamakis, and Kolter 2009; Chai *et al.* 2008; Branda *et al.* 2006). In our experiments, there were no appearances of structures like biofilm or endospores. The study of these characteristics of *B. subtilis* in MSCA requires further investigations.

The phenotype and morphology itself is very important phenomenon of bacterial physiology. Nevertheless, the physiological activity of cell and viability of cell cannot be easily seen by the morphology alone. In such a situation, the physiological analysis with the help of physiological markers is very helpful. Fluorescent dyes are widely used as a physiological indicator for the bacterial cells. Fluorescence analysis can give information of physiological activity and viability of bacterial cells. In section 4.3, the physiology analysis of *C. glutamicum* and *B. subtilis* was carried out on the basis of fluorescence signals. The analysis with the help of fluorescent dyes is presented and discussed in the following with the respective fluorescence graphs.

4.3. Physiology analysis with fluorescent dyes

Fluorescence microscopy is widely used to analyze various physiological functions in bacterial cells. Many fluorescent techniques are implemented to analyze viability, metabolic activity, dead cells, producer cells and many more. However, some techniques are complex and not easy to be employed directly to growing bacterial cells, unless any genetic modification of bacteria. The viability measurement methods presented in this thesis are based on non-invasive physiological analysis of a bacterial cell without the requirement of genetic modification. The method is proposed for an accurate evaluation of physiological activity of bacterial cells by using dynamic viability staining. In this chapter, the results of the physiological analysis with the help of fluorescent dyes are presented and discussed. The presented results are the mean of five microcolonies cultivated in the MGC. For *C. glutamicum,* dynamic viability staining approach was carried out with the use of calcein-AM to indicate live cells and PI for apparently dead cell detection. As *B. subtilis* cannot be stained by calcein-AM, another viability staining approach was used with PO-PRO1 and PI. PI indicated cells with damaged cell wall while PO-PRO1 indicated cells without membrane potential.

4.3.1. Physiology analysis of *C. glutamicum* with fluorescent dyes

Metabolic activity of *C. glutamicum* was analyzed by the use of calcein-AM and PI. Non-fluorescent calcein-AM can passively diffuse through plasma membrane and converted into fluorescent calcein by intracellular esterase. Efflux pump present in *C. glutamicum* might be involved in the efflux of calcein from the cell. Thus, calcein signal depend on the conversion and active efflux of calcein from intracellular space. Calcein signal was observed decreasing gradually for all reference channels from generation to generation. Decline in the calcein signal in actively growing cells was observed due to the cellular growth and changes in metabolic activity, and active efflux of calcein. On the other hand PI signal was constant. Hence, all the references were comparable.

4.3.1.1. Physiology analysis of *C. glutamicum* with AMP

Real time cellular activity of metabolically active *C. glutamicum* cells was observed by calcein fluorescence. Mean calcein fluorescence for microcolony inferred initial number of cells, growth and metabolic activity. If AMP at a concentration of 0.1 µg/mL was used, calcein signal of the cells was comparable to reference. If cells were grown with AMP concentration at 1 µg/mL, growth inhibition was observed after 2 hours and calcein signal reduced. PI signal was increased after 2 hours, which indicated the lysis of the cells. The cells grown with AMP at a concentration of 10 µg/mL showed initial increase in calcein signal and constant PI signal. After 1 hour, increase in PI signal was observed, which indicated that the cell wall was damaged and the cellular DNA was stained, while corresponding decrease of calcein signal also confirmed that the metabolic activity of cells was reduced to minimum. AMP at a concentration 1 µg/mL and 10 µg/mL inhibited the growth of cells. Thus, calcein fluorescence was independent on the change in number of cells and the variations in the calcein fluorescence was due to the changes in metabolic activity of individual bacterial cells. Additionally, variations were observed in calcein fluorescence, and it can be interpreted that due to AMP, cells could not pump out calcein, although the conversion by esterase was unaffected. Hence, the signal was increased. In addition to that, the remaining esterase activity in non-viable cells which do not have damages in cell wall might also have caused variations in calcein signal for a short period of time. Constant PI signal indicated the death of all cells present in the microcolony. High standard deviation was resulted due to the relative difference in the time of cell lysis (Figure 25).

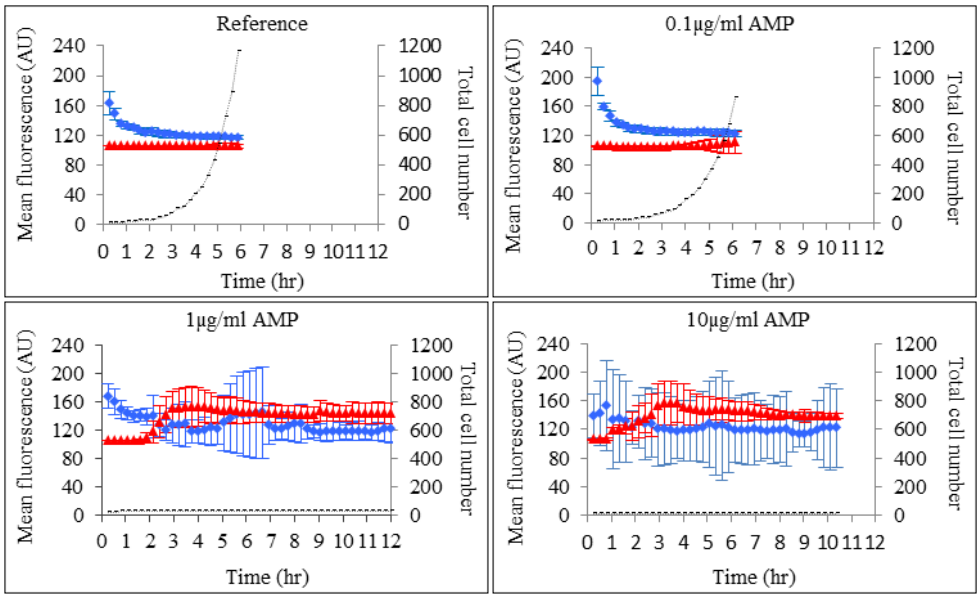

Figure 25. Graphs show mean fluorescence signal of calcein (blue) and PI (red) for five microcolonies, if treated with AMP at a concentration of 0.1 µg/mL, 1 µg/mL and 10 µg/mL along with reference. Black line indicates total cell number in five microcolonies.

4.3.1.2. Physiology analysis of *C. glutamicum* with CHL

CHL at a concentration of 0.1 µg/mL had no significant effect on cell physiology, thus found comparable to reference. If cells were grown CHL concentration at 1 µg/mL, calcein fluorescence was reduced and no significant fluorescence signals were observed (Figure 26). CHL is a bacteriostatic antibiotic and inhibits protein synthesis. Smith, Worrel, and Swanson in year 1949 discussed effects of different concentrations of CHL on bacterial growth and enzymatic activity of bacterial cells. They observed that, CHL inhibits the enzymatic activity in bacteria. Similar results were observed, if *C. glutamicum* cells were treated with CHL. Suppressed growth and enzyme inhibition by CHL at a concentration of 1 µg/mL might be the reasons of decreasing calcein signal. Additionally, CHL inhibit protein synthesis, and cell could not produce new functional enzyme for the conversion of non-fluorescent calcein-AM to fluorescent calcein. The efflux of calcein from the cell might also be unaffected which can also cause decline in calcein fluorescence. If *C. glutamicum* cells were grown in the medium containing CHL at a concentration of 10 µg/mL, reduction in cell number was observed in later half of experiment. Constant calcein signal indicated that the cell were not metabolically active. Slight increase in standard deviation for calcein was due to the presence of cells with

swelled and spindle shaped morphology (Figure 23). The increase in PI signal indicates that cells were lysed. The high standard deviation in PI signal was due to the fact that cells were bursted to form ghost cells and due to the temporal difference in cell lyses.

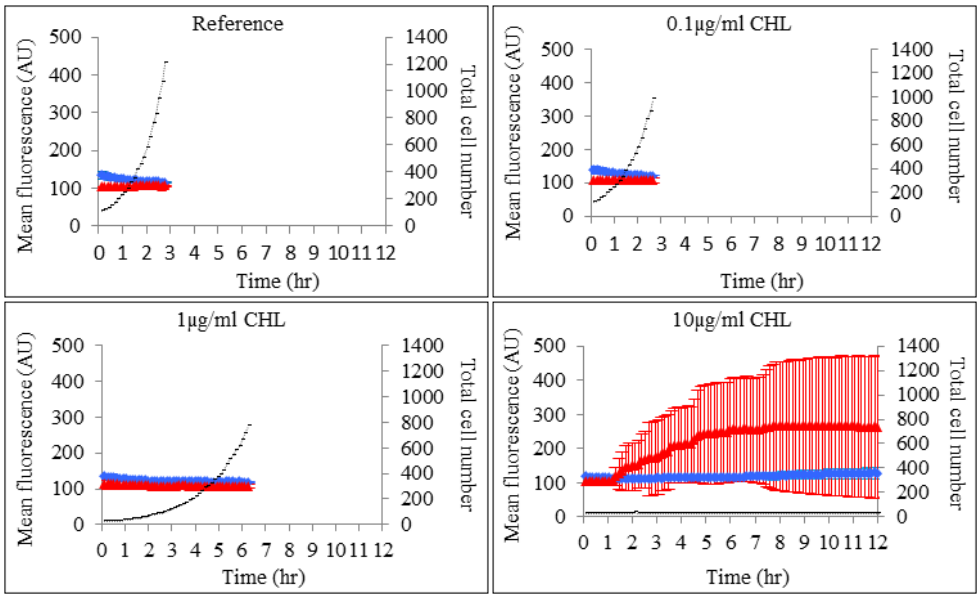

Figure 26. Graphs show mean fluorescence signal of calcein (blue) and PI (red) for five microcolonies, if treated with CHL at a concentration of 0.1 µg/mL, 1 µg/mL and 10 µg/mL along with reference. Black line indicates total cell number in five microcolonies.

4.3.1.3. Physiology analysis of *C. glutamicum* with KAN

If *C. glutamicum* cells were grown with KAN at a concentration of 10 µg/mL, a decrease in calcein signal was observed for first hour (Figure 27). The decrease in signal was due to the increase in the cell number and active efflux of calcein. Calcein signal reduced and became when cells were affected by KAN treatment. After 2 hours of the KAN treatment, an increase in calcein and PI signal was observed. The increase in PI signal resulted due to the cell lysis, while the increase in calcein signal might be due to the decrease in active efflux of calcein. Similar results were observed if KAN at a concentration of 1 µg/mL was used. The rise in PI signal was observed after 7 hours. The microcolony was highly heterogeneous in calcein fluorescence because of the presence of segmented cells, metabolically active cells, dead cells and ghost cells (Figure 23). High standard deviation in calcein signal was due to the heterogeneity of

cells in a microcolony. Additionally, the bursting of cell also resulted in high standard deviation in PI fluorescence.

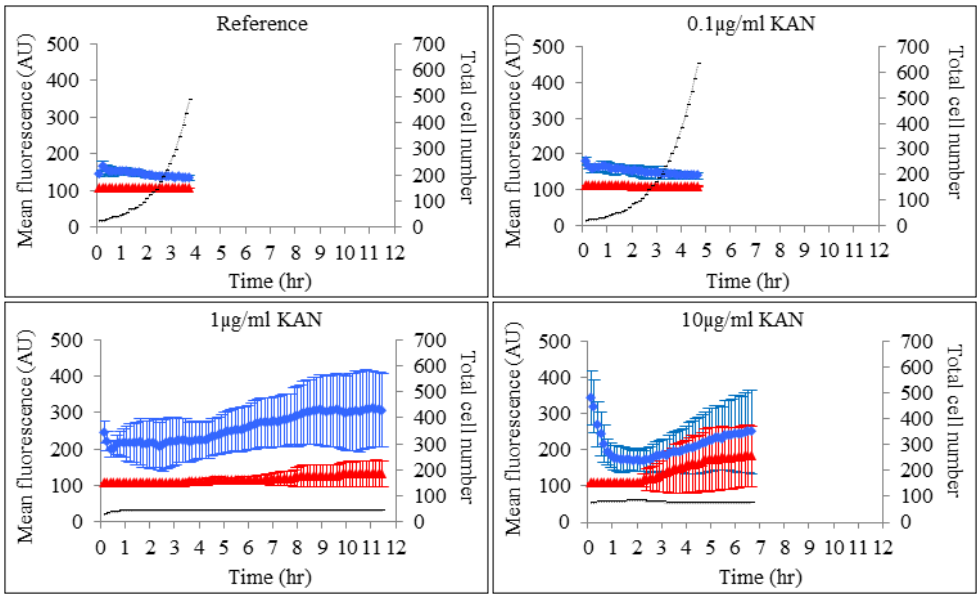

Figure 27. Graphs show mean fluorescence signal of calcein (blue) and PI (red) for five microcolonies, when treated with KAN at a concentration of 0.1 µg/mL, 1 µg/mL and 10 µg/mL along with reference. Black line indicates total cell number in five microcolonies.

4.3.1.4. Physiology analysis of *C. glutamicum* with STR

STR is a bactericidal antibiotic and its mode of action is same as that of KAN. Thus, the observations for STR were found comparable to KAN for all concentrations (Figure 28).

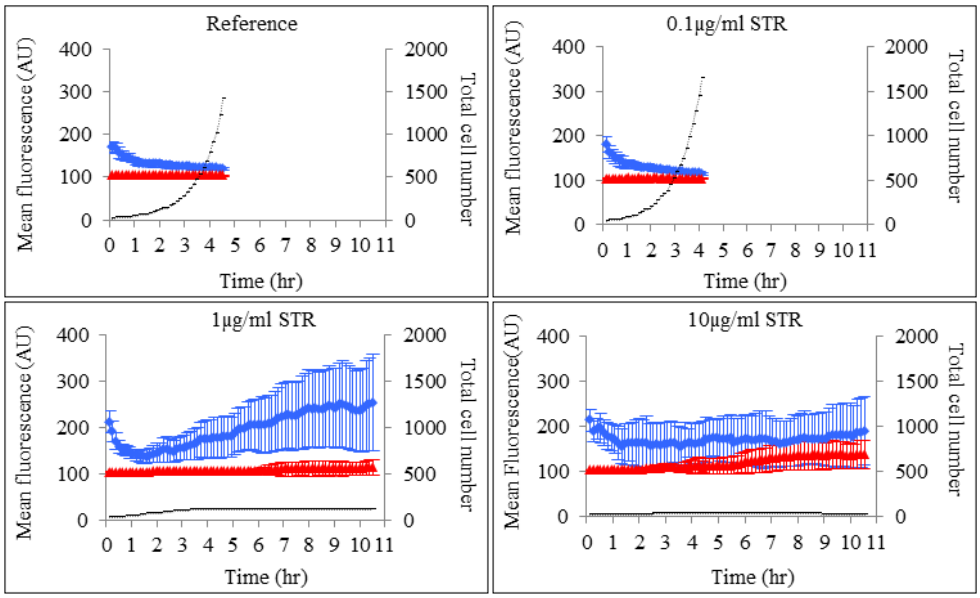

Figure 28. Graphs show mean fluorescence signal of calcein (blue) and PI (red) for five microcolonies, if treated with STR at a concentration of 0.1 µg/mL, 1 µg/mL and 10 µg/mL along with reference. Black line indicates total cell number in five microcolonies.

4.3.1.5. Physiology analysis of *C. glutamicum* with MMC

C. glutamicum was found less sensitive for MMC, nevertheless, phenotypic changes were observed and were discussed in previous chapter. The calcein and PI fluorescence for reference and all the MMC concentrations used were comparable. Calcein and PI signal did not show any increase and the signals were constant to the background signal. The constant calcein signal indicated that cells were actively pumping calcein out from the intracellular space. Hence, no increase in calcein signal was observed. PI signal was also constant and it indicated that, the cell wall was not damaged due to the MMC treatment (Figure 29).

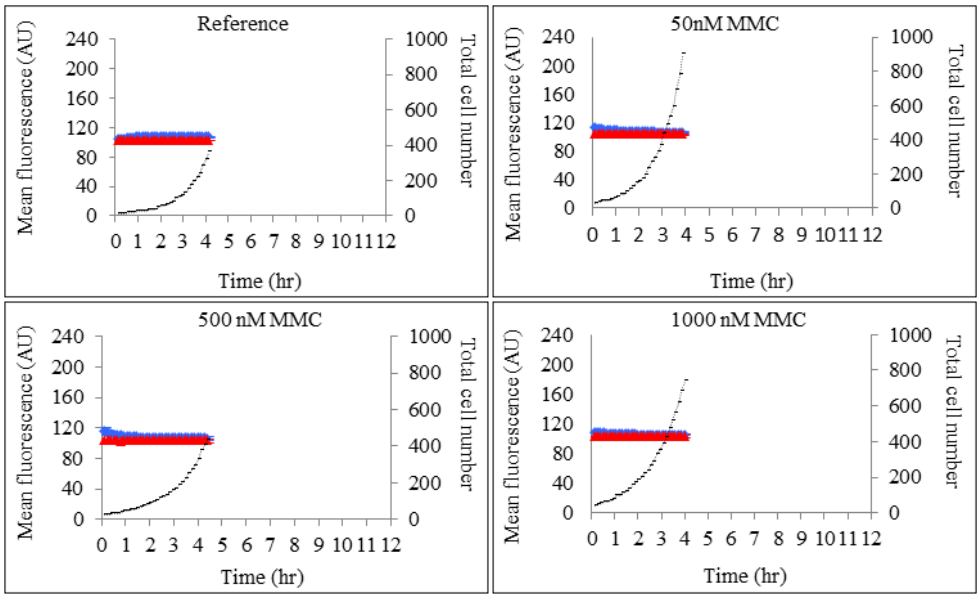

Figure 29. Graphs show mean fluorescence signal of calcein (blue) and PI (red) for five microcolonies, if treated with MMC at a concentration of 50 nM, 500nM and 1000 nM along with reference. Black line indicates total cell number in five microcolonies.

4.3.2. Physiology analysis of *B. subtilis* with fluorescent dyes

For *B. subtilis,* fluorescent stains PO-PRO1 and PI were used. The different mechanisms of the dyes helped to distinguish between the viable cells, cells without membrane potential and cells with damaged cell wall. The results are the mean of five microcolonies, for respective experiments of *B. subtilis* with different antibiotics. The results are presented and discussed in the following.

4.3.2.1. Physiology analysis of *B. subtilis* with AMP

If *B. subtilis* cells were grown with AMP concentration at 0.1 µg/mL, the fluorescence signals were comparable to reference. A slight increase in standard deviation of PO-PRO1 signal was observed in reference condition, which might be due to the autolysis of *B. subtilis* cells. The fluorescence analysis of *B. subtilis* indicated that AMP at a concentration of 0.1 µg/mL, resulted in the increase of standard deviation of PO-PRO1 as compared to the reference. An increase in standard in case 0.1 µg/mL AMP, indicated about the minor impact of AMP on *B. subtilis* cells. If cells were treated with AMP at a concentration of 1 µg/mL and 10µg/mL, an increase in PO-PRO1 signal was observed. This increase in PO-PRO1 signal indicated towards the loss of membrane potential of the cells. As soon as the cells were affected by AMP, they lost membrane potential and the signal correspond the loss of membrane potential. The intensity of fluorescence depended of the level of loss in membrane potential. At instance when the cell wall was ruptured, both PO-PRO1 and PI could enter the cell and increase in both fluorescence signals was observed. The high standard deviation was due to the different time intervals when cells had lost their membrane potential. A reduction in fluorescence signals was observed in later half of experiment in case of AMP concentration at 1 µg/ml. This loss of fluorescence was due to the loss of DNA from the ruptured cell wall.

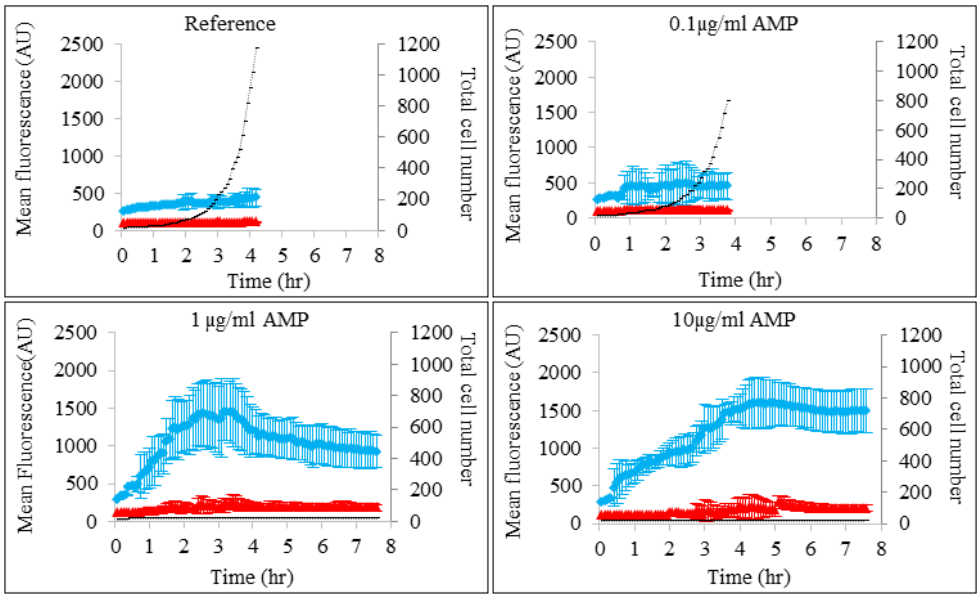

Figure 30. Graphs show mean fluorescence signal of PO-PRO1 (blue) and PI (red) for five microcolonies, if treated with AMP at a concentration of 0.1 µg/mL, 1 µg/mL and 10 µg/mL along with reference. Black line indicates total cell number in five microcolonies.

4.3.2.2. Physiology analysis of *B. subtilis* with CHL

If CHL at a concentration of 0.1 µg/mL and 1 µg/mL was used, the fluorescence signals were comparable to reference. If *B. subtilis* was treated with CHL at a concentration 10 µg/mL, it was observed that the PO-PRO1 signal started to increase after 3 hours. This might be due to the reason that, CHL is a bacteriostatic antibiotic and it suppressed bacterial growth initially, but the concentration was high enough to kill bacterial cell in later part of the experiment. CHL at a concentration of 10 µg/mL for 3 hours, resulted in loss of membrane potential. The variations in the signal were due to loss of membrane potential and of different cells at different time points. Gradual increase in PI signal after 5 hours, indicated that the cell wall began to get damaged and PI intruded cytoplasm and slowly cells were getting stained by PI (Figure 31).

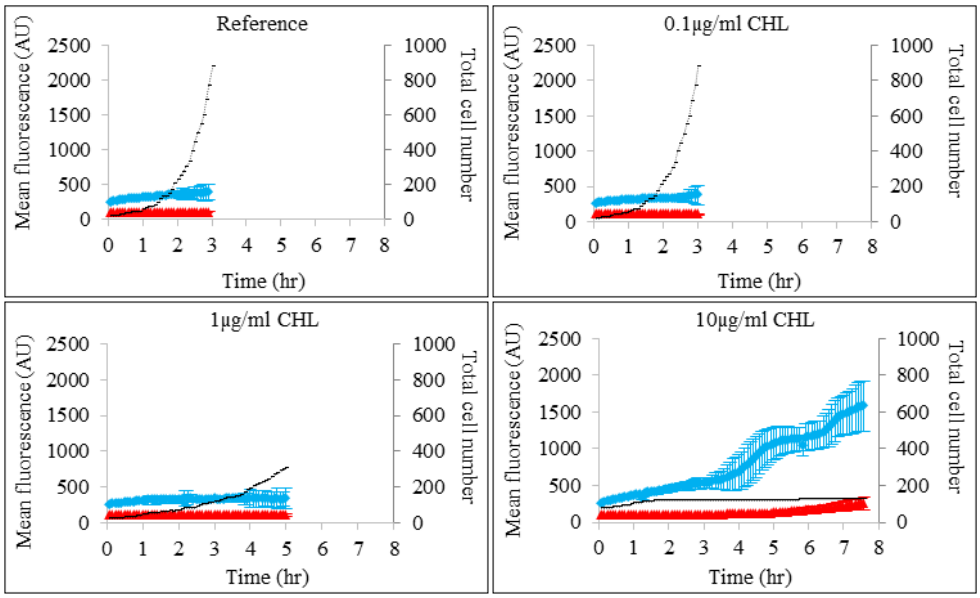

Figure 31. Graphs show mean fluorescence signal of PO-PRO1 (blue) and PI (red) for five microcolonies, if treated with CHL at a concentration of 0.1 µg/mL, 1 µg/mL and 10 µg/mL along with reference. Black line indicates total cell number in five microcolonies.

4.3.2.3. Physiology analysis of *B. subtilis* with KAN

In the fluorescence of analysis of *B. subtilis* with KAN, PO-PRO1 and PI signals were comparable for reference and KAN at a concentration of 0.1 µg/mL. If *B. subtilis* cells came in contact with KAN at a concentration of 1 µg/mL, the fluorescence signal of PO-PRO1 increased gradually. The course of fluorescence indicated that the loss of membrane potential occurred after 1 hour. The PO-PRO1 signal was observed to be constant gradual increase in PO-PRO1 fluorescence was observed after 5 hours. Initial increase in PO-PRO1 fluorescence indicated that few cells had lost their membrane potential and the increase in PO-PRO1 after 5 hours indicated that the number of cells which had lost their membrane potential were increasing. If *B. subtilis* grown in medium with KAN at a concentration of 10 µg/mL, an increase in the PO-PRO1 signal was observed from the beginning of the experiment. This indicated that as soon as cells came in the contact with KAN, they had started to loss their membrane potential. The standard deviation of PO-PRO1 signal also indicated that although cells were affected by the KAN treatment, there were temporal differences in the loss of membrane potential. The reduction in standard deviation during the latter part of the experiment also indicated that all cells were getting PO-PRO1 positive and finally have lost their membrane potential.

If *B. subtilis* was treated with KAN, no significant increase in PI signal was observed. It indicated that, KAN in the tested concentrations was lethal, but caused no damage to the cell wall (Figure 32).

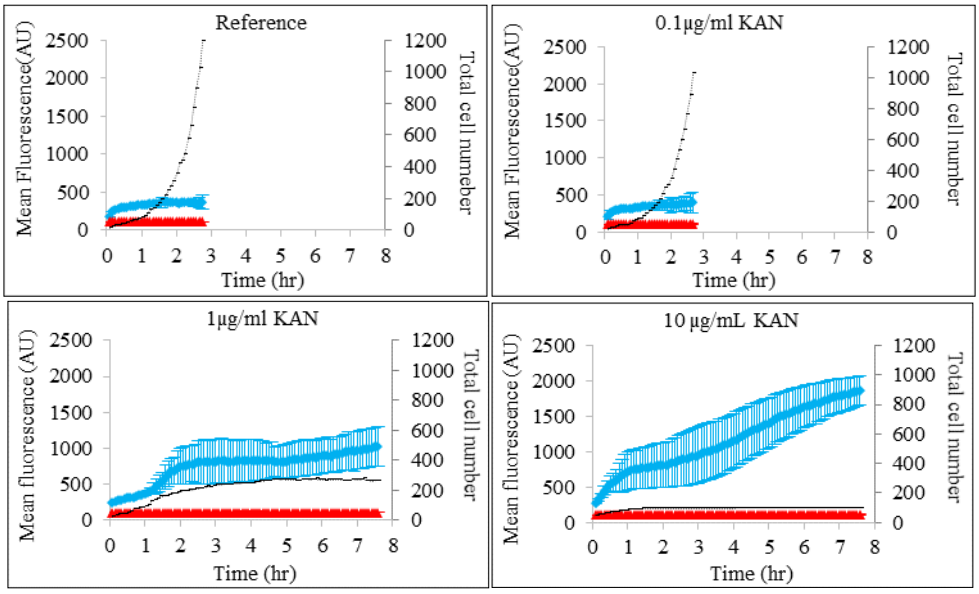

Figure 32. Graphs show fluorescence signal of PO-PRO1 (blue) and PI (red) for five microcolonies, if treated with KAN at a concentration of 0.1 µg/mL, 1µg/mL and 10 µg/mL along with reference. Black line indicates total cell number in five microcolonies.

4.3.2.4. Physiology analysis of *B. subtilis* with STR

As discussed earlier, the mode of action of STR is same as that of KAN but *B. subtilis* was appeared to be less sensitive for STR. The fluorescence of STR at a concentration lower than 1 µg/mL was found comparable to the reference. A slight increase in the standard deviation for these concentrations might be due to the autolysis of few cells. After 1 hour treatment of STR concentration at 10 µg/mL, increase in PO-PRO1 fluorescence was observed with high standard deviation. An increase in the PO-PRO1 indicated the loss of membrane potential of the cells. By the interpretation of PO-PRO1 fluorescence, it can be seen that, the fluorescence was not very high. As the cell number was increasing, the results can be concluded as, only a few cells in the growing population had lost their membrane potential. This also explains the reason of the high standard deviation in the PO-PRO1 fluorescence. No increase in the PI signal was observed (Figure 33).

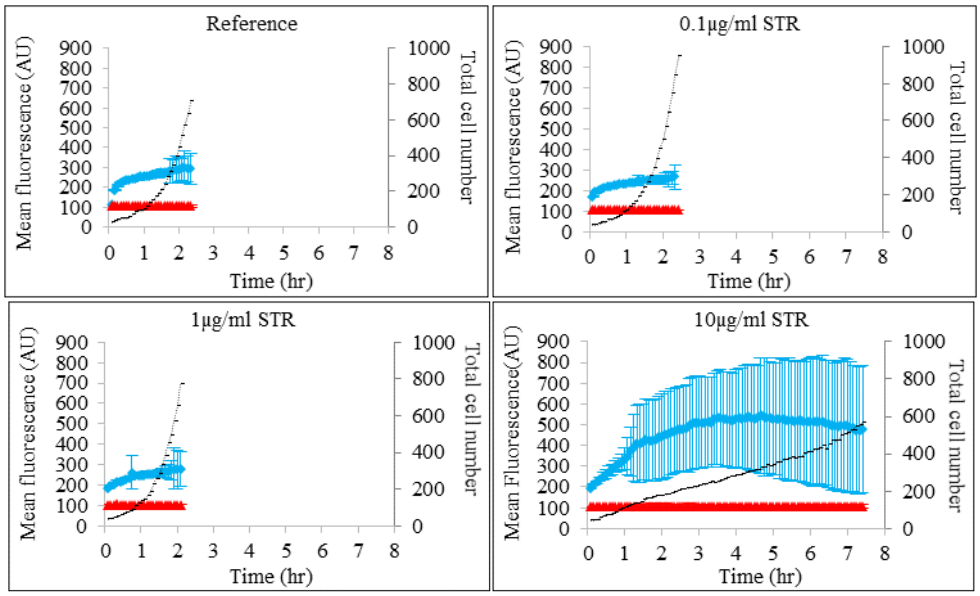

Figure 33. Graphs show fluorescence signal of PO-PRO1 (blue) and PI (red) for five microcolonies, if treated with STR at a concentration of 0.1 µg/mL, 1 µg/mL and 10 µg/mL along with reference. Black line indicates total cell number in five microcolonies.

4.3.2.5. Physiology analysis of *B. subtilis* with MMC

The fluorescence for MMC at a concentration of 50 nM was found comparable to reference. When *B. subtilis* was treated with MMC at a concentration of 500 nM and 1000 nM, total lethality was observed and the cell disintegrated. This aspect was already discussed earlier. As the cells bursted due to antibiotic, fluorescence signal did not show any significant change. High standard deviation for MMC at a concentration of 500 nM was due to the slow bursting of cell so that, cells could give detectable PO-PRO1 signal before bursting. The disintegration of cells for MMC concentration at 1000 nM was very fast, therefore, no fluorescence signal was observed (Figure 34).

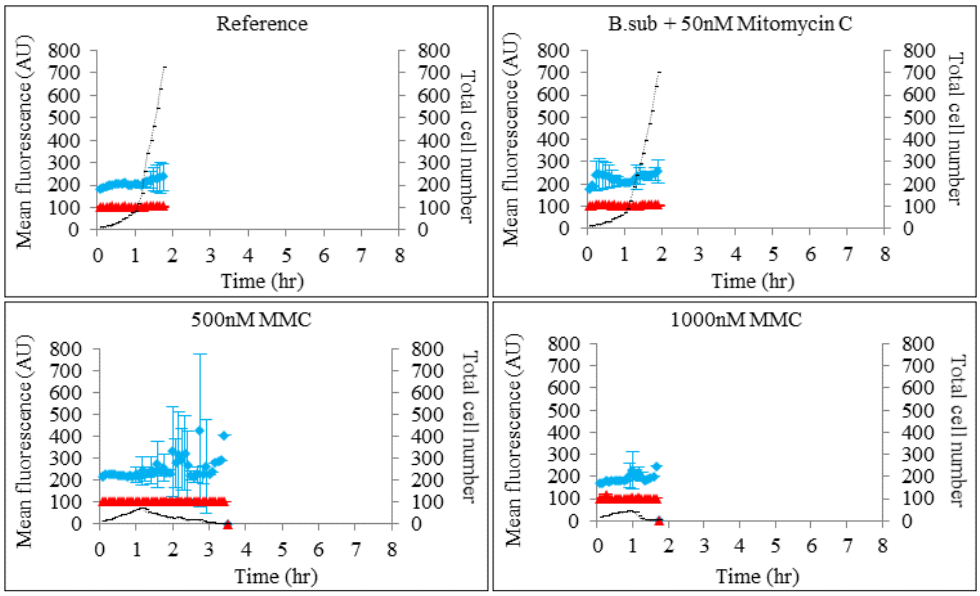

Figure 34. Graphs show fluorescence signal of PO-PRO1 (blue) and PI (red) for five microcolonies, if treated with MMC at a concentration of 50 nM, 500 nM and 1000 nM along with reference. Black line indicates the total cell numbers in five microcolonies.

In the discussion, it can be seen that for *C. glutamicum* and *B. subtilis*, different fluorescent dyes were used which have different mechanisms of action. Thus cannot be compared directly. Although the antibiotic used was similar, hence the action of an antibiotic in different concentrations can be compared. Thus, the action of antibiotic can be seen precisely on the basis of metabolic activity, membrane potential and cell wall integrity. It is often discussed that, the PI staining not always indicates the dead cell and there are often chances for the false PI positive cells (Neumeyer *et al.* 2013). The use of second fluorescence dye with PI for *C. glutamicum* and *B. subtilis* minimizes the chances of getting false PI positive cells.

C. glutamicum was grown with perfusion media containing antibiotic and the effect of antibiotic was observed with the use of dynamic staining method using PI and calcein-AM. Thus, not only sensing of alive and dead cells was acquired, but also the metabolically activity could also be sensed. By interpreting calcein signals and with the knowledge of mode of action of antibiotic, a wide range of physiological information of cell can be obtained. Bacterial susceptibility to antibiotic is highly relevant to its metabolism. Most of the bactericidal antibiotics interact with their targets and stimulate the production of hydroxyl radical which would cause cellular death (Martínez and Rojo 2011). By interpreting the calcein fluorescence, it can be seen that the

energy status of cells also changed due to antibiotic. For instance, cells which were giving high calcein signal can be interpreted as ATP-low cells. Since, the efflux pumps need ATP to pump out calcein from the cell, the low ATP status in cell might stop efflux, leading to increase of calcein fluorescence into the cell. As passive diffusion of calcein-AM into the cell and its conversion into calcein are energy independent processes, an increase in the calcein fluorescence (Krämer unpublished) reflects the low or no ATP status of cell. Additionally, the expression of efflux pump is also energy dependent. It might also possible that due to the low energy status of cells, the reduction in the number of pumps might have occurred, which could have reduced calcein efflux. (Martínez and Rojo 2011; Andersson and Levin 1999; Andersson 2006; Baquero, Coque, and De La Cruz 2011).

On the contrary to *C. glutamicum*, different staining strategy was used for *B. subtilis*, it cannot be stained with calcein-AM. The reason for this might be the physiological differences of both bacteria. Nevertheless, a novel staining method was developed by combining PO-PRO1 and PI. With the use of this combination for bacterial staining, the discussion over dead stage of bacteria can be resolved. As discussed earlier, PI staining alone can give false positive results. The uncertainty over the death of bacteria can be analyzed better by using counter stain PO-PRO1 along with PI. PO-PRO1 indicated the cells without membrane potential and such cells were metabolically dead. The cells which gave PO-PRO1 and PI could be declared as dead with no doubt, as the fact that a cell could not survive without membrane potential and damaged cell wall. Physiology analysis with PO-PRO1 also assisted in gaining the information that, membrane potential of *B. subtilis* was lost prior to the cell wall damage due to the antibiotic treatment. PO-PRO1 can also indirectly illustrate the metabolic activity of the cell. Metabolic activity within the cell produces the potential gradient between the intra and extra cellular environment. Therefore, a reduction in the membrane potential can be caused due to a reduction in metabolic activity of cell. Hence, physiological activity of cell can be sensed by interpreting PO-PRO1 fluorescence signals. Furthermore, to see the response of individual bacterial cell due to the antibiotic treatment, fluorescence analysis based on individual single-cell during the course of experiment was carried out.

In section 4.4, the results from the single-cell fluorescence analysis of *C. glutamicum* and *B. subtilis* are presented and discussed.

4.4. Single-cell fluorescence analysis

Mean fluorescence analysis demonstrated the changes in calcein and PI fluorescence over microcolony temporally resoluted. As it is based on the mean value of every single-cell mean fluorescence of the microcolony, it cannot reveal the heterogeneity of microcolony and how individual single-cells respond to antibiotic treatment. Single-cell analysis can demonstrate how an individual cell reacted to an antibiotic and when the cell was lysed. Single-cell fluorescence traces gave information about the metabolic activity, membrane potential and cell wall integrity of a particular cell over time. In case of antibiotic concentrations where cell number in a single microcolony was too low, single-cell data from five microcolonies was pooled to form a significant population. The single-cell fluorescence results are presented with the corresponding number of microcolonies analyzed.

4.4.1. Single-cell analysis of *C. glutamicum*

Single-cell analysis of *C. glutamicum* was carried out to elucidate the response of single cells under the treatment of different concentrations of antibiotics. Single-cell analysis for *C. glutamicum* is presented and discussed in the following.

4.4.1.1. Single-cell analysis of *C. glutamicum* with AMP

Single cell analysis of *C. glutamicum* under AMP treatment revealed that there was an inverse relation between antibiotic concentration and the time of cellular lysis. Single-cell analysis with AMP revealed that increasing concentration of AMP also increases the PI signals. The time of increase in the PI signal was found to have co-relation with the increase in AMP concentration. The range of the time in which PI signal was noticed under different concentrations of AMP was from 1 hour to 4 hours after the beginning of experiment. Corresponding decrease in calcein signal was also noticed for most of the cells. AMP at a concentration of 10 µg/mL, demonstrated the variations in the calcein and PI fluorescence of few single-cells in the microcolony.

Single-cell traces were prepared for the cells, which were different from others and gave peculiar fluorescence. Single-cell fluorescence traces depicted varied response of individual single-cells to AMP (Figure 35). The reason for the variation in the fluorescence was the heterogeneity of cells. As can be seen from the single-cell traces of cell number 1 (Figure 36) the calcein signal was high initially. The drop in the calcein signal corresponds to the increase in the PI fluorescence. Increase in PI fluorescence and sudden decrease in calcein signal, indicated the damage of cell wall after 5 hours. On the other hand, cell number 2 (Figure 36) did not show much variation in fluorescence signals for first four hours of experiment. After 4 hours, sudden increase in the calcein fluorescence indicated intracellular changes and metabolic activity of cells. Hence, an increase in calcein signal was observed.

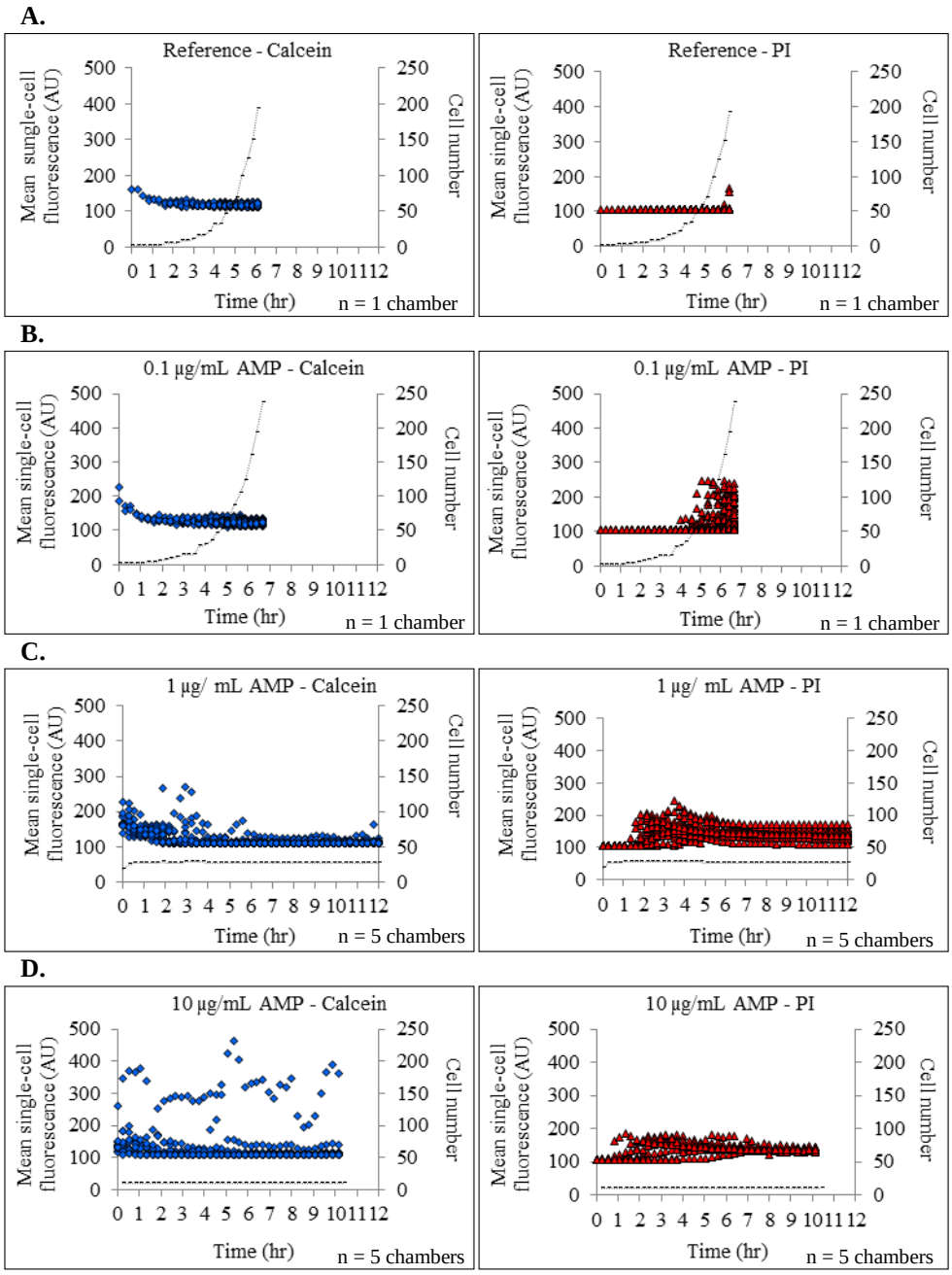

Figure 35. Single-cell analysis of *C. glutamicum* with AMP. (A. B. C. D.) Single-cell mean fluorescence of calcein (blue) and PI (red) over microcolony for reference and AMP at a concentration of 0.1 µg/mL, 1 µg/mL and 10 µg/mL are presented, respectively. Black line indicates cell number.

Single-cell fluorescence traces for the representative cells are presented in the diagrams below.

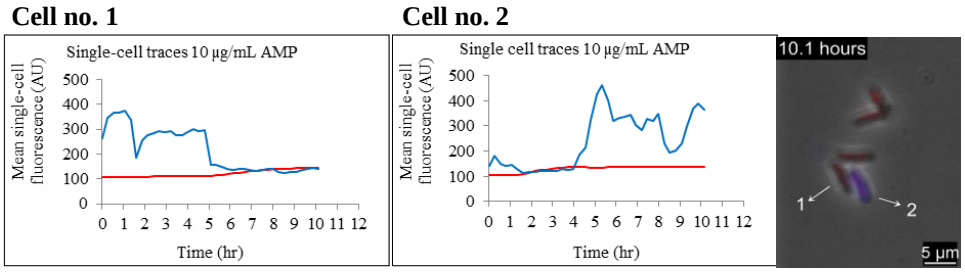

Figure 36. Single-cell fluorescence (calcein and PI) traces of representative *C. glutamicum* cells are presented with AMP concentration at 10 µg/mL. Corresponding cells are marked with numbers in the image.

4.4.1.2. Single-cell analysis of *C. glutamicum* with CHL

CHL is a bacteriostatic antibiotic and inhibit protein synthesis. By the single-cell fluorescence data it can be seen that CHL at a concentration lower than 1 µg/mL, did not have significant impact on the single-cell fluorescence. An increase in the PI signal for a minority of cells at CHL concentration lower than 1 µg/mL, could be explained by ageing, and spontaneous death in bacteria growing under normal conditions (Keren *et al.* 2004). Few PI positive cells can also be seen even though there is not much impact of antibiotic on the cell physiology. If *C. glutamicum* was grown with 10 µg/mL CHL, high heterogeneity was observed in single-cell PI fluorescence and comparatively less variation in the single-cell calcein fluorescence. Single-cell fluorescence traces have revealed that one bacterial cell can give both calcein and PI fluorescence (Figure 37). This was due to segmented cells. Single-cell traces of cell number 1 demonstrated that PI fluorescence had pulsing signal (Figure 38). First increase in PI signal was observed after 2 hours while second increase in PI signal was observed after 4 hours. The reason for this pulsing signal was the temporal difference in the lysis of each part of a segmented cell. After 2 hours, first pulse in PI fluorescence was due to the lysis of one sister cell and lysis of second sister cell occurred after 4 hours. Additionally, single-cell fluorescence trace of cell number 2 depicted the occurrence of increase in calcein and PI signal in a single cell. It can be elucidated as, high PI signal from one sister cell was observed after 5 hours of CHL treatment. This sudden increase in PI signal

indicated the death of cell while the gradually increasing calcein signal indicated about the metabolically activity of second sister cell (Figure 38).

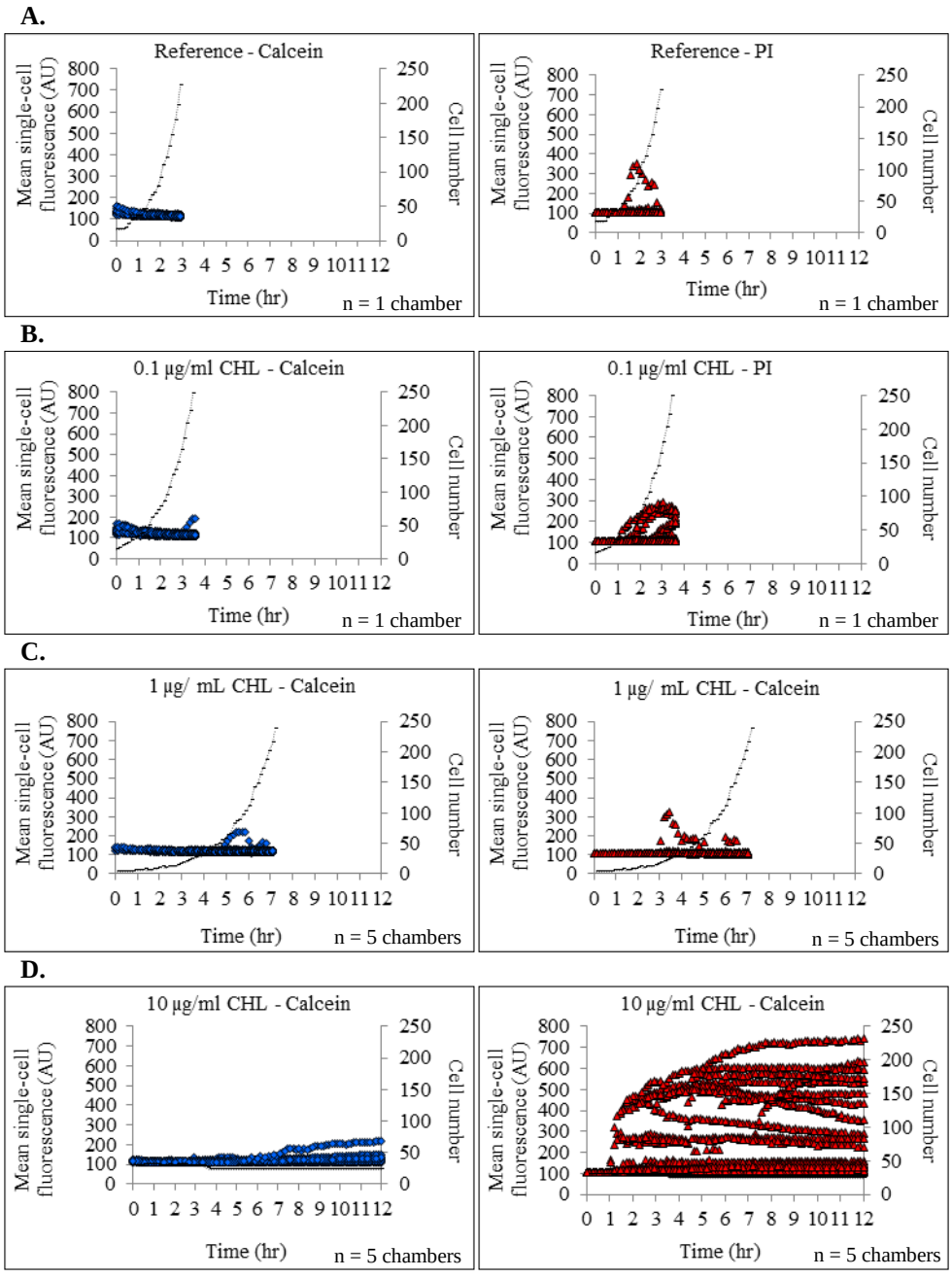

Figure 37. Single-cell analysis of *C. glutamicum* with CHL. (A. B. C. D.) Single-cell mean fluorescence of calcein (blue) and PI (red) over microcolony for reference and CHL at a concentration of 0.1 µg/mL, 1 µg/mL and 10 µg/mL are presented, respectively. Black line indicates cell number.

Single-cell fluorescence traces for the representative cells are presented in the diagrams below.

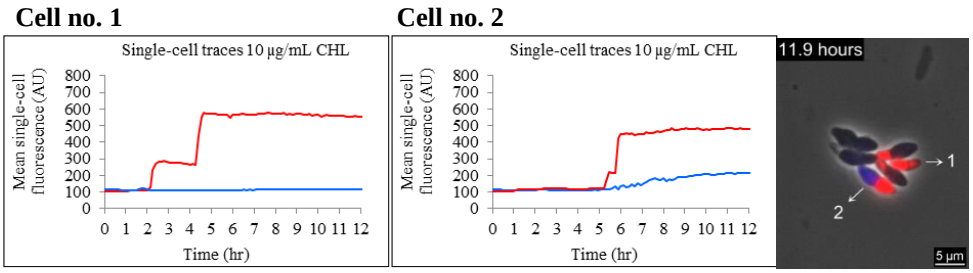

Figure 38. Single-cell fluorescence (calcein and PI) traces of representative *C. glutamicum* cells are presented with CHL concentration at 10 µg/mL. Corresponding cells are marked with numbers in the image.

4.4.1.3. Single-cell analysis of *C. glutamicum* with KAN

KAN inhibits protein synthesis and is bactericidal. Single-cell analysis revealed that cell population was highly different in calcein signal. The corresponding PI signal was comparatively more homogeneous. The PI fluorescence of single cells in KAN at a concentration of 1 µg/mL increased after 3 hours of treatment and few cells were PI positive. The increase in the PI signal of single-cells was not high as compared to the KAN at a concentration of 10 µg/mL. While the courses of PI signal with KAN at a concentration of 10 µg/mL demonstrated sudden increase in PI signal for most of the cells after 2 hours (Figure 39). Single-cell fluorescence traces for the cell number 1 indicated the continuous increase in calcein signal and no increase in PI signal. This indicated that the cell did not have damage in cell wall and it was metabolically active (Figure 40). Single-cell fluorescence traces of cell number 2 showed the variations in calcein signal. The signals were changing due to the changes in metabolic activity of cell or partial loss of calcein by leakage. Sudden decrease in calcein signal and increase in PI signal point out towards the lysis of cell (Figure 40). By comparing cell number 1 and 2 it can be seen that cell lysis, largely depended on the duration of KAN treatment and the ability of cells to tolerate the effect of KAN.

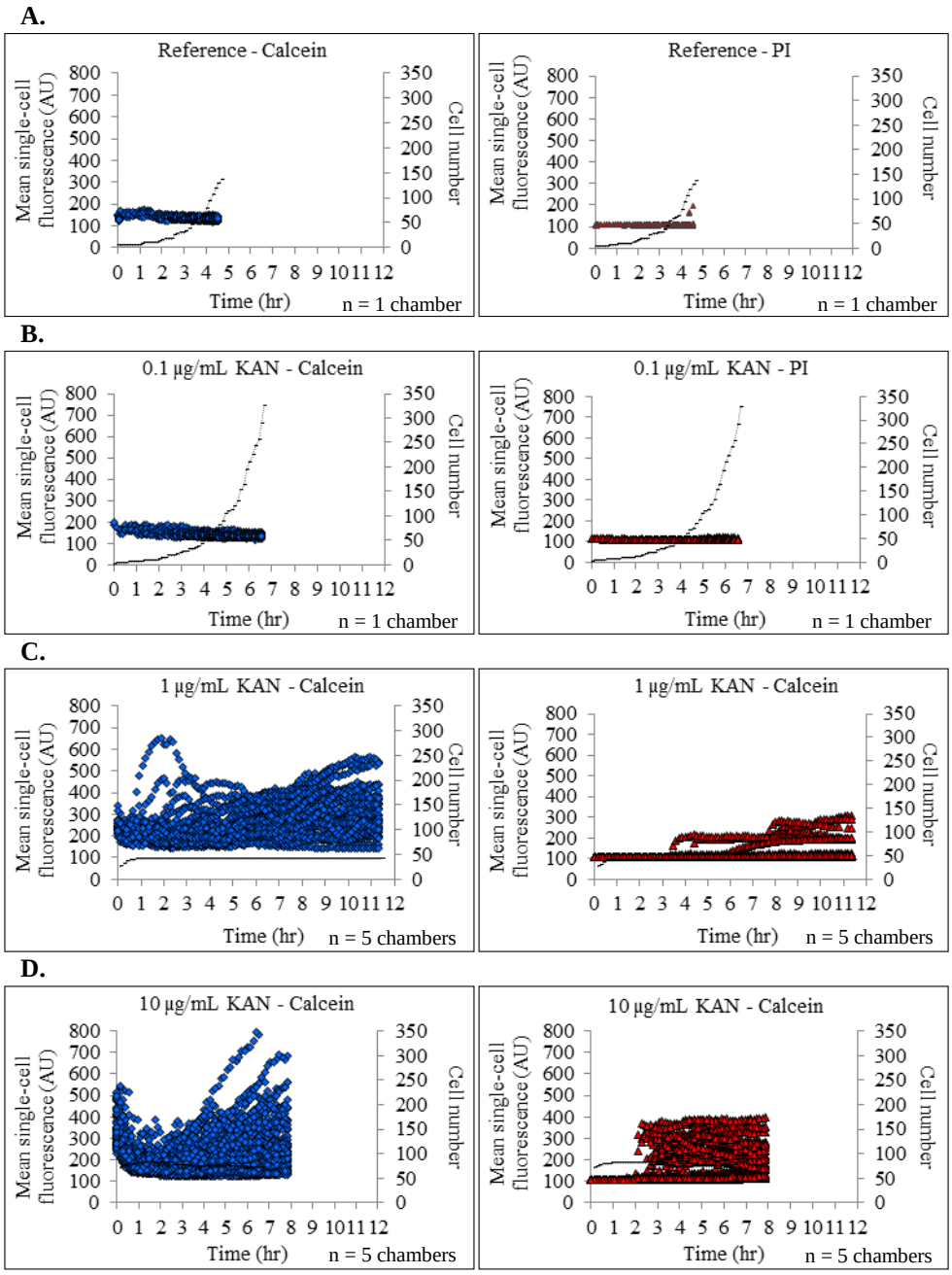

Figure 39. Single-cell analysis of *C. glutamicum* with KAN. (A. B. C. D.) Single-cell mean fluorescence of calcein (blue) and PI (red) over microcolony for reference and KAN at a concentration of 0.1 µg/mL, 1 µg/mL and 10 µg/mL are presented, respectively. Black line indicates cell number.

Single-cell fluorescence traces for the representative cells are presented in the diagrams below.

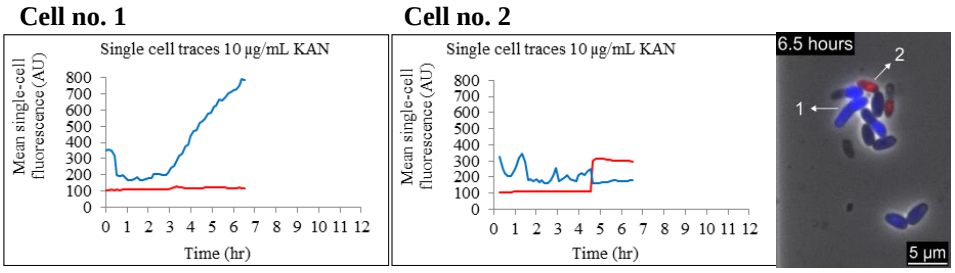

Figure 40. Single-cell fluorescence (calcein and PI) traces of representative *C. glutamicum* cells are presented with KAN concentration at 10 µg/mL. Corresponding cells are marked with numbers in the image.

4.4.1.4. Single-cell analysis of *C. glutamicum* with STR

The mode of action of STR is same as that of KAN. Single cells of *C. glutamicum* growing in the medium containing STR demonstrated similar behavior in the course of PI and calcein signal as observed with KAN. As described in previous chapters, STR at a concentration equal to and lower than 0.1 µg/mL, did not have significant effect on the physiology of cells. Single-cell analysis also elucidates similar results and no heterogeneity was found at single-cell level. Cells were found to have high heterogeneity in calcein signal if the concentration of STR was equal to and higher than 1 µg/mL. Increase in the calcein signal was observed to have temporal shift with increase in concentration of STR. If STR at a concentration of 1 µg/mL was used, single-cell calcein fluorescence started increasing and getting heterogeneous after 1 hour of experiment. While single-cell calcein fluorescence at a concentration higher than 1 µg/mL indicated less increase and calcein signals and cells were comparatively less heterogeneous. Similar temporal shift was also observed in single-cell PI fluorescence if the concentration of STR was increased. Single-cell PI signal was increased after 5 hours of experiment with STR at a concentration of 1 µg/mL, while single-cell PI signal appeared to be increased after 2 hours of experiment. Hence, there was a temporal shift of 3 hours in PI signal if the concentration of STR was increase from 1 µg/mL to 10 µg/mL (Figure 41). Single-cell fluorescence traces of cell number 1 demonstrate high variations in calcein signal during the course of experiment. It indicated that

there were changes in metabolic activity of the cell. The PI signal was not increased from the background signal, therefore, is can be concluded that the cell wall was not damaged (Figure 42). Single-cell fluorescence traces of cell number 2 indicated the presence of segmented cells. One sister cell gave high PI signal after 6 hours and other sister cell had very reduced calcein signal. High PI signal can be interpreted as the signal for cell death while reduced calcein indicated about the traces of cellular activity within the cell (Figure 42).

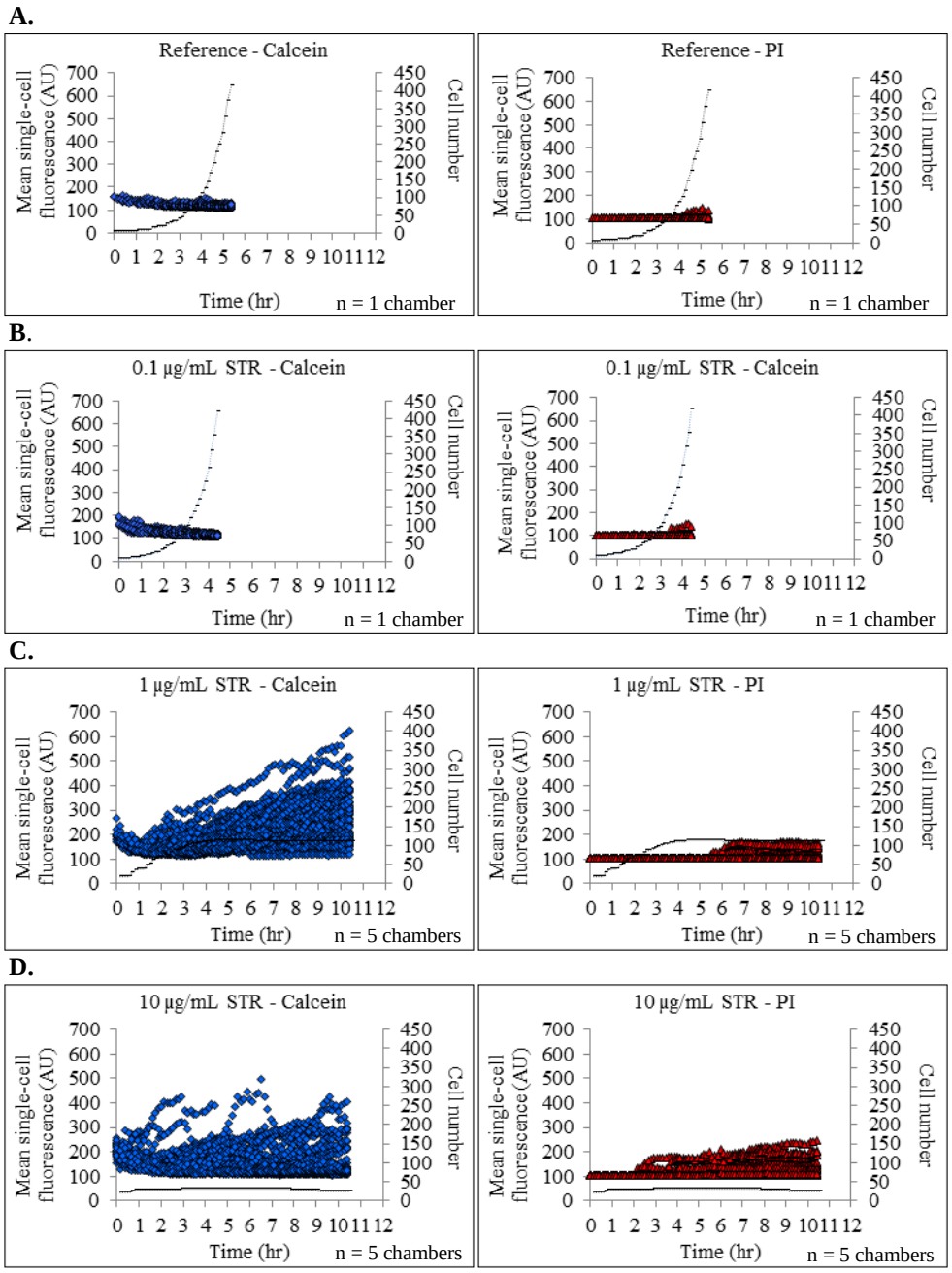

Figure 41. Single-cell analysis of *C. glutamicum* with STR. (A. B. C. D.) Single-cell mean fluorescence of calcein (blue) and PI (red) over microcolony for reference and STR at a concentration of 0.1 µg/mL, 1 µg/mL and 10 µg/mL are presented, respectively. Black line indicates cell number.

Single-cell fluorescence traces for the representative cells are presented in the diagrams below.

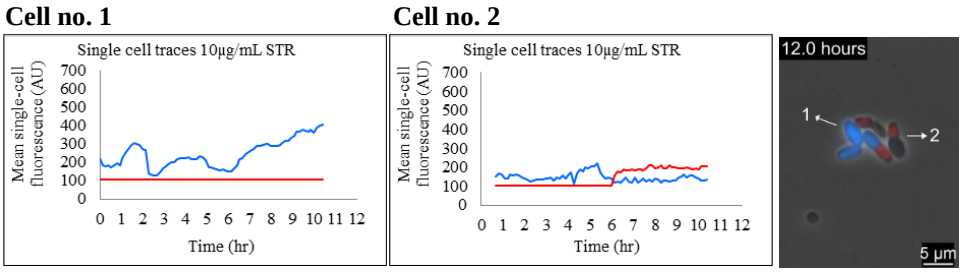

Figure 42. Single-cell fluorescence (calcein and PI) traces of representative *C. glutamicum* cells are presented with STR concentration at 10 µg/mL. Corresponding cells are marked with numbers in the image.

4.4.1.5. Single-cell analysis of *C. glutamicum* with MMC

MMC is an antibiotic which acts as DNA cross-linker and selectively inhibits the synthesis of DNA. As shown in previous chapters, MMC at concentration lower than 1000 nM, did not have significant effect on the physiology of cells in microcolony. Single-cell fluorescence analysis also demonstrated that there was a petite effect on the physiology of cells. Single-cell analysis indicated that, a minority of cells had increase in calcein signal after 3 hours for MMC concentration at 1000 nM. Similar increase was observed for MMC at a concentration of 500 nM after 5 hours. Thus if concentration of MMC was increased 2 folds, calcein signal indicated the temporal shift of 2 hours towards the start of experiment. Only a minority of the cells demonstrated this increase in calcein signal. An increase in calcein signal might be due to the reduced efflux of calcein and low energy of cells. Similarly, a rare appearance increase in PI signal was observed at different concentrations of MMC. Our single-cell analysis demonstrated that, *C. glutamicum* cells can tolerate MMC, if the concentration is lower than and equal to 1000 nM. As *C. glutamicum* cells did not show any peculiar difference in the physiology and fluorescence signals, single-cell traces were not prepared.

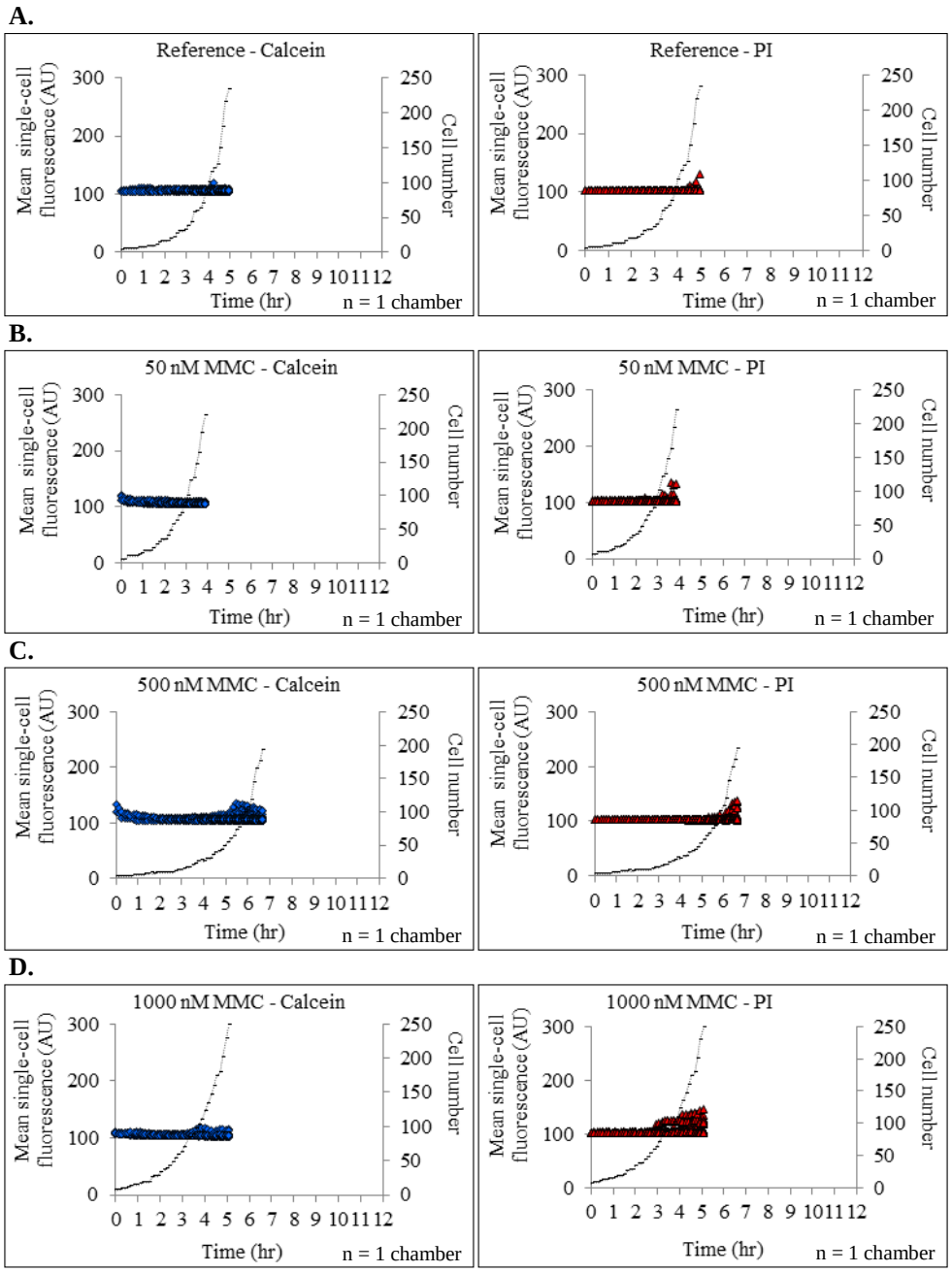

Figure 43. Single-cell analysis of *C. glutamicum* with MMC. (A. B. C. D.) Single-cell mean fluorescence of calcein (blue) and PI (red) over microcolony for reference and MMC at a concentration of 50 nM, 500 nM and 1000 nM are presented, respectively. Black line indicates cell number.

4.4.2. Single-cell analysis of *B. subtilis*

Single-cell fluorescence analysis of *C. glutamicum* demonstrated the heterogeneity of cells under the treatment of different concentrations of antibiotics. Similar analysis was carried out for *B. subtilis* to know its response to different antibiotics at single-cell level. As discussed in previous chapters, *B. subtilis* is a fast growing bacteria and show autolysis in normal conditions. Due to the autolysis of *B. subtilis* cells, fluorescence signals were observed for the reference. Single-cell analysis of *B. subtilis* is presented and discussed subsequently.

4.4.2.1. Single-cell analysis of *B. subtilis* with AMP

Single-cell analysis of *B. subtilis* under a treatment of AMP at a concentration lower than 0.1 µg/mL did not have much impact on the physiology of cells. Single-cell heterogeneity was increased by increasing AMP concentration higher than 0.1 µg/mL. PO-PRO1 signals were observed to be increased rapidly, shortly after the start of experiment. There was an abrupt increase in PO-PRO1 signal for AMP at a concentration of 1 µg/mL, while increase in single-cell PO-PRO1 fluorescence of AMP at a concentration of 10 µg/mL had a pattern. In this pattern, a gradual increase in the PO-PRO1 signal continued till 3 hours after the start of experiment and a sudden increase was observed thereafter. Comparing the PO-PRO1 signals for both the concentrations, it was observed that, the cells lost their membrane potential faster at a concentration of 1 µg/mL. Similarly, single-cell PI fluorescence demonstrated an increase in PI signal apparently at 1 hour for AMP at a concentration of 1 µg/mL. Increase in PI signal for a concentration higher than 1 µg/mL was observed after 2 hours. Hence, it can be said that the cells were lysed faster with AMP concentration at 1 µg/mL. Single-cell fluorescence traces were prepared for the cells growing with AMP at a concentration of 10 µg/mL (Figure 44). Single-cell fluorescence traces of cell number 1 demonstrated a sudden increase in PO-PRO1 signal after 1 hour while the PI signal was increased after 3 hours. This illustrated that there was not necessary a co-relation in the time of increase in PO-PRO1 and PI signals (Figure 45). Single-

cell fluorescence traces of cell number 2 showed sudden and simultaneous increase in PO-PRO1 and PI signal. A sudden increase in both signal indicated the cell lysis. Simultaneous increase in both fluorescence signals was a proof of cell death (Figure 45).

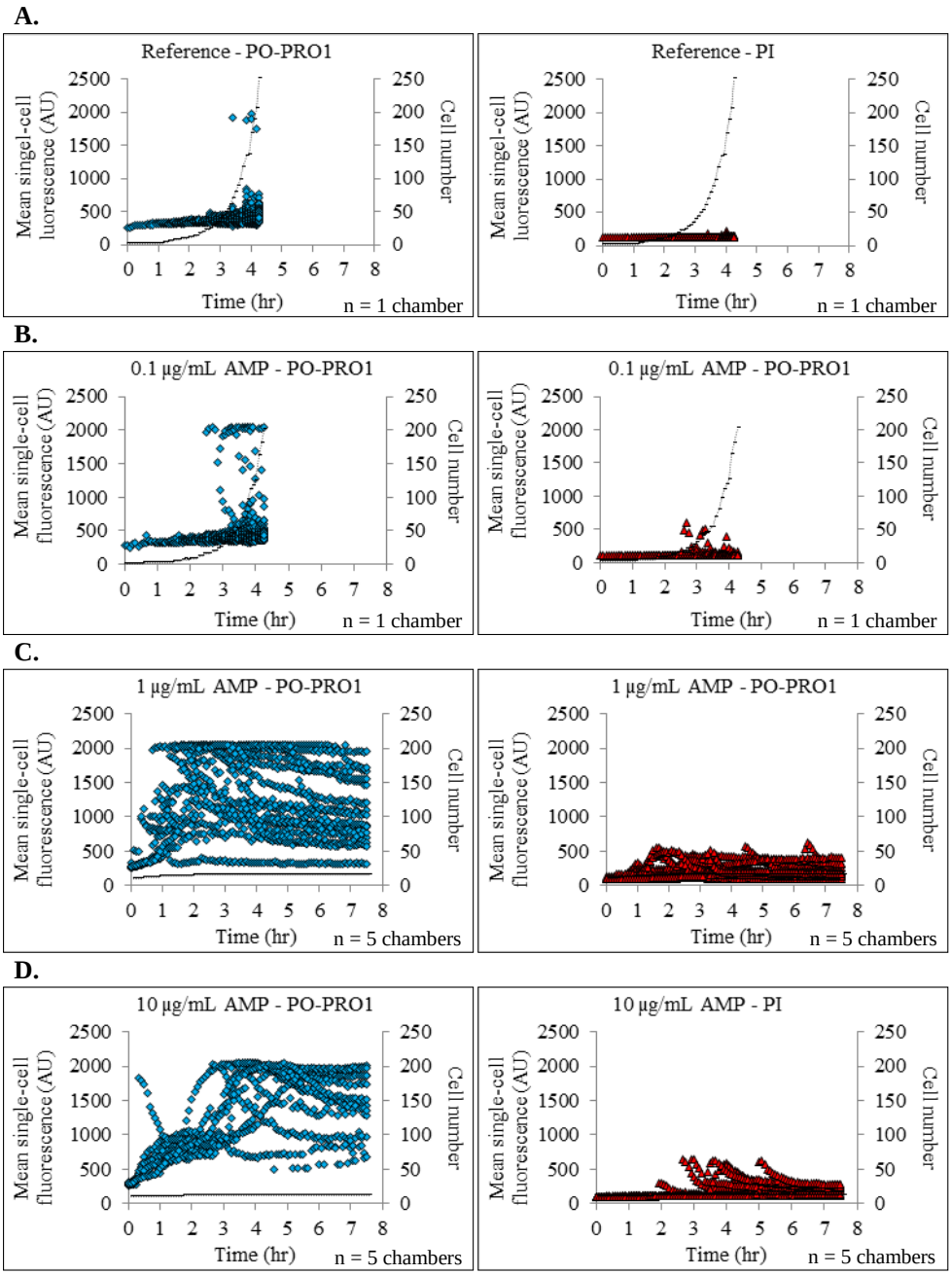

Figure 44. Single-cell analysis of *B. subtilis* with AMP. (A. B. C. D.) Single-cell mean fluorescence of PO-PRO1 (blue) and PI (red) over microcolony for reference and AMP at a concentration of 0.1 µg/mL, 1 µg/mL and 10 µg/mL are presented, respectively. Black line indicates cell number.

Single-cell fluorescence traces for the representative cells are presented in the diagrams below.

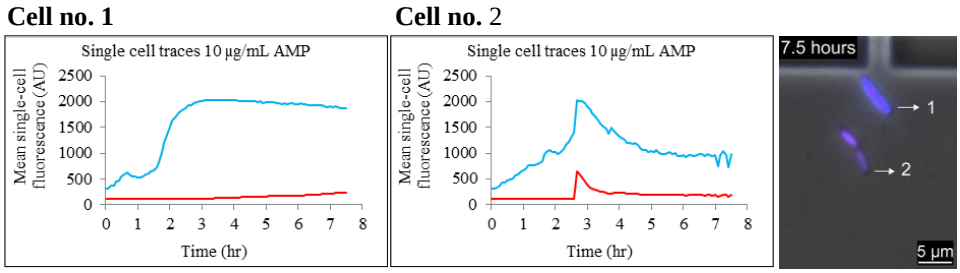

Figure 45. Single-cell fluorescence (PO-PRO1 and PI) traces of representative *B. subtilis* cells are presented with AMP concentration at 10 µg/mL. Corresponding cells are marked with numbers in the image.

4.4.2.2. Single-cell analysis of *B. subtilis* with CHL

As described in previous chapters that CHL at a concentrations lower than and equal to 1 µg/mL, did not have any impact on the fluorescence of the cells. Single-cell fluorescence analysis also indicated that, in spite of the suppression in growth and change in morphology, single-cells did not give PO-PRO1 and PI fluorescence signals. If the concentration of CHL was increased to 10 µg/mL, a uniform increase was observed in the course of single-cell PO-PRO1 fluorescence signal during the experiment. There was a slight increase observed in the PI fluorescence towards the end of the experiment. The PO-PRO1 signal indicated towards the slow loss of membrane potential due to the impact of CHL (Figure 46). In a minority of cells represented by cell number 1, sudden increase in the PO-PRO1 fluorescence was observed after a gradual increase. A slight increase in PI signal was also observed simultaneously. This sudden increase in the fluorescence signals illustrated the damage in cell wall so that both dyes could enter the cell and bind to the DNA (Figure 47). Single-cell traces of cell number 2 demonstrate the gradual increase in the PO-PRO1 fluorescence. Thus, cell number 2 represents the response of majority of cells in the microcolony towards the treatment (Figure 47).

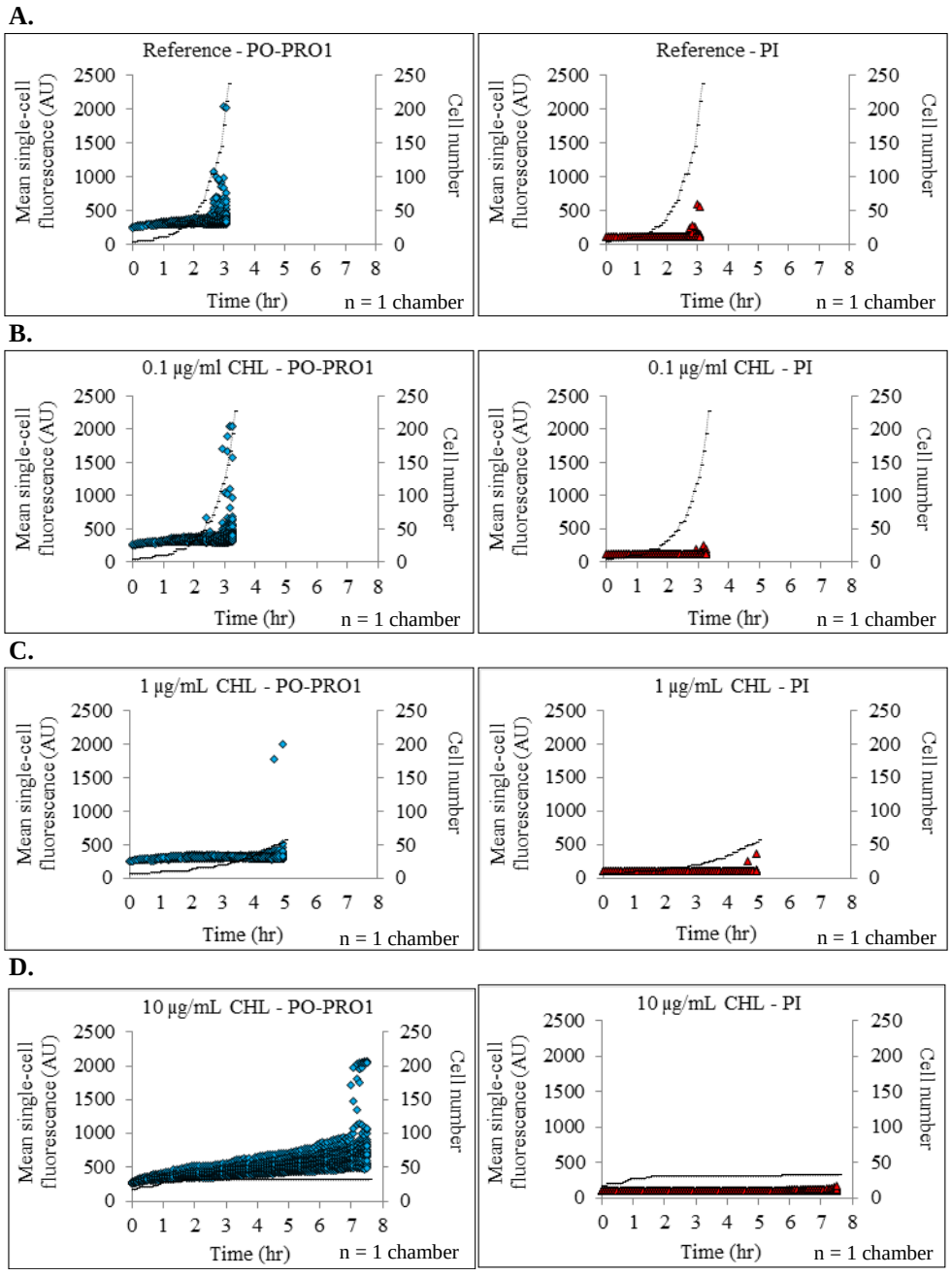

Figure 46. Single-cell analysis of *B. subtilis* with CHL. (A. B. C. D.) Single-cell mean fluorescence of PO-PRO1 (blue) and PI (red) over microcolony for reference and CHL at a concentration of 0.1 µg/mL, 1 µg/mL and 10 µg/mL are presented, respectively. Black line indicates cell number.

Single-cell fluorescence traces for the representative cells are presented in the diagrams below.

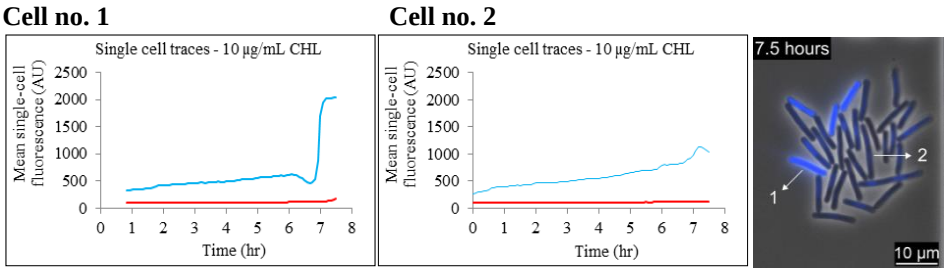

Figure 47. Single-cell fluorescence (PO-PRO1 and PI) traces of representative *B. subtilis* cells are presented with CHL concentration at 10 µg/mL. Corresponding cells are marked with numbers in the image.

4.4.2.3. Single-cell analysis of *B. subtilis* with KAN

Single-cell fluorescence analysis *B. subtilis* with KAN revealed that, PO-PRO1 signal followed a pattern, if concentration was increased to 1 µg/mL and higher. Single-cell PO-PRO1 fluorescence increased gradually for first hour of the experiment and thereafter signal became very high as compared to previous signals. Similar patterns for majority of cell in a microcolony with KAN at a concentration of 1 µg/mL and 10 µg/mL demonstrated that 2 hours of KAN treatment at a concentration higher than 1 µg/mL can kill *B. subtilis* cells. However, no increase in the PI fluorescence signal also indicated that, the death of cells was caused due to the inhibition of cellular metabolic functions without significant damage to the cell wall (Figure 48). Single-cell traces were prepared for representative cells grown with KAN at a concentration of 10 µg/mL, to visualize the change in fluorescence over time. Cell number 1 and 2 demonstrated the similar pattern of change in fluorescence signal, although there were temporal differences in the signals. The temporal differences in fluorescence caused due to relatively different times of the loss in the membrane potential of cell number 1 and 2 (Figure 49).

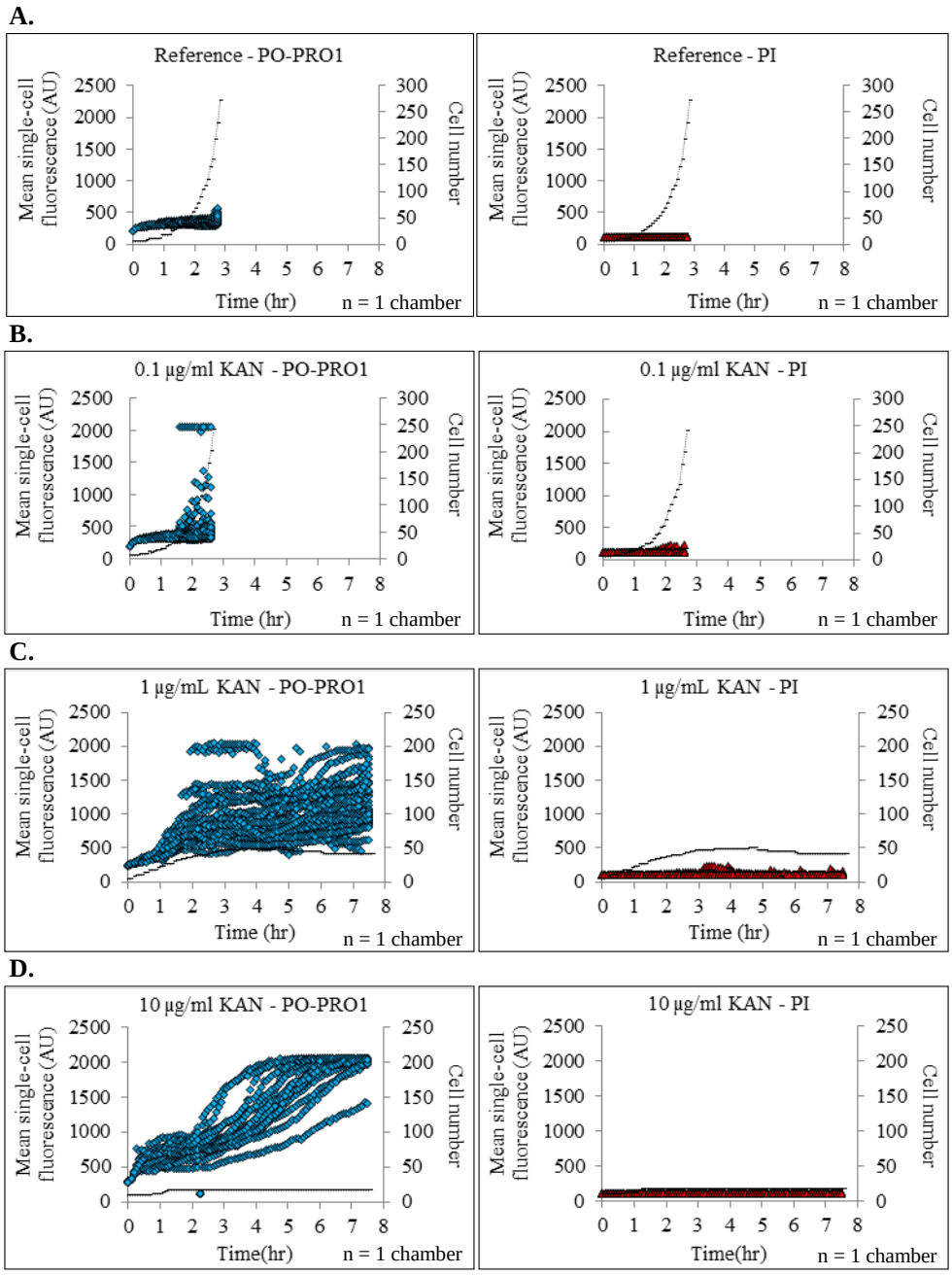

Figure 48. Single-cell analysis of *B. subtilis* with KAN. (A. B. C. D.) Single-cell mean fluorescence of PO-PRO1 (blue) and PI (red) over microcolony for reference and KAN at a concentration of 0.1 µg/mL, 1 µg/mL and 10 µg/mL are presented, respectively. Black line indicates cell number.

Single-cell fluorescence traces for the representative cells are presented in the diagrams below.

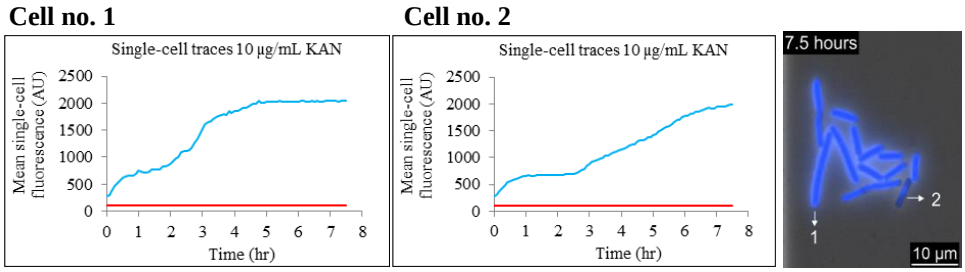

Figure 49. Single-cell fluorescence (PO-PRO1 and PI) traces of representative *B. subtilis* cells are presented with KAN concentration at 10 µg/mL. Corresponding cells are marked with numbers in the image.

4.4.2.4. Single-cell analysis of *B. subtilis* with STR

On the contrary to KAN, *B. subtilis* appeared to be less susceptible towards STR treatment. Single-cell analysis demonstrated that majority of cells in the microcolony were PO-PRO1 negative. Only a minority of the cells were observed to be PO-PRO1 positive. Single-cell traces for the representative PO-PRO1 positive cells were prepared, which indicated about the time difference and variations in the PO-PRO1 signal during the experiment. PO-PRO1 signal of cell number 1 increased gradually for first two hours and sudden increase was observed after 2 hours of STR treatment (Figure 51). Cell number 2 originated 1 hour after the start of experiment. Hence, the beginning of fluorescence signal represents the birth of cell. A sudden increase in the PO-PRO1 fluorescence of cell number 2 was observed after 5 hours. The sudden increase indicated the loss of membrane potential and death of cells (Figure 51). The temporal differences in the fluorescence signal of both cells might be due to the difference in susceptibility of individual cell towards STR. As both the cells did not give PI fluorescence signal, it can be interpreted that PI could not intrude the cells because the cell wall did not produce damages.

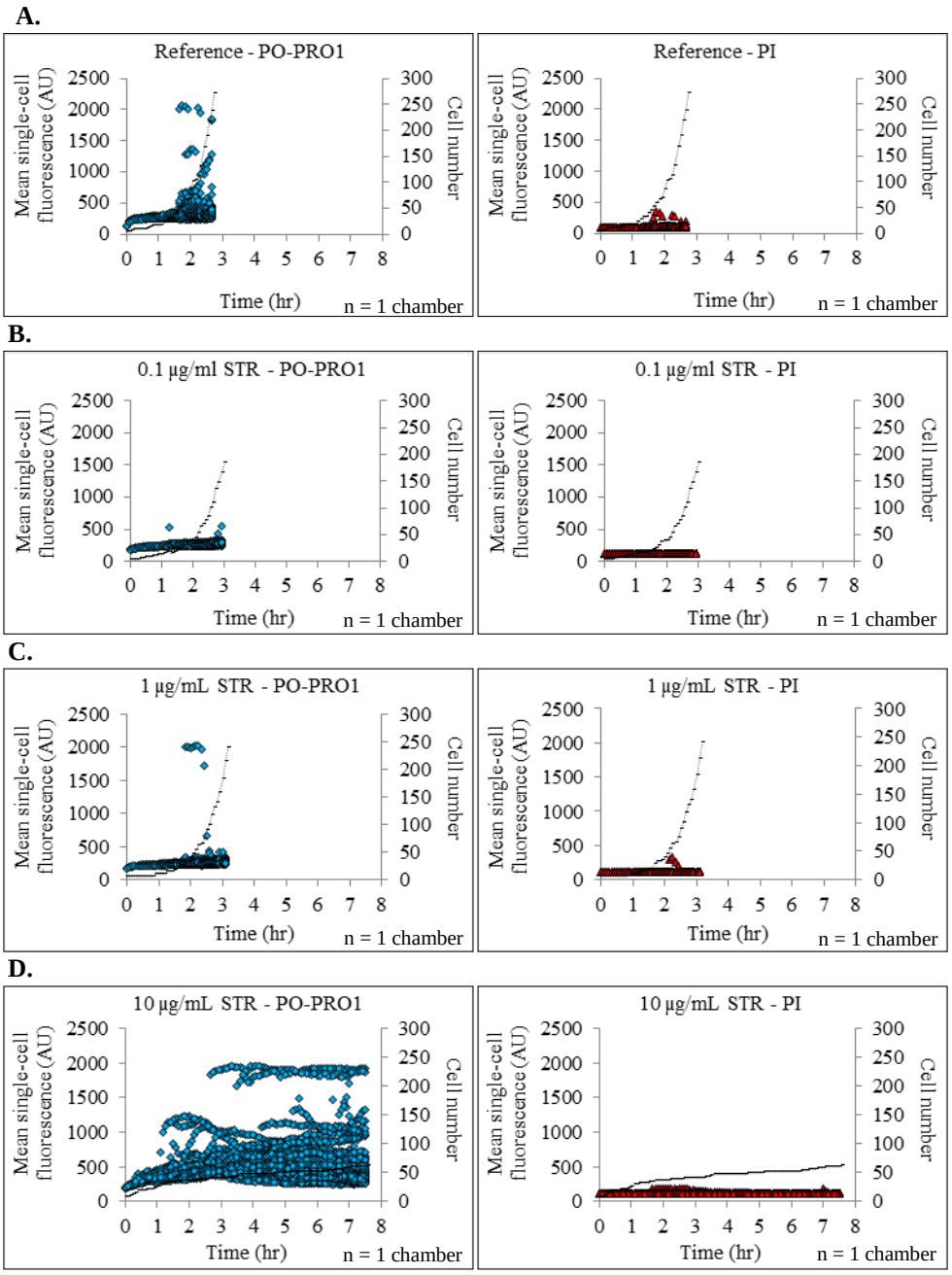

Figure 50. Single-cell analysis of *B. subtilis* with STR. (A. B. C. D.) Single-cell mean fluorescence of PO-PRO1 (blue) and PI (red) over microcolony for reference and STR at a concentration of 0.1 µg/mL, 1 µg/mL and 10 µg/mL are presented, respectively. Black line indicates cell number.

Single-cell fluorescence traces for the representative cells are presented in the diagrams below.

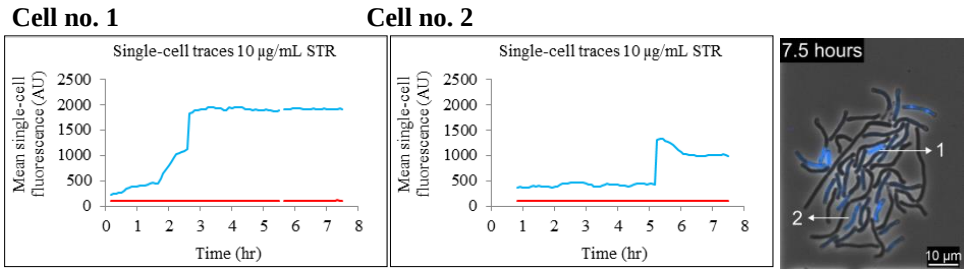

Figure 51. Single-cell fluorescence (PO-PRO1 and PI) traces of representative *B. subtilis* cells are presented with STR concentration at 10 µg/mL. Corresponding cells are marked with numbers in the image.

4.4.2.5. Single-cell analysis of *B. subtilis* with MMC

As described before, *B. subtilis* was highly susceptible to MMC at a concentration equal to and higher than 500 nM. Single-cell analysis of *B. subtilis* with MMC demonstrated that in spite of disintegration of cells, a majority of cell did not give PO-PRO1 and PI fluorescence signal. In the single-cell analysis of *B. subtilis* with MMC at a concentration of 500 nM, few cells appeared to have high PO-PRO1 signal, while relatively no PO-PRO1 signal with MMC concentration at 1000 nM. It can be explained by the fact that, increased concentration of MMC made disintegration process rapid and lysis of cells occurred before the appearance of fluorescence signals. Single-cell analysis indicated towards the co-relation between the MMC concentration and the dynamics of disintegration of *B. subtilis* cells.

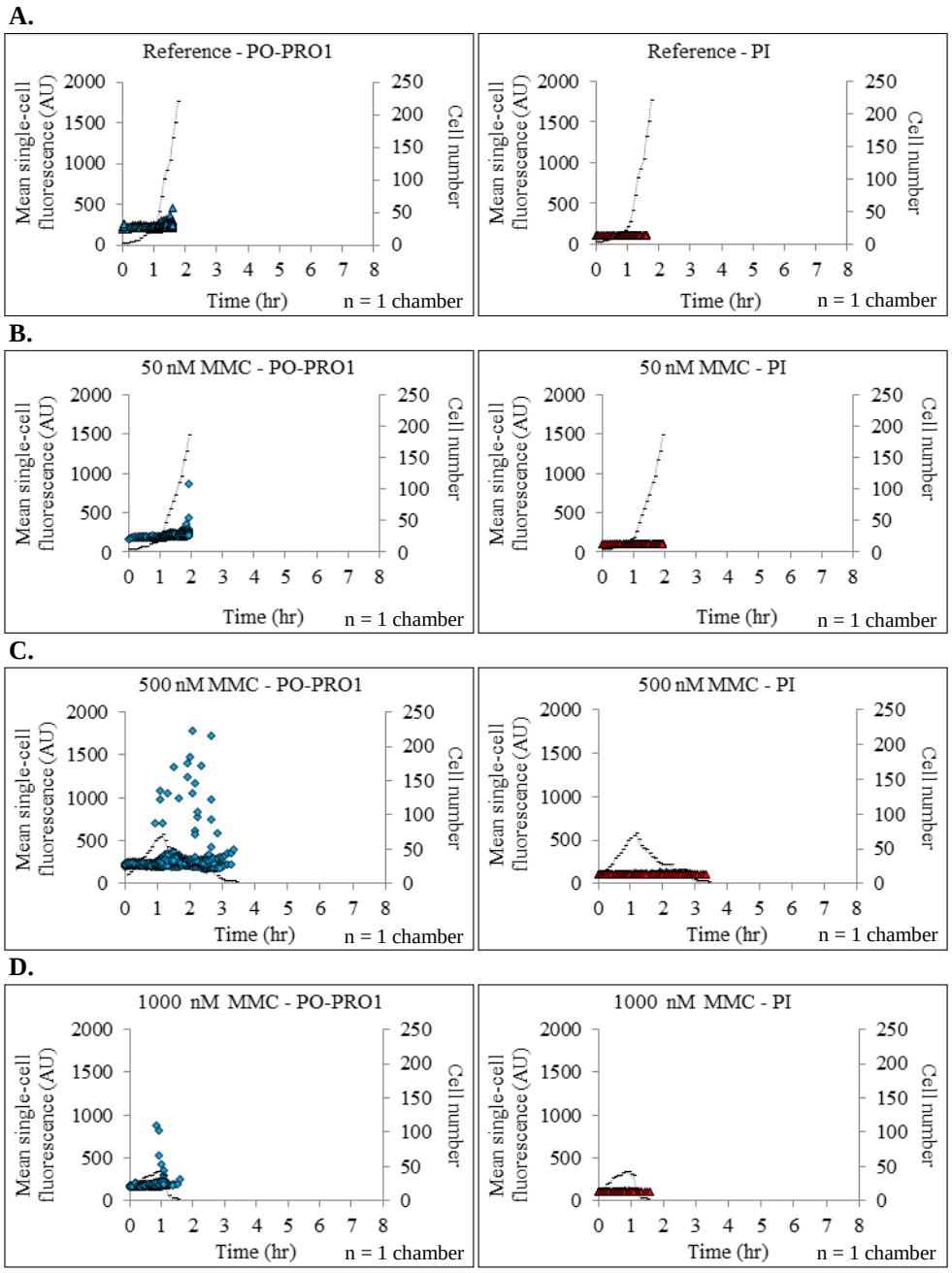

Figure 52. Single-cell analysis of *B. subtilis* with MMC. (A. B. C. D.) Single-cell mean fluorescence of PO-PRO1 (blue) and PI (red) over microcolony for reference and MMC at a concentration of 50 nM, 500 nM and 1000 nM are presented, respectively. Black line indicates cell number.

Single-cell analysis revealed the heterogeneous response of individual bacterial cells of a microcolony during the long period of antibiotic treatment. The appearance of segmented *C. glutamicum* cells during the antibiotic treatment was the most important aspect illustrated by the single-cell fluorescence analysis. It demonstrated the phenotypic tolerance of few cells which kept their metabolic activity when majority of cells were dead due to the

antibiotic treatment. The different responses of individual bacterial cells of a population to antibiotic treatment is known as heteroresistance (El-Halfawy and Valvano 2015). The phenomenon of heteroresistance is not yet properly characterized and concensus based definations are not established. They have critically reviewed the phenomenon of heteroresistance and found out that there are discrepancies in the heteroresistance analysed by different methods. Therefore, there is a need for the method which can assist in the characterization of heteroresistance, because lack of the standard definition might cause misidentification of homogeneous strains as heteroresistant and impede an accurate assesment of its clinical relevance. Thus, MSCA can be very much helpful in the characterization of heteroresistance.

Single-cell analysis also illustrated the reason for the high standard deviation in the mean fluorescence analysis. The standard deviation in the mean fluorescence was caused due to the heterogeneous response of individual single-cells of bacteria in an isogenic micropopulation. Thus the variation in the individual cell response can be accurately analysed by single-cell fluorescence analysis.

4.5. Regrowth experiments of *C. glutamicum*

Regrowth of bacteria after the antibiotic treatment has a very high clinical relevance in the treatment of infectious bacterial diseases. It is important because, the recurrence of disease after an antibiotic therapy or the infection of bacteria after a disinfection treatment causes severe losses to lives and economy every year (Keller and Kuijper 2015; Prantera *et al.* 2002). If the antibiotic therapy is not followed properly followed according to the prescription, the chances of the regrowth of bacteria are very high. To understand the effect of brief period of antibiotic treatment, regrowth experiments were performed with *C. glutamicum* and antibiotic candidates AMP and CHL. In the start of the experiment, bacterial cells were allowed to grow with the normal culture media without antibiotics for 1 hour. This allowed them to reach the exponential phase of growth. Normal culture media was switched with the media containing respective antibiotic at a concentration of 10 µg/mL. The antibiotic treatment was carried out for one hour and after that, media was again switched with the normal media. To sense the changes in the metabolic activity of the bacteria due to antibiotic shock, calcein-AM was used as a fluorescence sensor. The results are the mean value of five microcolonies. Single-cell fluorescence traces for one representative microcolony were prepared to see the response of individual single bacterial cell during the experiment. The results are presented and discussed simultaneously in the following.

4.5.1. Regrowth experiments of *C. glutamicum* with AMP

C. glutamicum grown for an hour without antibiotic exhibited the increase in the cell number and decrease in the calcein fluorescence. As discussed earlier, the decrease in the calcein fluorescence was due to the fast cell growth and energy dependent efflux of calcein from the cell. The decrease in the calcein signal was observed for 1 hour of undisturbed growth. After initial 1 hour, *C. glutamicum* was treated with AMP at a concentration of 10 µg/mL for 1 hour (Figure 53). As soon as normal media was switched to the media with antibiotic, sudden increase in the calcein fluorescence was observed, which indicated the stress on the metabolic activity of *C. glutamicum*. During the

antibiotic treatment, growth of the cells was suppressed and the reduction in calcein signal was observed. As cells were not growing, the reduction in calcein signal indicated the changes in metabolic activity of cells. After 1 hour of AMP treatment, perfusion media was again changed to normal medium without AMP. After a shift in culture medium, increase in calcein fluorescence was observed and cell did not grow for almost 3 hours. This was the recovery phase (~3 hours) of the cells. As AMP was not present in the microenvironment of cells, an increase in calcein signal was observed. During the recovery phase, variations in the calcein signal indicted the increase in the metabolic activity after antibiotic shock. After 4 hours, a decrease in the calcein signal was observed along with the increase in the cell number. In this condition, as cells had recovered from the antibiotic shock and started to multiply, the decrease in calcein signal can be explained due to the growth of *C. glutamicum* cells. Single-cell fluorescence traces were prepared which indicated that, after the antibiotic shock, cells responded differently. Few cells did not grow and few cells had variations in calcein fluorescence. The variations were seen during the recovery phase which was for 3 hours after the AMP treatment. After the recovery phase, cells started to grow and the variations were also gradually reduced. Few cells were also found to have difference in calcein signal after the recovery phase. It might be due to the heterogeneity in metabolic activity and physiology of these cells after antibiotic contact.

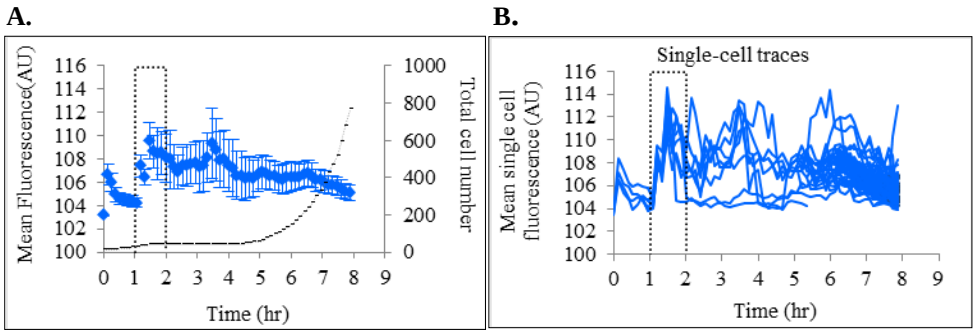

Figure 53. Regrowth experiment of *C. glutamicum* with AMP. (A) Mean calcein (blue) fluorescence of five microcolonies. Black line indicates the cell numbers present in five MGC. (B) Mean single-cell calcein traces for the cells in one representative microcolony. The window represent the period of 1 hour AMP treatment at a concentration of 10 µg/mL.

4.5.2. Regrowth experiments of *C. glutamicum* with CHL

To see the effect of brief period of CHL treatment with *C. glutamicum*, regrowth experiment was carried out CHL. Cells were allowed to grow without CHL for 1 hour. As soon as cells came in contact with calcein, increase in the fluorescence signal was observed followed by gradual decrease in signals. The decrease was caused due to growth and calcein efflux in undisturbed conditions, as described earlier. After initial growth, the media was shifted to media with CHL. When the cells came in contact with CHL at a concentration of 10 µg/mL, a slight increase was observed followed by sudden decrease in calcein fluorescence. There are two interrelated reasons for this. One is the fact that CHL induced stress in the cells thus initially a slight increase in the calcein signal was seen as soon as cell came in contact with CHL. Furthermore, it is known that CHL inhibits cellular enzymatic activity (Smith, Worrel, and Swanson 1949). The sudden decrease in calcein fluorescence was due to the CHL stress which inhibited the enzymatic activity in cells (Figure 54). After 1 hour of CHL treatment, media was shifted to the normal perfusion medium for regrowth. The recovery phase for the cells was short as compared to AMP. It lasted for 1.5 hours and after that, cells started to grow and divide. Increase in the calcein signal was observed after the recovery phase, which indicated the regaining of enzymatic activity by *C. glutamicum* cells. Single-cell calcein traces were prepared for one representative microcolony and it was observed that individual cells were having similar course of fluorescence as the mean fluorescence of microcolony. After the recovery phase, except few cells, all cells were having similar course of calcein signal. Single-cell fluorescence traces indicated that, after the recovery phase, few cells were appeared to have high calcein signal in respect to other cells in the microcolony. It indicated towards the possibility that, 1 hour of treatment with CHL at a concentration of 10 µg/mL, resulted some changes in the cells which might have caused abnormalities in the further generations. As CHL inhibits protein synthesis, one reason might also be the chances of faulty protein synthesis which might have induced by CHL in generations of which were not in the direct contact with CHL.

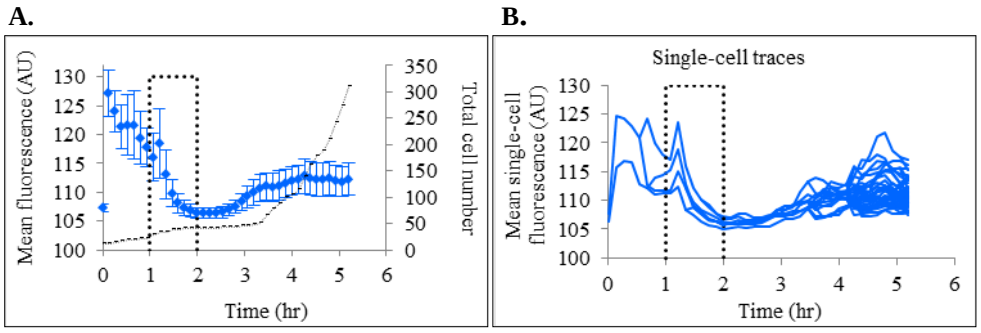

Figure 54. Regrowth experiment of *C. glutamicum* with CHL. (A) Mean calcein (blue) fluorescence of five microcolonies. Black line indicates the cell numbers present in five MGC. (B) Mean single-cell calcein traces for the cells in one representative microcolony. The window represent the period of 1 hour chloramphenicol treatment at a concentration of 10 µg/mL.

Regrowth experiments of *C. glutamicum* showed that AMP was a strong antibiotic as compared to CHL. The stress caused by both the antibiotic could be seen by the calcein signals which have much differences. On one hand, AMP caused high variation in the calcein signal and longer recovery phase, while on the other hand calcein signal was more homogeneous with a short recovery phase. Regrowth of bacteria after an antibiotic therapy is very important parameter in the treatment of diseases. There are many diseases like tuberculosis and Crohn's disease, which causes many deaths due to the recurrence of disease, and economic losses due to regrowth of bacteria in processed food products. The regrowth experiments with the MSCA method can be very helpful in understanding the dynamics of bacterial regrowth and physiology thus can directly assist in deciding the course and duration of antibiotic therapy.

5. Conclusions and outlook

In this thesis, microfluidic single-cell studies have been conducted for *C. glutamicum* and *B. subtilis* with different concentrations of AMP, CHL, KAN, STR and MMC. These studies were focused on the analysis of bacterial physiology growth with the use of different dynamic fluorescence staining methods under antibiotic treatment. The fluorescent dyes used for *C. glutamicum* were calcein-AM and PI whereas the fluorescent dyes used for *B. subtilis* were PO-PRO1 and PI, because calcein-AM was not metabolized by *B. subtilis*. With the help of these fluorescence signals, real time analysis of bacterial physiological changes upon antibiotic treatment had been performed.

The dynamic fluorescence staining assisted MSCA has shown the potential to be an ideal assay for the assessment of bacterial physiology and susceptibility towards an antibiotic. MSCA provides in-depth real time information of bacterial physiological changes in growth rate, metabolic activity, viability, microbial heterogeneity.

In order to analyze the antibiotic susceptibility, detailed studies on the basis of aforesaid physiological parameters have been conducted. These studies have shown in detail, the interactions of *C. glutamicum* and *B. subtilis* with antibiotics of different modes of action. Coherent results were obtained in the analysis with agar plate and MSCA method. But in case of *C. glutamicum* and AMP, higher sensitivity was observed with MSCA method. The explanation of an increased antibiotic sensitivity of *C. glutamicum* in MSCA analysis could be due to the absence of diffusional limitations of AMP into the cells. Based on this result a hypothesis can be made that, diffusion of antibiotics into bacterial cells might depend on the physical state of the media in which antibiotics are present, and it can be estimated that diffusion of antibiotics improves, if they are present in liquid medium.

Furthermore, the fluorescence analysis of bacterial physiology has shown the effect of the antibiotics on metabolic activity and viability of bacterial cells. The results of the fluorescence analysis revealed that different antibiotics had different effects on the physiology of the bacterial cells. For instance, the fluorescence analysis with *C. glutamicum* and AMP illustrated

that the antibiotics, which inhibit cell wall synthesis were more effective in changing the morphology and physiology of bacterial cells, if the cells were actively growing (Neumeyer *et al.* 2013). The fluorescence analysis with *C. glutamicum* and *B. subtilis* with CHL indicated that the nature of antibiotics depends on the concentration of antibiotics. The high concentration of bacteriostatic antibiotics can be bactericidal, as observed in case of CHL.

Moreover, fluorescence analysis of *C. glutamicum* indicated towards the changes in the metabolic activity of the cells due to antibiotic treatment. For instance, CHL inhibits protein synthesis, thus blocks the formation of new enzymes in the cells. Also, it had an inhibiting effect on intracellular enzymes (Smith, Worrel, and Swanson 1949). In case of KAN and STR, which inhibits protein synthesis, the variations in the intracellular metabolic activity were observed for individual cells. These variations in the metabolic activity might be caused due to the changes in energy status of cells (Martínez and Rojo 2011; Andersson and Levin 1999; Andersson 2006; Baquero, Coque, and De La Cruz 2011) upon antibiotic treatment. *C. glutamicum* was found to be more susceptible for KAN as compared to STR. The instance when MMC was used with *C. glutamicum*, the result indicated that *C. glutamicum* was less sensitive for the concentration of MMC used in the experiments.

Fluorescence analysis of *B. subtilis* with PO-PRO1 has revealed that in the progress of cell death, the membrane potential was lost prior to the damage in cell wall. Bacterial physiology and morphology had a significant role in the response towards antibiotics (Novo *et al.* 1999). For instance, *C. glutamicum* was more susceptible towards cell lysis in highest concentration of antibiotics (AMP, CHL, STR, KAN) tested as compared to *B. subtilis.* The reason for the different susceptibility towards cell lysis could be due to the differences in the cell morphology, architecture of cell wall and the growth characteristics of both bacteria (Daniel and Errington 2003). Hence, the choice of an antibiotic for the treatment of specific bacterial infection depends on the bacterial species (El-Halfawy 2015).

Single-cell fluorescence analysis has illustrated the heterogeneous response of individual bacterial cells under an antibiotic treatment. The individuals of an isogenic population can differ widely in physiology under an

antibiotic treatment, but these heterogeneous responses of various bacteria is not yet completely characterized for different antibiotics (El-Halfawy 2015). Nevertheless, heteroresistance has high relevance in the antimicrobial susceptibility analysis. As the lack of a standard definition of heteroresistance might hamper the assessment of its clinical significance and might lead to the misinterpretation of homogeneous strains as heteroresistant. The MSCA can be a powerful tool in the characterization of bacterial heterogeneity under antibiotic treatment.

The aforesaid experiments were performed to analyze the effect of long period of antibiotic treatment on the bacterial physiology. In order to analyze the changes in bacterial physiology upon a brief period of antibiotic treatment, separate experiments have been performed with *C. glutamicum* and two antibiotic candidates *i.e.* AMP and CHL. It has been found out that, upon exposure to the antibiotics for a short period of time (1 hour), AMP caused high variation in the calcein signals, which indicated the varied responses of the individual bacterial cell in the metabolic activity. 1 hour of treatment with CHL did not caused high variation in the fluorescence in recovery phase. After 1 hour of antibiotic treatment, the recovery of the bacteria was slow in case of AMP as compared to CHL. Hence, the MSCA method also paved the possibility of regrowth studies of bacteria with real time observation of physiology and metabolic responses under an antibiotic treatment. Additionally, the real time observation of growth based on the individual cells indicated that there was a time dependent death of bacterial cells in the long antibiotic treatment experiment. The characterization of the relation of time and cell death in various concentrations of antibiotics needs further studies. The precise characterization of the time dependent dynamics of cell growth and death in AST could be very helpful in the development of pharmacodynamic models of antibiotics (Hou *et al.* 2014).

To summarize the results of the antibiotic susceptibility analysis, MSCA method for the AST has revealed many interesting responses of *C. glutamicum* and *B. subtilis* upon antibiotic treatment. Thus, MSCA method not only provides the antibiotic susceptibility information on the basis of bacterial growth, but also it provides the information of physiological changes of

bacteria. The results of physiological analysis with different antibiotics might provide a background for the future studies of bacteria with different antibiotics. Such studies could be very helpful in the clinical applications and development of new antibiotics in pharmaceutical industries. As MSCA method provides high throughput single-cell information of bacterial physiology, it can be widely used for the studies of bacteria in agriculture, food processing industries, waste water treatment plants and environmental microbiology.

References

Andersson, Dan I. 2006. "The Biological Cost of Mutational Antibiotic Resistance: Any Practical Conclusions?" *Current Opinion in Microbiology* 9 (5): 461–65. doi:10.1016/j.mib.2006.07.002.

Andersson, Dan I., and Bruce R. Levin. 1999. "The Biological Cost of Antibiotic Resistance." *Current Opinion in Microbiology* 2 (5): 489–93. doi:10.1016/S1369-5274(99)00005-3.

Andrews, Jennifer M. 2001. "JAC Determination of Minimum Inhibitory Concentrations," 5–16.

Baquero, Fernando, Teresa M. Coque, and Fernando De La Cruz. 2011. "Ecology and Evolution as Targets: The Need for Novel Eco-Evo Drugs and Strategies to Fight Antibiotic Resistance." *Antimicrobial Agents and Chemotherapy* 55 (8): 3649–60. doi:10.1128/AAC.00013-11.

Binder, Dennis, Alexander Grünberger, Anita Loeschcke, Christopher Probst, Claus Bier, Jörg Pietruszka, Wolfgang Wiechert, Dietrich Kohlheyer, Karl-Erich Jaeger, and Thomas Drepper. 2014. "Light-Responsive Control of Bacterial Gene Expression: Precise Triggering of the Lac Promoter Activity Using Photocaged IPTG." *Integrative Biology : Quantitative Biosciences from Nano to Macro* 6 (8): 755–65. doi:10.1039/c4ib00027g.

Branda, Steven S., Frances Chu, Daniel B. Kearns, Richard Losick, and Roberto Kolter. 2006. "A Major Protein Component of the *Bacillus subtilis* Biofilm Matrix." *Molecular Microbiology* 59 (4): 1229–38. doi:10.1111/j.1365-2958.2005.05020.x.

Breeuwer, P., and T. Abee. 2000. "Assessment of Viability of Microorganisms Employing Fluorescence Techniques." *International Journal of Food Microbiology* 55 (1-3): 193–200. doi:10.1016/S0168-1605(00)00163-X.

Brehm-stecher, Byron F, Eric A Johnson, Byron F Brehm-stecher, and Eric A Johnson. 2004. "Single-Cell Microbiology : Tools , Technologies , and Applications Single-Cell Microbiology : Tools , Technologies , and Applications" 68 (3). doi:10.1128/MMBR.68.3.538.

Chai, Yunrong, Frances Chu, Roberto Kolter, and Richard Losick. 2008. "Bistability and Biofilm Formation in *Bacillus subtilis*." *Molecular Microbiology* 67 (2): 254–63. doi:10.1111/j.1365-2958.2007.06040.x.

Chen, Chia Hsiang, Yi Lu, Mandy L Y Sin, Kathleen E Mach, Donna D Zhang, Vincent Gau, Joseph C Liao, and Pak Kin Wong. 2010. "Antimicrobial Susceptibility Testing Using High Surface-to-Volume Ratio Microchannels" 82 (3): 1012–19.

Chmielewski, R. A. N., and J. F. Frank. 2003. "Biofilm Formation and Control in Food Processing Facilities" 2.

Choi, Jungil, Yong-gyun Jung, Eun Keun Kim, Minchul Lee, Jeongheon Yoo, and Sunghoon Kwon. 2013. “Rapid and High Throughput Antimicrobial Susceptibility Test Using Morphological Analysis of Single Cells With Microfluidic Channel in 96 Well Platform,” no. October: 548–50.

Choi, Jungil, Yong-Gyun Jung, Jeewoo Kim, Seongbum Kim, Ushin Jung, Hunjong Na, and Sunghoon Kwon. 2012. “Rapid Antibiotic Susceptibility Testing by Tracking Single Cell Growth in a Microfluidic Agarose Channel System.” *Lab on a Chip*. doi:10.1039/c2lc41055a.

Daniel, Richard a., and Jeff Errington. 2003. “Control of Cell Morphogenesis in Bacteria: Two Distinct Ways to Make a Rod-Shaped Cell.” *Cell* 113 (6): 767–76. doi:10.1016/S0092-8674(03)00421-5.

Donovan, Catriona, and Marc Bramkamp. 2014. “Cell Division in Corynebacterineae.” *Frontiers in Microbiology* 5 (APR): 1–16. doi:10.3389/fmicb.2014.00132.

Dubnau, D. 1991. “The Regulation of Genetic Competence in *Bacillus subtilis*.” *Molecular Microbiology* 5 (1): 11–18. doi:10.1111/j.1365-2958.1991.tb01820.x.

Dusny, Christian, Alexander Grünberger, Christopher Probst, Wolfgang Wiechert, Dietrich Kohlheyer, and Andreas Schmid. 2015. “Technical Bias of Microcultivation Environments on Single-Cell Physiology.” *Lab Chip* 15. Royal Society of Chemistry: 1822–34. doi:10.1039/C4LC01270D.

El-Halfawy. 2015. “Antimicrobial Heteroresistance: An Emerging Field in Need of Clarity.” Clin Microbiol Rev 28:191–207. doi:10.1128/CMR.00058-14.

Ferreira, J H S, F N Matthee, and a C Thomas. 1991. “Biological Control of Eutypa Lata on Grapevine by an Antagonistic Strain of *Bacillus subtilis*.” *Phytopathology*.

Gefen, Orit, and Nathalie Q Balaban. 2009. “The Importance of Being Persistent : Heterogeneity of Bacterial Populations under Antibiotic Stress” 33: 704–17. doi:10.1111/j.1574-6976.2008.00156.x.

Gram, Lone, Lars Ravn, Maria Rasch, Jesper Bartholin, Allan B Christensen, and Michael Givskov. 2002. “Food Spoilage — Interactions between Food Spoilage Bacteria” 78: 79–97.

Gruenberger Alexander, Christopher Probst, Antonia Heyer, Wolfgang Wiechert, Julia Frunzke, and Dietrich Kohlheyer. 2013. “Microfluidic Picoliter Bioreactor for Microbial Single-Cell Analysis: Fabrication, System Setup, and Operation.” *Journal of Visualized Experiments : JoVE* 50560 (82): 50560. doi:10.3791/50560.

Gruenberger, A. M., 2014. Single-Cell Analysis of Microbial Production Strains in Microfluidic Bioreactors. Ph.D. Thesis. Rheinisch-Westfälischen Technischen Hochschule Aachen Universität.

Helfrich, S. et al., 2015. Vizardous: Interactive Analysis of Microbial Populations with Single Cell Resolution. Bioinformatics (Oxford, England).

Helfrich, S., 2012. A (semi-)automatic image analysis approach to lineage tree generation from time-lapse microscopy. Master Thesis. Universität des Saarlandes.

Hett, Erik C., Michael C. Chao, and Eric J. Rubin. 2010. "Interaction and Modulation of Two Antagonistic Cell Wall Enzymes of Mycobacteria." *PLoS Pathogens* 6 (7): 1–14. doi:10.1371/journal.ppat.1001020.

Hou, Zining, Yu An, Karin Hjort, Klas Hjort, Linus Sandegren, and Zhigang Wu. 2014. "Lab on a Chip Using a Microfluidic Linear Gradient 3D Culture Device †," 3409–18. doi:10.1039/c4lc00451e.

Ikeda, M., and S. Nakagawa. 2003. "The *Corynebacterium glutamicum* Genome: Features and Impacts on Biotechnological Processes." *Applied Microbiology and Biotechnology* 62 (2-3): 99–109. doi:10.1007/s00253-003-1328-1.

Iyer, V N, and W Szybalski. 1964. "Mitomycins and Porfiromycin: Chemical Mechanism of Activation and Cross-Linking of Dna." *Science (New York, N.Y.)*. doi:10.1126/science.145.3627.55.

Jorgensen, James H, and Mary Jane Ferraro. 2009. "Antimicrobial Susceptibility Testing: A Review of General Principles and Contemporary Practices." *Clinical Infectious Diseases : An Official Publication of the Infectious Diseases Society of America* 49 (11): 1749–55. doi:10.1086/647952.

Joux, Fabien, and Philippe Lebaron. 2000. "Use of Fluorescent Probes to Assess Physiological Functions of Bacteriaat Single-Cell Level." *Microbes and Infection* 2 (12): 1523–35. doi:10.1016/S1286-4579(00)01307-1.

Kahlmeter, Gunnar, Derek F J Brown, Fred W. Goldstein, Alasdair P. MacGowan, Johan W. Mouton, Anders Österlund, Arne Rodloff, Martin Steinbakk, Pavla Urbaskova, and Alkiviadis Vatopoulos. 2003. "European Harmonization of MIC Breakpoints for Antimicrobial Susceptibility Testing of Bacteria." *Journal of Antimicrobial Chemotherapy* 52 (2): 145–48. doi:10.1093/jac/dkg312.

Kalashnikov, Maxim, Jean C Lee, Jennifer Campbell, and Alexis F Sauer-budge. 2012. "Lab on a Chip A Microfluidic Platform for Rapid , Stress-Induced Antibiotic Susceptibility Testing of Staphylococcus Aureus," 4523–32. doi:10.1039/c2lc40531h.

Kalinowski, Jörn, Brigitte Bathe, Daniela Bartels, Nicole Bischoff, Michael Bott, Andreas Burkovski, Nicole Dusch, et al. 2003. "The Complete *Corynebacterium glutamicum* ATCC 13032 Genome Sequence and Its Impact on the Production of L-Aspartate-Derived Amino Acids and Vitamins." *Journal of Biotechnology* 104 (1-3): 5–25. doi:10.1016/S0168-1656(03)00154-8.

Kell, Douglas B., Arseny S. Kaprelyants, Dieter H. Weichart, Colin R. Harwood, and Michael R. Barer. 1998. "Viability and Activity in Readily Culturable Bacteria: A Review and Discussion of the Practical Issues." *Antonie van Leeuwenhoek, International Journal of General and Molecular Microbiology* 73 (2): 169–87. doi:10.1023/A:1000664013047.

Keller, J.J., and E.J. Kuijper. 2015. "Treatment of Recurrent and Severe Clostridium Difficile Infection." *Annual Review of Medicine* 66 (1): 373–86. doi:10.1146/annurev-med-070813-114317.

Kennedy, K. a., S. Rockwell, and a. C. Sartorelli. 1980. "Preferential Activation of Mitomycin C to Cytotoxic Metabolites by Hypoxic Tumor Cells." *Cancer Research* 40 (7): 2356–60.

Keren, Iris, Niilo Kaldalu, Amy Spoering, Yipeng Wang, and Kim Lewis. 2004. "Persister Cells and Tolerance to Antimicrobials." *FEMS Microbiology Letters* 230 (1): 13–18. doi:10.1016/S0378-1097(03)00856-5.

Koul, Anil, Luc Vranckx, Neeraj Dhar, Hinrich W H Göhlmann, Emre Özdemir, Jean-Marc Neefs, Melanie Schulz, et al. 2014. "Delayed Bactericidal Response of *Mycobacterium tuberculosis* to Bedaquiline Involves Remodelling of Bacterial Metabolism." *Nature Communications* 5: 3369. doi:10.1038/ncomms4369.

Kunst, F, N Ogasawara, I Moszer, a M Albertini, G Alloni, V Azevedo, M G Bertero, et al. 1997. "The Complete Genome Sequence of the Gram-Positive Bacterium *Bacillus subtilis*." *Nature* 390 (6657): 249–56. doi:10.1038/36786.

Lee, Soo Youn, Bit Na Kim, Ji Hye Han, Suk Tai Chang, Young Woo Choi, Yang Hoon Kim, and Jiho Min. 2010. "Treatment of Phenol-Contaminated Soil by *Corynebacterium glutamicum* and Toxicity Removal Evaluation." *Journal of Hazardous Materials* 182 (1-3). Elsevier B.V.: 937–40. doi:10.1016/j.jhazmat.2010.06.092.

Lopez, Daniel, Hera Vlamakis, and Roberto Kolter. 2009. "Generation of Multiple Cell Types in Bacillus Subtilis." *FEMS Microbiology Reviews* 33 (1): 152–63. doi:10.1111/j.1574-6976.2008.00148.x.

López, Daniel, Hera Vlamakis, Richard Losick, and Roberto Kolter. 2009. "Cannibalism Enhances Biofilm Development in *Bacillus subtilis*." *Molecular Microbiology* 74 (3): 609–18. doi:10.1111/j.1365-2958.2009.06882.x.

Maglica, Željka, Emre Özdemir, and John D. McKinney. 2015. "Single-Cell Tracking Reveals Antibiotic-Induced Changes in Mycobacterial Energy Metabolism." *MBio* 6 (1): 1–11. doi:10.1128/mBio.02236-14.Editor.

Martínez, José L., and Fernando Rojo. 2011. "Metabolic Regulation of Antibiotic Resistance." *FEMS Microbiology Reviews* 35 (5): 768–89. doi:10.1111/j.1574-6976.2011.00282.x.

Mateos, Luís M., Efrén Ordóñez, Michal Letek, and José a. Gil. 2006. "*Corynebacterium glutamicum* as a Model Bacterium for the Bioremediation of Arsenic." *International Microbiology* 9 (3): 207–15.

Mendelson, N. H. 1982. "Dynamics of Bacillus Subtilis Helical Macrofiber Morphogenesis: Writhing, Folding, Close Packing, and Contraction." *Journal of Bacteriology* 151 (1): 438–49.

Mohan, Ritika, Chotitath Sanpitakseree, Amit V Desai, Selami E Sevgen, Charles M Schroeder, and Paul J A Kenis. 2015. "RSC Advances A Micro Fl Uidic Approach to Study the E Ff Ect of Bacterial Interactions on Antimicrobial Susceptibility in Polymicrobial Cultures †," 35211–23. doi:10.1039/C5RA04092B.

Morikawa, Masaaki, Shinji Kagihiro, Mitsuru Haruki, Kazufumi Takano, Steve Branda, Roberto Kolter, and Shigenori Kanaya. 2006. "Biofilm Formation by a *Bacillus subtilis* Strain That Produces Γ-Polyglutamate." *Microbiology* 152 (9): 2801–7. doi:10.1099/mic.0.29060-0.

Neumeyer, Andrea, Thomas Hübschmann, Susann Müller, and Julia Frunzke. 2013. "Monitoring of Population Dynamics of *Corynebacterium glutamicum* by Multiparameter Flow Cytometry." *Microbial Biotechnology* 6 (2): 157–67. doi:10.1111/1751-7915.12018.

Nicolas, Pierre, Ulrike Mäder, Etienne Dervyn, Tatiana Rochat, Aurélie Leduc, Nathalie Pigeonneau, Elena Bidnenko, et al. 2012. "Condition-Dependent Transcriptome Architecture in Bacillus Subtilis," no. March: 1103–6.

Novo, David, Nancy G. Perlmutter, Richard H. Hunt, and Howard M. Shapiro. 1999. "Accurate Flow Cytometric Membrane Potential Measurement in Bacteria Using Diethyloxacarbocyanine and a Ratiometric Technique." *Cytometry* 35 (1): 55–63. doi:10.1002/(SICI)1097-0320(19990101)35:1<55::AID-CYTO8>3.0.CO;2-2.

Ogura, Mitsuo, Kana Shimane, Kei Asai, Naotake Ogasawara, and Teruo Tanaka. 2003. "Binding of Response Regulator DegU to the aprE Promoter Is Inhibited by RapG, Which Is Counteracted by Extracellular PhrG in Bacillus Subtilis." *Molecular Microbiology* 49 (6): 1685–97. doi:10.1046/j.1365-2958.2003.03665.x.

Piggot, Patrick J., and David W. Hilbert. 2004. "Sporulation of *Bacillus subtilis*." *Current Opinion in Microbiology* 7 (6): 579–86. doi:10.1016/j.mib.2004.10.001.

Prantera, C, M L Scribano, G Falasco, a Andreoli, and C Luzi. 2002. "Ineffectiveness of Probiotics in Preventing Recurrence after Curative Resection for Crohn's Disease: A Randomised Controlled Trial with Lactobacillus GG." *Gut* 51 (3): 405–9. doi:10.1136/gut.51.3.405.

Probst, Christopher, Alexander Grünberger, Wolfgang Wiechert, and Dietrich Kohlheyer. 2013. "Polydimethylsiloxane (PDMS) Sub-Micron Traps for Single-Cell Analysis of Bacteria." *Micromachines* 4 (4): 357–69. doi:10.3390/mi4040357.

Pulido, Marina R., Meritxell García-Quintanilla, Reyes Martín-Peña, José Miguel Cisneros, and Michael J. McConnell. 2013. "Progress on the Development of Rapid Methods for Antimicrobial Susceptibility Testing." *Journal of Antimicrobial Chemotherapy* 68 (12): 2710–17. doi:10.1093/jac/dkt253.

Sargent, M. G. 1975. "Control of Cell Length in Bacillus Subtilis." *Journal of Bacteriology* 123 (1): 7–19.

Sim, Soo Yeon, Eun Ji Hong, Younhee Kim, and Heung Shick Lee. 2014. "Analysis of cepA Encoding an Efflux Pump-like Protein in *Corynebacterium glutamicum*." *Journal of Microbiology* 52 (4): 278–83. doi:10.1007/s12275-014-3461-1.

Smith, Grant N, Cecilia S Worrel, and A N N L Swanson. 1949. "Inhibition of Bacterial Esterases by Chloramphenicol."

Stein, Torsten, Institut Mikrobiologie, and Johann Wolfgang Goethe-. 2005. "MicroReview *Bacillus subtilis* Antibiotics : Structures , Syntheses and" 56: 845–57. doi:10.1111/j.1365-2958.2005.04587.x.

Sutton, Scott. 2011. "Accuracy of Plate Counts," 42–46.

Teicher, Beverly a, Charles D Kowal, Katherine a Kennedy, and Alan C Sartorelli. 1981. "Enhancement by Hyperthermia of the in Vitro Cytotoxicity of Mitomycin C toward Hypoxic Tumor Cells Enhancement by Hyperthermia of the in Vitro Cytotoxicity of Mitomycin C toward Hypoxie Tumor Cells1." *Cancer Research* 41 (March): 1096–99.

Tomasz, M. 1995. "Mitomycin C: Small, Fast and Deadly (but Very Selective)." *Chemistry and Biology* 2 (9): 575–79. doi:10.1016/1074-5521(95)90120-5.

Vos, Logan and De. 2011. *Endospore Forming Soil Bacteria*.

Yassin, a. F., R. M. Kroppenstedt, and W. Ludwig. 2003. "*Corynebacterium glaucum* Sp. Nov." *International Journal of Systematic and Evolutionary Microbiology* 53 (3): 705–9. doi:10.1099/ijs.0.02394-0.

Decleration

Herewith, I declare that this thesis has been completed independently and unaided and that no other sources others then the ones given here have been used.

Furthermore, I declare that this work has never been submitted at any other time and anywhere else as a final thesis. The thesis was prepared at the Microscale Bioengineering group at the IBG-1 of the Forschungszentrum Jülich, 52428, Jülich.

The submitted written version of this work is the same as the one electronically saved and submitted on CD. The CD also contains the video of the time lapse experiments.

Kiel, June, 2015

Abhijeet Singh

Abhijeet Singh

Acknowledgements

I would like to thank all those who supported and helped me directly or indirectly in my master thesis project and in writing this thesis. First of all, I want to thank JuniorProf. Dr. Dietrich Kohlheyer, for providing me an opportunity to conduct my master thesis at the Microscale Bioengineering group, IBG-1 of the Forschungszentrum Jülich and for being my examiner. He always supported and encouraged me in all steps of my project.

I want to express my gratitude for Prof. Dr. Ralf-Udo Ehlers, for being my examiner. I have always been motivated by his lectures and Biocontrol biotechnology course at e-nema GmbH, was a great experience in the knowing the real application of biotechnology on an industrial basis.

I am grateful to my supervisor Dipl. Ing. Christina Krämer, for being someone I could turn to for advice and counsel. I thank her expertise and for teaching me the fluorescence microscopy and microfluidic techniques necessary to succeed in my experiments. Her scientific counsel and positive attitude played a very important in producing the results and presenting them in form of this thesis. I am fortunate that our paths crossed at Microscale Bioengineering group.

I am also very thankful to Dr. Alexander Grünberger, Christopher Probst, Agnes Müller-Schröer, and Nadja Braun, who supported me in my experiments. They were always helpful and patient and supported in all scientific queries. I want to thank Stefan Helfrich for all his support and troubleshooting regarding software. Without his help, I could not have completed my work in such a short period of time.

Furthermore, I want to thank my friends Gaurav Pandharikar, Amit Sagervanshi, Kiran Singewar and Ankush Borlepawar for motivating and encouraging me during my whole master studies. I want to thank all my batch mates of AgriGenomics for all their support and help.

Last but not least, I want to thank my parents for allowing and motivating me to pursue my higher studies in Germany. I am indebted to my father Mr. Ramesh Kumar Didot, for all his inspiration and financial support, without which I could not have come to Germany. I want to express my deepest regards to my mother Mrs. Jyoti Bala, for her unconditional love and care. I am also grateful to my master and guardians Pandit Shriram Sharma Acharya and Mata Bhagwati Devi Sharma, for their cosmic presence and guidance in every situation of my life. I am obliged to my parents and guardians for their boundless love and care, which I cannot be able to pay back.

Appendix I

1. Materials

Name	Company	Comments
Drigalski spatula	VWR	
Glass slide	Schott AG, Ger-many	D263 T eco, 30 mm x 25 mm x 0.17 mm
Needles	Nordsen EFD	Precision Tips 27 GA; ID = 0.2 mm, OD = 0.42 mm
Poly(dimethyl)siloxane (PDMS)	Dow corning	Sylgard 184 Slilicone Elastomer Kit
Syringes	Braun	Disposable Syringes – Omnifix Spritzen BRAUN Omnifix 40 Duo, 1 mL
Tubing	Tygon	Tygon S-54-HL, ID = 0.25 mm, OD = 0.76 mm

2. Equipment

Name	Company	Comments
Incubator	PECON	Incubator NL 2000
Incubator	Ecotron	Infors HT
Magnetic stirrer	Stuart	VWR 442-0304/CB 162
Microscope	Nikon	Nikon Eclipse Ti
Oven	Memmert	UN 200
Photometer	Eppendorf	Eppendorf BioPhotometer plus/6132000008
Plasma Cleaner	Diener Electronics	Femto Plasma Cleaner
Syringe pumps	Centoni GmbH	neMESYS Syringe pumps

3. Chemicals

Name	Company	Comments
Agar-agar	Applichem GmbH	Bacteriology grade
BactoTM Brain heart Infusion	Becton, Dickinson	
NaCl	ROTH	

4. Fluorescent dyes

Name	Company	Comments
Calcein acetoxymethyl ester (calcein-AM)	Life technologies	excitation/emission maximum ~400/452 nm
PO-PRO1	Life technologies	excitation/emission maximum ~435/455 nm
Propidium Iodide (PI)	Carl Roth	excitation/emission maximum ~535/617 nm

Appendix II – Videos on CD ROM

List of videos

1. *B. subtilis*

S. no.	Name of video
1.	*B. subtilis* with AMP
2.	*B. subtilis* with CHL
3.	*B. subtilis* with KAN
4.	*B. subtilis* with MMC
5.	*B. subtilis* with STR

2. *C. glutamicum*

S. no.	Name of video
1.	*C. glutamicum* with AMP
2.	*C. glutamicum* with CHL
3.	*C. glutamicum* with KAN
4.	*C. glutamicum* with MMC
5.	*C. glutamicum* with STR

2. *C. glutamicum* regrowth experiment

S. no.	Name of video
1.	*C. glutamicum* with AMP
2.	*C. glutamicum* with CHL